LAWRENCE
LIVERMORE
NATIONAL
LABORATORY

Substrate-Integrated Hollow Waveguides (iHWG) for Infrared (IR) and Raman Gas Sensing: Volume 2

J. C. Carter, B. Mizaikoff, A. Wilk, S. S. Kim

October 15, 2012

Disclaimer

This document was prepared as an account of work sponsored by an agency of the United States government. Neither the United States government nor Lawrence Livermore National Security, LLC, nor any of their employees makes any warranty, expressed or implied, or assumes any legal liability or responsibility for the accuracy, completeness, or usefulness of any information, apparatus, product, or process disclosed, or represents that its use would not infringe privately owned rights. Reference herein to any specific commercial product, process, or service by trade name, trademark, manufacturer, or otherwise does not necessarily constitute or imply its endorsement, recommendation, or favoring by the United States government or Lawrence Livermore National Security, LLC. The views and opinions of authors expressed herein do not necessarily state or reflect those of the United States government or Lawrence Livermore National Security, LLC, and shall not be used for advertising or product endorsement purposes.

SUBSTRATE-INTEGRATED HOLLOW WAVEGUIDES (IHWG) FOR INFRARED (IR) & RAMAN GAS SENSING

VOLUME 2

J. Chance Carter[1], Boris Mizaikoff[2], Andreas Wilk[2], Seong-Soo Kim[2]

[1]Lawrence Livermore National Laboratory, Livermore CA
[2]Institute of Analytical and Bioanalytical Chemistry, Ulm University, Ulm Germany

TABLE OF CONTENTS

APPENDICES

Substrate-Integrated Hollow Waveguides (iHWG) for Infrared (IR) & Raman Gas Sensing

Volume 2

1.1   Introduction

This document is the third in a series[1-2] that describes the development of substrate-integrated hollow waveguides (iHWG) for infrared (IR) and Raman gas sensing applications. This work is a collaborative effort between Lawrence Livermore National Laboratory and the Institute of Analytical and Bioanalytical Chemistry at Ulm University.

1.2   Meandering Hollow Waveguide Design II: size and mass reduction

Waveguide miniaturization (i.e, size and mass reduction) was the primary design objective during this project phase. Prior waveguide prototypes having a 2x2.1mm channel size and made from aluminum were based mainly on a 5.0x7.5cm form factor; the overall dimensions of the latest aluminum waveguide prototypes, while maintaining the same channel size, are 5.0x5.0cm, resulting in a ~33% reduction in volume and weight. Consequently, the smaller form factor required new waveguide design concepts providing sufficient waveguide channel pathlength for high sensitivity gas measurements.

Figure 1 illustrates five new waveguide designs developed and reduced to practice (see Appendix A) during this project phase; each design is based on the 5.0x5.0cm form factor. The key feature that differentiates these prototypes from prior designs is the ability to incorporate a reflective optic effectively doubling the pathlength over which the IR radiation interacts with the gas molecules within the waveguide channel volume. The double-pass design also enables tailoring of the meandering hollow waveguide to the specific sensing application resulting in (1) minimal optical losses due to scattering, (2) minimal optical reflections (reflection = losses); (3) minimal losses per reflection, and (4) maximum light in-coupling and out-coupling.

S2*

S3*

← 50 mm →

50 mm

Central geometric (channel) pathlength

S2: 109.7 mm
S3: 204.1 mm
D2: 141.1 mm
D3: 233.1 mm
D4: 299.9 mm

* Single or double pass

(optional)

(optional)

D2

D3

D4

← 50 mm →

50 mm
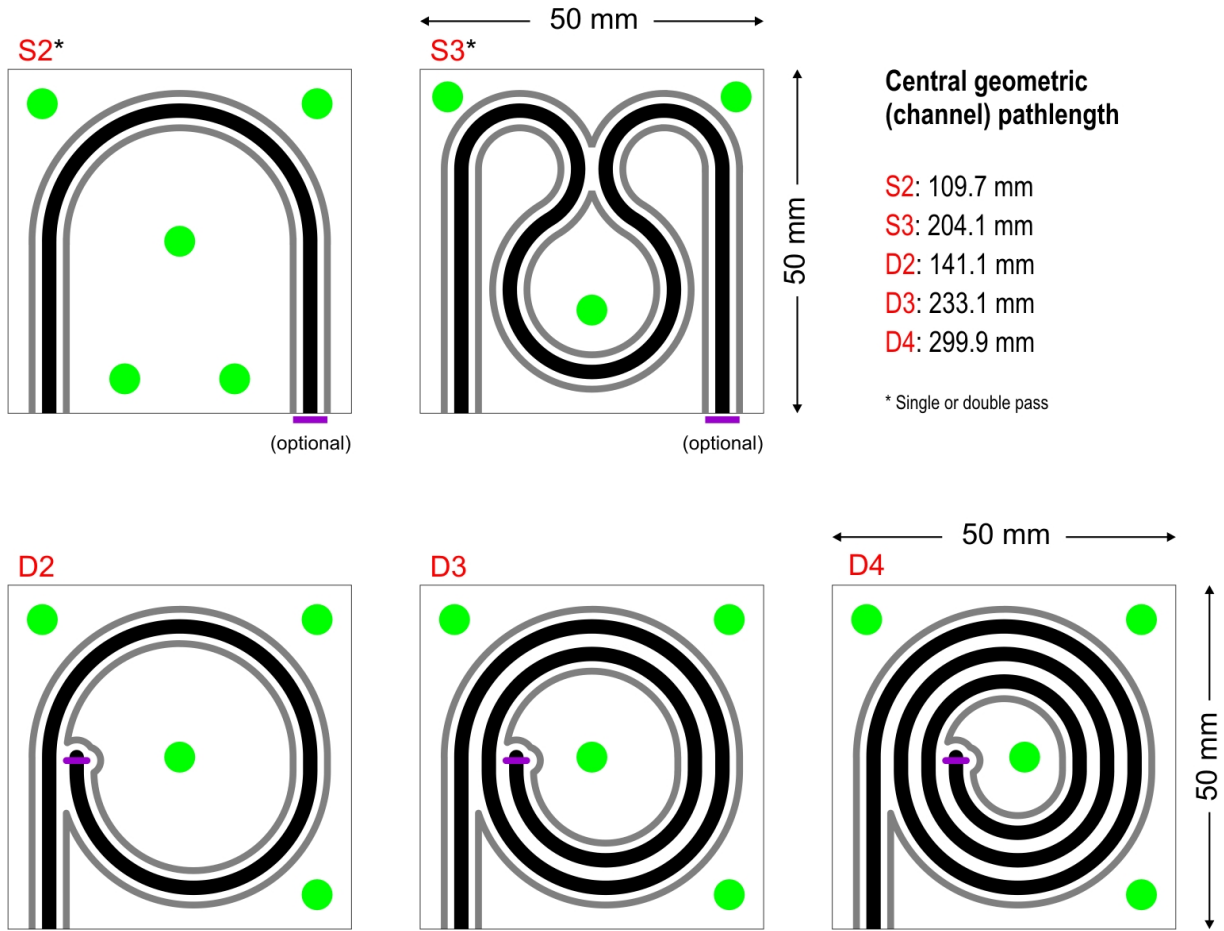
Figure 1. The new waveguide prototype designs feature the addition of a reflective optic (purple) that effectively doubles the optical channel (black) pathlength (i.e. double-pass waveguide configuration). The pathlength in millimeters of a light ray traversing the central path (i.e. no reflections) of each channel is provided; multiplying this value by 2 provides a conservative estimate of the double-pass pathlength [Note: the S2 and S3 waveguide designs can function as either single or double-pass configurations]. The waveguide top plate (not shown) can be secured in a variety of ways including clamping with screws (green) or adhesion (e.g. epoxies). Outer channels (grey) serve as a containment berm to prevent the adhesive from entering the optical channel (black). Alternatively, these channels (grey) may serve as conduits for introducing fluids (e.g. for brazing, etc.) or other materials (e.g. nanolaminates, etc.) or other sensors (e.g. temperature, etc.).

In operation, light is directed to the meandering waveguide channel port via a fiber or fiber array or conventional optics (not shown). For the spiral designs (i.e. D2, D3, D4), light entering the meandering hollow waveguide propagates via interactions with the channel surfaces toward the innermost spiral where an optic (e.g. retro-reflector, mirror,

grating, etc.) is located. The propagation direction of the light is reversed by the optic and the light passes a second time through the waveguide channel. As the light traverses the entire pathlength of the hollow channel in either direction, it interacts with gas/vapor and/or liquid phase molecules co-located in the hollow channel. Light exiting the waveguide channel port is directed via a fiber or fiber array or optical elements (not shown) to the analyzer[3].

This meandering waveguide configuration can be described as a multi-pass or, in these embodiments, double-pass waveguide design since light traverses the meandering waveguide channel more than once. An advantage of the multi-pass meandering design is increased optical pathlength within the same meandering waveguide channel volume and dimensions (i.e. in this case, 5.0x5.0 cm) as a similar device designed to allow light to traverse once. As an example, Appendix B details the geometrical channel length calculation for the Figure 1, D4 design. This calculation assumes a central ray passing down the center of the meandering waveguide channel and only interacting at the inner spiral termination point with an optical element (i.e. never interacting with the channel surfaces). The calculated spiral channel geometric length of 299.9 millimeters is, of course, less than the true optical pathlength of a light ray traveling from the meandering waveguide port to the termination point of the inner spiral because this calculation estimate does not take into account the added pathlength provided by reflections along the channel surfaces in both directions. Nonetheless, this is a useful (conservative) estimate for demonstrating that a total optical pathlength estimate of 599.8 millimeters (2 x 299.9 millimeters) is achievable within a 5.0 x 5.0 cm form factor. For comparison, a similar sensor comprising a

conventional hollow waveguide of equivalent optical pathlength, and for a central ray propagating down the center, would require the full 599.8 millimeters in length.

1.3   Meandering Hollow Waveguide Fabrication II:
macro- and micro- techniques

Two different manufacturing approaches, macro- and micro-fabrication, were investigated for fabricating meandering hollow waveguide prototypes; a discussion of both methods is detailed in the FY11 Annual Report[4]. At the end of FY11 the only prototype waveguide devices fabricated were those using conventional milling macrofabrication. Regardless of the substrate material, all early devices suffered from surface features that were on the same order of magnitude as the mid-IR wavelengths (3-20 microns), resulting in significant scattering losses. By our summation, the most limiting factor in surface roughness precision was the vibrations of the machine during the milling process. Therefore, for macrofabrication to remain a viable method for hollow waveguide device fabrication, the surface roughness precision had to be improved by at least an order of magnitude.

Even though diamond milling had been investigated in FY11 and quickly ruled out because of its high demand and the resulting expense per unit device (based on the small numbers of devices for our R&D efforts), it was reconsidered but ruled out again on the basis of device delivery schedule (again, based on the small numbers of devices). While in discussions with the Fraunhofer Institute of Fabrication (IOF), we learned of the KERN Evo Ultra Precision Computer Numerical Control (CNC) Machine (see Appendix C), which is specially designed, among other things, for applications requiring the highest positional precision and excellent surface quality. The key difference between the KERN Evo CNC and

others is the 1.8-ton polymer concrete monobloc machine frame, which provides maximum rigidity, vibration dampening, and low sensitivity to temperature fluctuations. Eventually, several test pieces produced by Fraunhofer on the KERN Evo CNC using our substrate materials were measured using atomic force microscopy (AFM) to have a surface roughness of ~100-500nm, which represents a 10 to 20-fold improvement over prior prototype surface roughness (see Appendix D). Figure 2 shows an AFM image of the roughest test sample site. Figure 3 shows the waveguide devices fabricated by Fraunhofer using the KERN Evo CNC and based on the designs illustrated in Figure 1.

1.4   IR Waveguide/Optical Fiber Interface

All double-pass waveguide designs discussed herein utilize the same channel port for radiation in- and out-coupling. Thus, the optical fiber probe must also provide for radiation in- and out-coupling and ideally terminate in a common connector. Silica-based optical fiber probe designs that accomplish this are well known to those skilled in the art of remote Raman spectroscopy and are the subject of numerous reports[5]. Borrowing from those design concepts, a prototype IR fiber probe comprising a bundle of eight individual fibers was fabricated in a 7-around-1 geometry using $AgCl_{0.5}Br_{0.5}$ solid-core fibers as illustrated in Figure 4. Assuming an optimal butt-coupled alignment with the 2x2.1mm waveguide channel port, the fiber out-coupling ratio is ~48% (see Appendix F). This ratio could be improved if square optical fibers were used instead of round fibers. Unfortunately, square Ag-halide fibers are not commercially available even though manufacturing such geometries is feasible.[6]
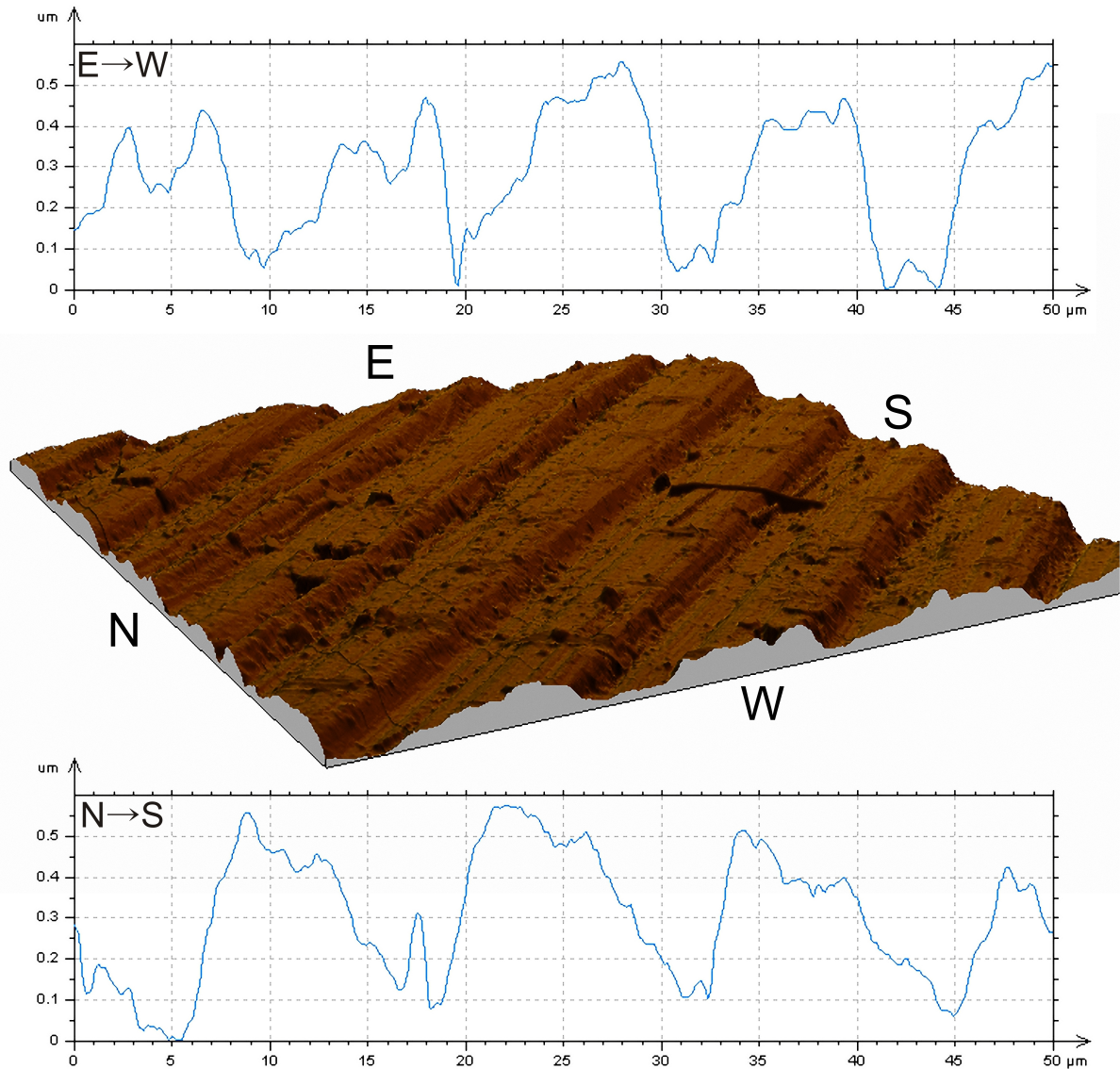
Figure 2. An AFM image of a 50x50 micron section of an aluminum test sample milled using the KERN Evo CNC Milling Machine with a HAM 430 precision end mill is shown. The surface roughness varies from ~100 to 550 nm in the AFM measurements that transect east (E) to west (W) and north (N) to south (S)

Figure 3. Meandering hollow waveguide prototypes were fabricated based on the design illustrations of Figure 1 using aluminum substrates with a final surface roughness of 100-200nm. The Fraunhofer IOF used the KERN Evo CNC Machine technology to fabricate these devices. A solid carbide end mill, HAM 430 precision milling tool (see Appendix E), was used for waveguide channel cuts. Note: the top plates for all waveguide devices were fabricated and polished at the Uni Ulm University Workshop.

1.5   IR Waveguide Testing II

In FY12 W-program sensors adopted a hierarchical gas test matrix consisting of eight tiers for comparing different gas sensing technologies. At the highest tier, the test consists of several dozen gas/vapor analytes and represents a high fidelity representation of gas environments relevant to the program customer; the lowest tier test matrix consists of only five gases: carbon dioxide, butane, methane, cyclopropane, and isobutylene. A non-fiber coupled single-pass meandering hollow waveguide was configured as a gas cell (see

Appendix G) and subjected to the Tier 0 test matrix. Individual calibrated standards (1000 ppm$_v$) of all five gases were purchased and interfaced with LLNL's custom gas calibration and mixing system (see Appendix H) for introducing individual gases and mixtures to the gas cell for mid-IR analysis (see Appendix I).
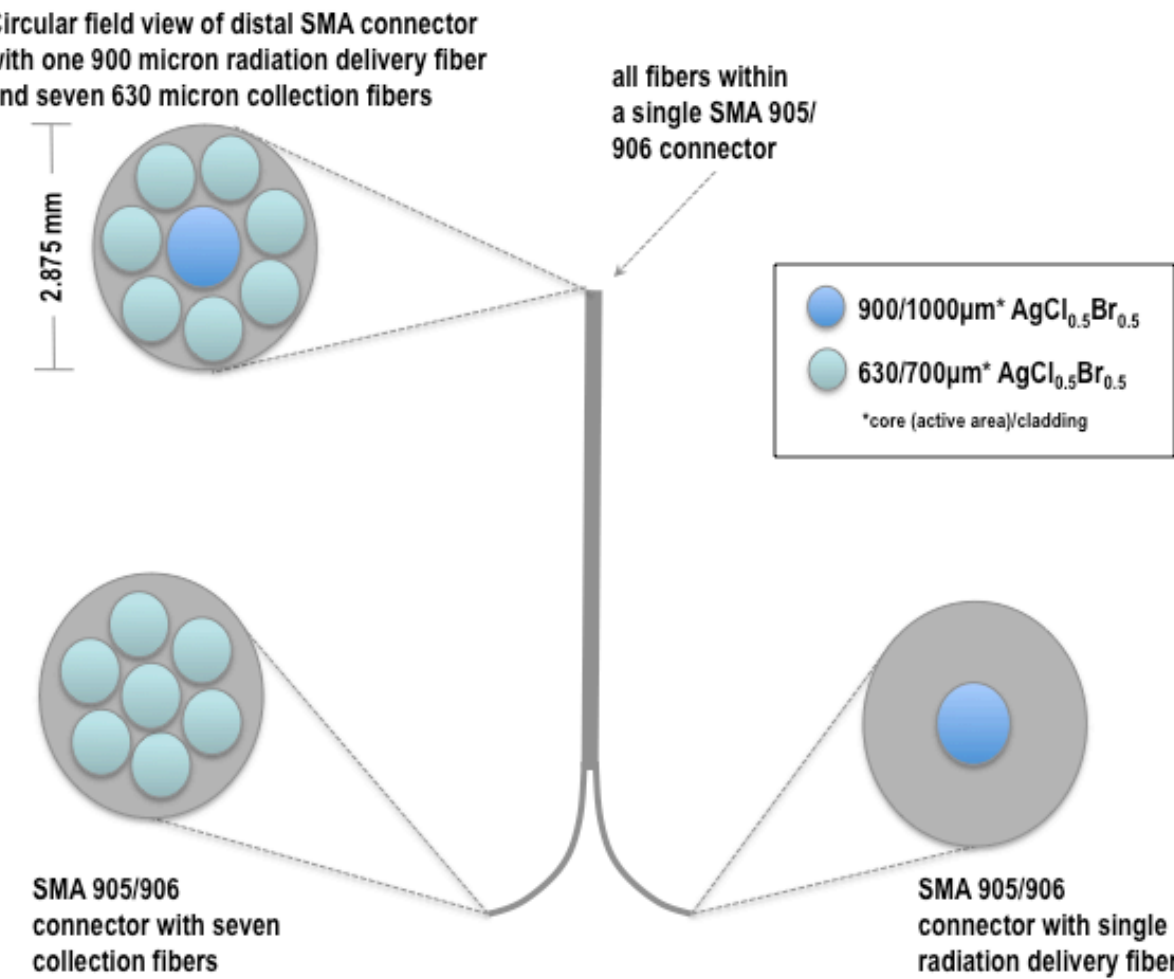

Figure 4. The cross-sectional packing geometry of a 7-around-1 optical fiber probe configuration for use with the double-pass waveguide designs of Figure 1 is shown in this illustration. This probe design comprises one fiber for delivering radiation to the distal tip for in-coupling to the double-pass waveguide port and 7 fibers for collecting radiation not absorbed by the sample. A single fiber connector was used to secure one end of the source and collection fibers, and the two remaining fiber ends were placed in separate fiber connectors. This arrangement is commonly referred to as a 'Y' design. All probes were connectorized using SMA type fiber connectors. The epoxy used to secure all fibers in SMA connectors was Torr Seal® epoxy (Varian, CA, part no. 9530001).

Table 1 summarizes the limits of detection (LODs) for the mid-IR measurements (1000ppm$_v$) of individual gas analytes of the Tier 0 test matrix. It is important to note that the LODs are only estimates as further studies at or near the estimated LOD are required to confirm these results. Furthermore, these tests did not include optical fiber coupled measurements, which will certainly limit the device throughput and lower the LODs. Even so these measurements serve as valuable data as we develop, in parallel, the smaller and lighter double-pass waveguides.

Mid-IR Gas Cell Sensing Results for Tier 0 gas Matrix test		
Analyte	UNIVARIATE SNR (1000 ppm standard)	UNIVARIATE LOD [ppm] (estimate)
Isobutylene	324	10.2 (2)
Methane	314	10.5 (2)
Cyclopropane	337	9.77 (C)
Butane	507	6.50 (1)
Carbon dioxide	156	21.1 (1)

Table 1. A summary of SNR and estimated LODs from gas measurements of the Tier 0 test matrix conducted using a single-pass meandering hollow waveguide configured as a gas cell.

1.6 Conclusions/Future Work

A significant reduction in waveguide mass and volume has been realized via the double-pass geometry during this project phase. The new waveguide designs also include design features that allow multiple options for integrating the various waveguide components. An optical fiber probe has also been developed for interfacing to the double-pass waveguide designs. The next steps will involve the addition of optical coatings (e.g. Au) to the waveguide and the insertion of retro-reflecting optics made from Au coated silica. The new waveguides will be fiber coupled and subjected to the same Tier 0 test matrix as summarized for the single-pass waveguide gas cell measurements.

1.7 References/Notes

1. Carter et al, "Substrate-integrated Hollow Waveguides (iHWG) for Infrared (IR) and Raman Gas Sensing", FY11 Annual Report for NWE Sensors, **Vol. 1**, pages 1-255 (2011).
2. "Substrate-integrated Hollow Waveguides (iHWG)", non-provisional patent application, filed October 1, 2012, which claims priority to provisional application 61/542,162.
3. Single-pass waveguide geometries have separate radiation input and output apertures unlike double-pass geometries, which utilize the same aperture for radiation in- and out-coupling.
4. Carter et al., "Substrate-integrated Hollow Waveguides (iHWG) for Infrared (IR) and Raman Gas Sensing", FY11 Annual Report for NWE Sensors, **Vol. 1**, pages 6-9 and Appendix H; H7-H28, (2011).
5. Cooney et al, "Comparative Study of Some Fiber-Optic Remote Raman Probe Designs. Part I: Model for Liquids and Transparent Solids", *Appl. Spectrosc.*, **50**, 836 (1996).
6. Personal communication with Viacheslav Artyushenko

Meandering Hollow Waveguide Design II: size and mass reduction

Appendix A

Waveguide design
Final substrate dimensions
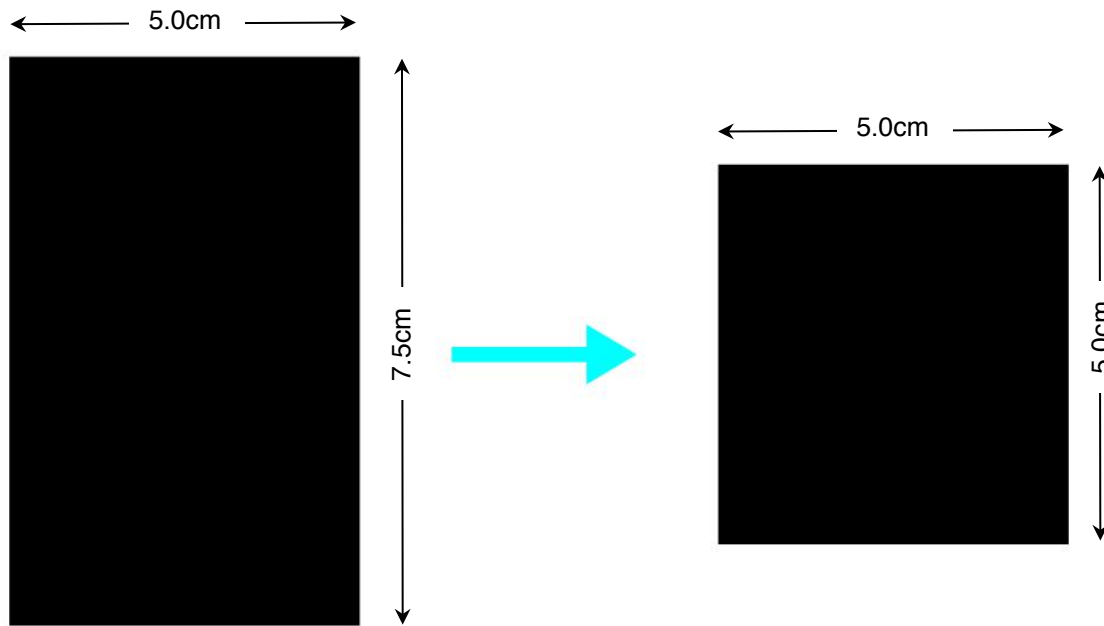
5.0cm

7.5cm

5.0cm

5.0cm

- **During this project phase there was an effort to reduce the size of the waveguide substrate dimensions from 5.0x7.5 cm to 5.0x5.0 cm.**

  Straightforwardly, this naturally reduces both volume and weight of all future meandering hollow waveguide (iHWGs) by 33%.

Lawrence Livermore National Laboratory

Waveguide design
Effects on weight and volume
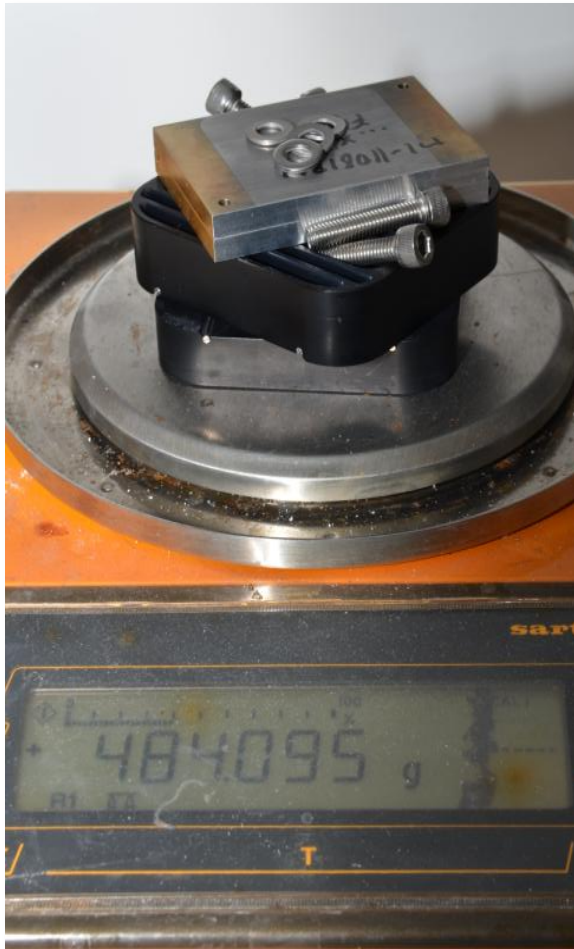
- **Weight of former assembly: ~ 484 g; anticipated weight of future devices: ~ 85 g.**

- **Occupied volume of assembly including clamp: roughly 275 cm3; new design without clamp: roughly 25 cm3.**

- **Total anticipated reduction in volume:**

- **~ 90%.**

- **Total anticipated reduction in weight:**

- **~ 82%.**

Waveguide design
Single- vs. double path
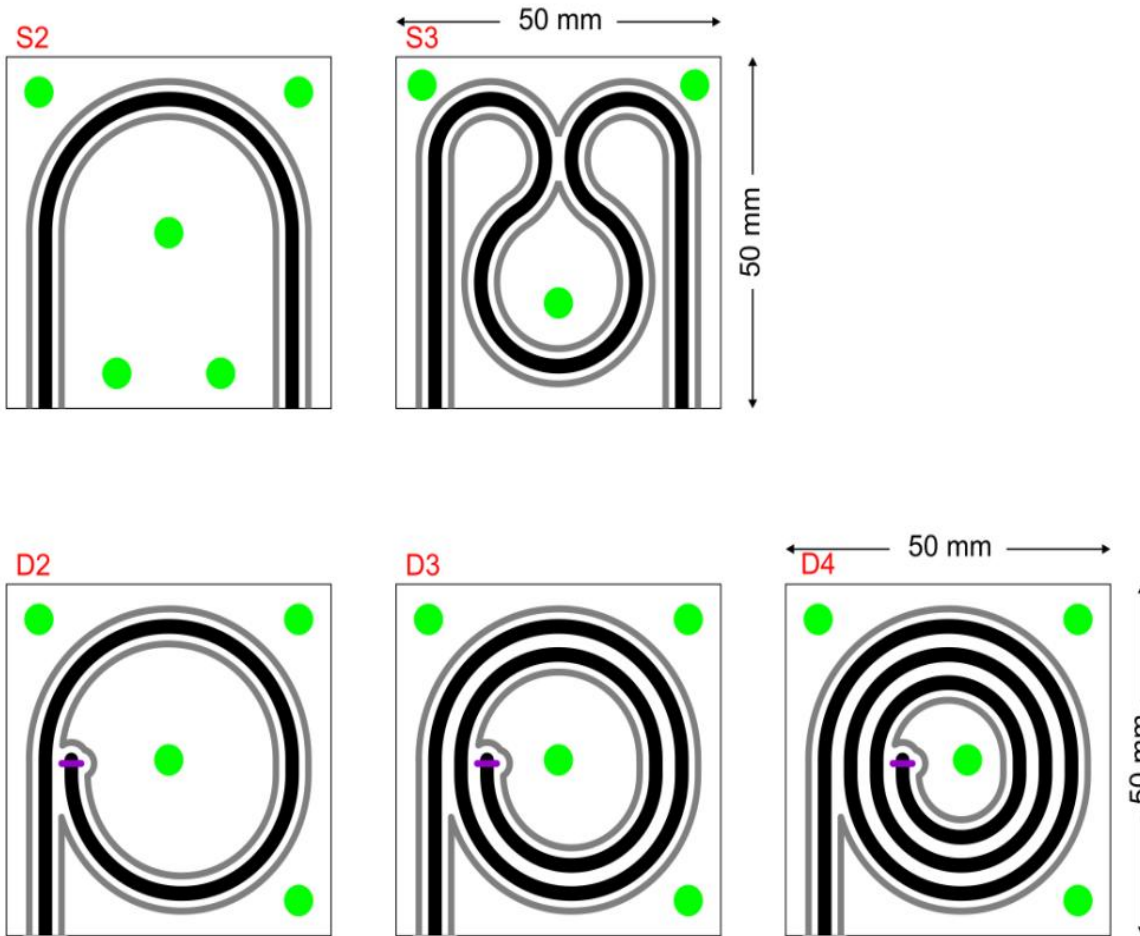
- **The planned iHWG structures that will be fabricated are shown to the left. For internal references, they are labeled S2, S3 and D2 – D4.**

- **The central path lengths are**

  S2: 109.7 mm

  S3: 204.1 mm

 **D2: 140.1 mm**

  D3: 232.0 mm

  D4: 298.9 mm

Waveguide design
Single- vs. double path
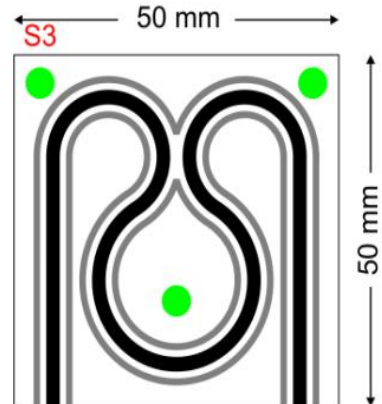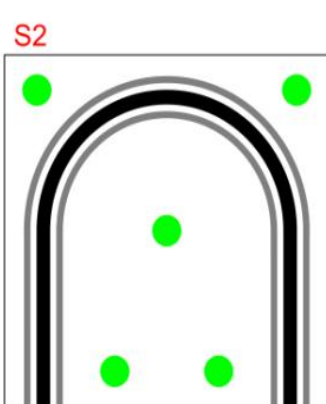
- **For the double-pass devices (D2-D4) that will require a retro-reflecting end, the effective optical path length doubles – see previous slide for single path lengths.**
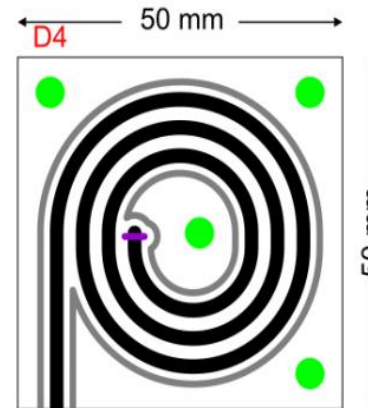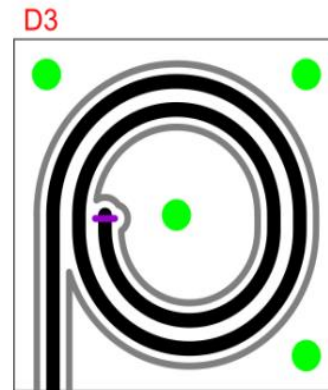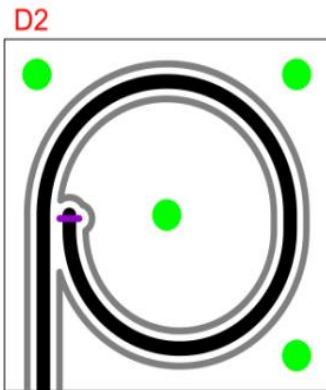
Waveguide design
Single- vs. double path
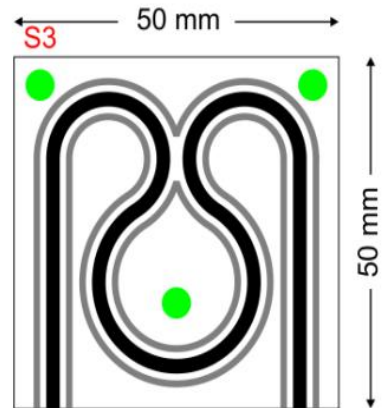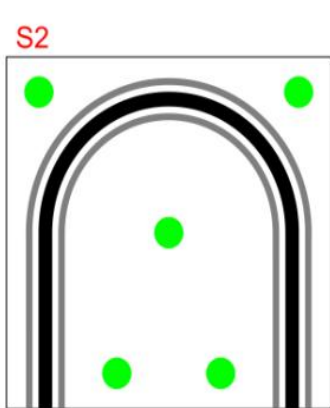
- **The (grey) channels parallel to each iHWG optical channel (black)serves as a containment berm to prevent adhesive from entering the iHWG optical channel (black).**
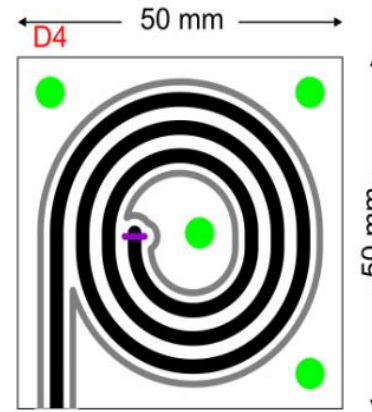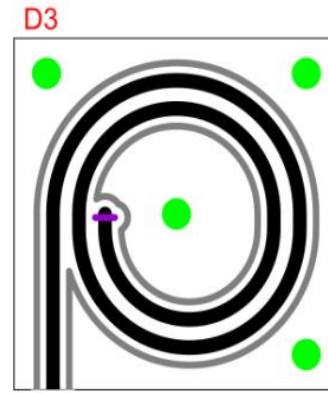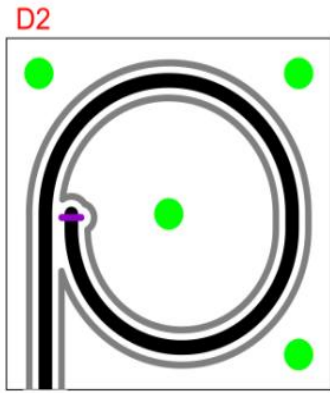
Waveguide design
Double-path designs: construction of the retroreflecting end I
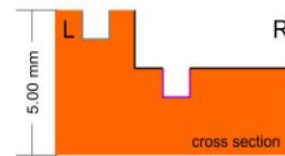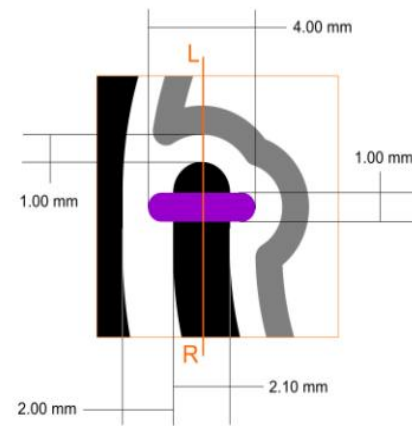
- **To the left we display a closeup view of the spiral terminal end.**

- **Since conventional (round) milling tools produced rounded ends, we plan to mill an additional relief perpendicular to the iHWG channel (purple).**

- **This relief could in consequence accommodate a mirror made from e.g., an Au coated silicon wafer slightly larger than the iHWG cross section.**

- **The mirror may be held in place by an adhesive.**

Waveguide design
Double-path designs: construction of the retroreflecting end II
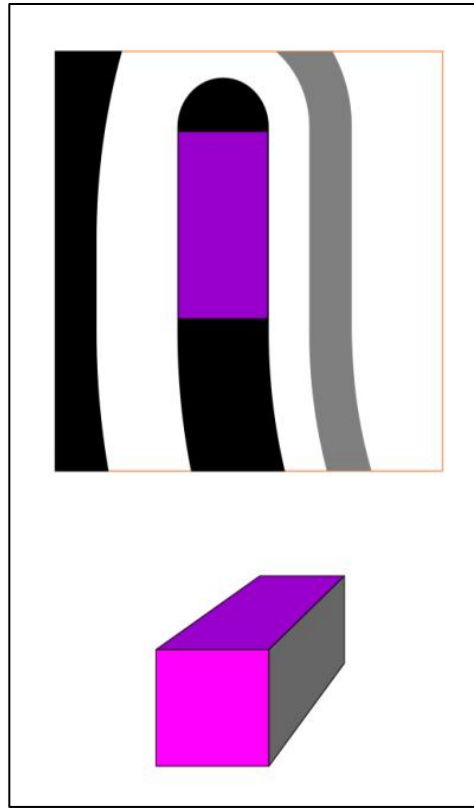
- Here, we show an alternative design for the terminal end, which is realized by inserting a block-like insert that closely matches the iHWG cross sectional dimensions into a straight part of the channel.

- The front facet of the insert (made from the same material as the waveguide) features a polished end.

- The insert could be of the same size as the iHWG (and would then have to be press-fitted into the iHWG) or slightly smaller (which would require the application of adhesive).

- Cold shrinking the parts (i.e., via cooling the insert to the temperature of liquid nitrogen) could be achieved, but requires very low manufacturing tolerances.

- Although this alternative design is very elegant, the manufacturing requirements are more demanding.

Lawrence Livermore National Laboratory

Waveguide design
Ultra-precision machining

- **All geometries shown on slide #6 are commissioned to be manufactured on state-of-the-art conventional milling machines (macrofabrication) that are anticipated to meet surface roughness specs of 100-200 nm for mid-IR gas sensing applications.**

- **A 100-200nm surface roughness would represent a 10-20 fold improvement compared to the surface roughness of devices manufactured previously at the University Ulm workshops, thereby surpassing the lambda/10 target.**

- **Funds were not sufficient to manufacture waveguide device design S2 using a diamond milling tool providing the unltimate in ultra-high precision machining. The achievable surface roughness is yet to be demonstrated for our application, however, it is thought that a 10 fold improvement over the 100-200nm surface roughness could be realized. S2 has the advantage that it can be connected to both OAPMs (this direct coupling helps characterizing the channel), two fibers (i.e., one in-coupling and one out-coupling fiber), but also to a single bundled fiber (e.g., a 7-around-1 configuration) by simply adding a planar mirror to one channel port.**

Lawrence Livermore National Laboratory

Considerations on single- vs. double-pass
Double-pass

- **Double-pass configurations (#D2-D4) allow for significantly increased optical path lengths (OPLs) on the same footprint.**

- **Moreover, throughput & absorption data collected on double-pass configurations might yield more useful insight into the effects of device scaling. This is because of the similarity of the geometries (i.e., 1 turn, 2 turns, 3 turns, with only slight changes in curvature), whereas an increase in OPL for single-path geometries requires entirely different geometries (S2 vs. S3). Scaling studies are necessary for determining the optimum optical pathlength(OPL), i.e., the geometry with the best SNR.**

- **Similarly, single-pass OPLs are only achievable at the cost of much smaller bending radii. Small radii on the other hand are known to increase the numerical aperture of the transmitted radiation to a greater extent than larger curvatures do. This consideration is important if fibers shall be used for radiation outcoupling, as the numerical aperture for any fiber is limited (e.g., for a silver halide fiber NA=0.3, corresponding to an acceptance angle of q=17.5°). Consequently, a significant decrease in outcoupling efficiency is expected for small curvatures.**

Lawrence Livermore National Laboratory

Considerations on single- vs. double-pass
Single-pass

- **Single-pass geometries on the other hand have the following advantages:**

  - **Any channel characterization requires constant (carefully controlled) coupling conditions. With double-pass geometries, however, only total throughput losses are measurable. It is impossible to decide which fraction of the measured losses is due to A) the fiber itself, B) the iHWG structure or C) misalignment. On the other hand, single-pass geometries allow for in- and outcoupling using OAPMs, thus ensuring easily achieveable constant coupling conditions.**

  - **Design S2 and S3 can be easily converted into a double-pass configuration by attaching a planar mirror to one of the end facets.**

Considerations on single- vs. double-pass
Conclusion

- **In the mid and long-term, double-pass geometries are favored. However, the acquisition of some of the data needed for building a sound simulation model also requires the investigation of single-pass geometries (i.e, thus the inclusion of S2 and S3 designs).**

- **Double-pass geometries are only advantageous when combined with bundled fiber probes (also favored, because only one connection is needed).**
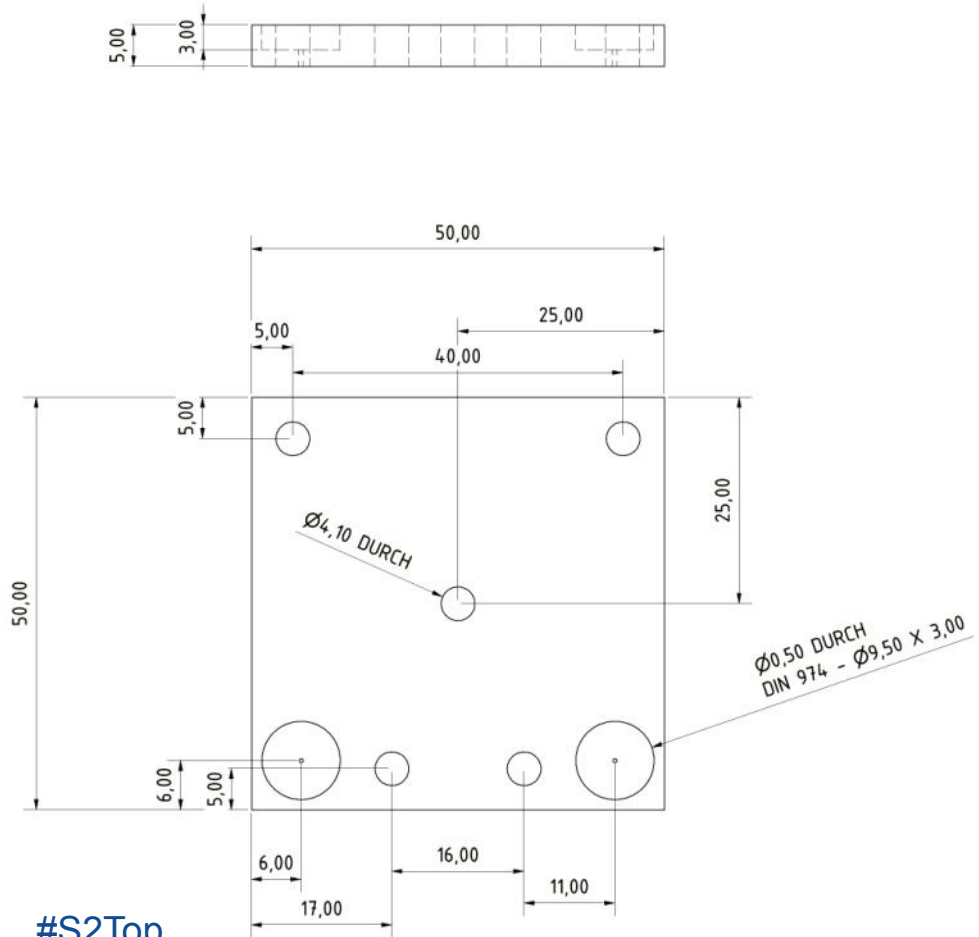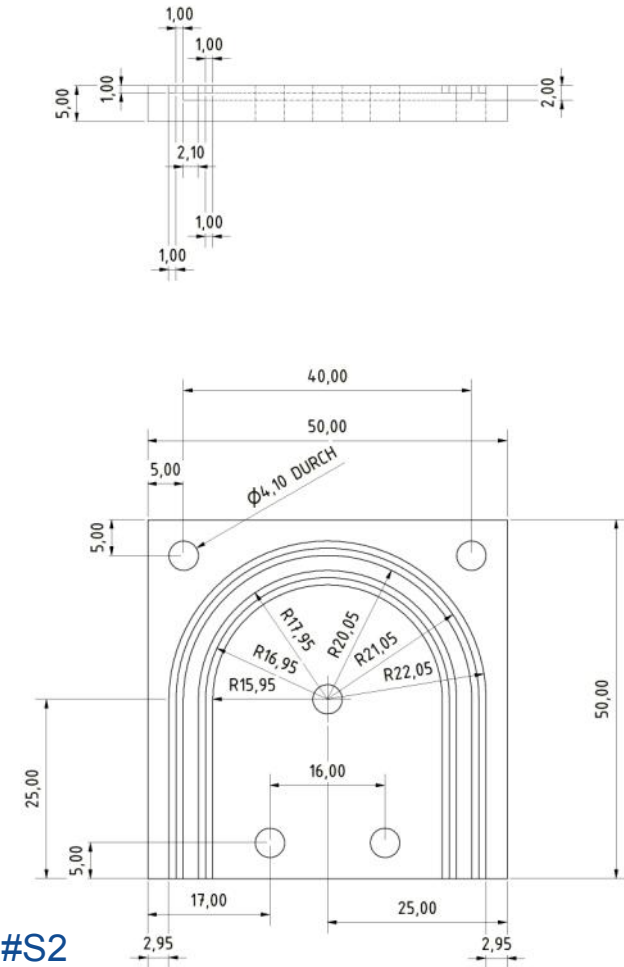
Lawrence Livermore National Laboratory

Waveguide design
Engineering drawings contd. I

#S2

#S2Top

Waveguide design
Engineering drawings contd. II

#S3

#S3Top
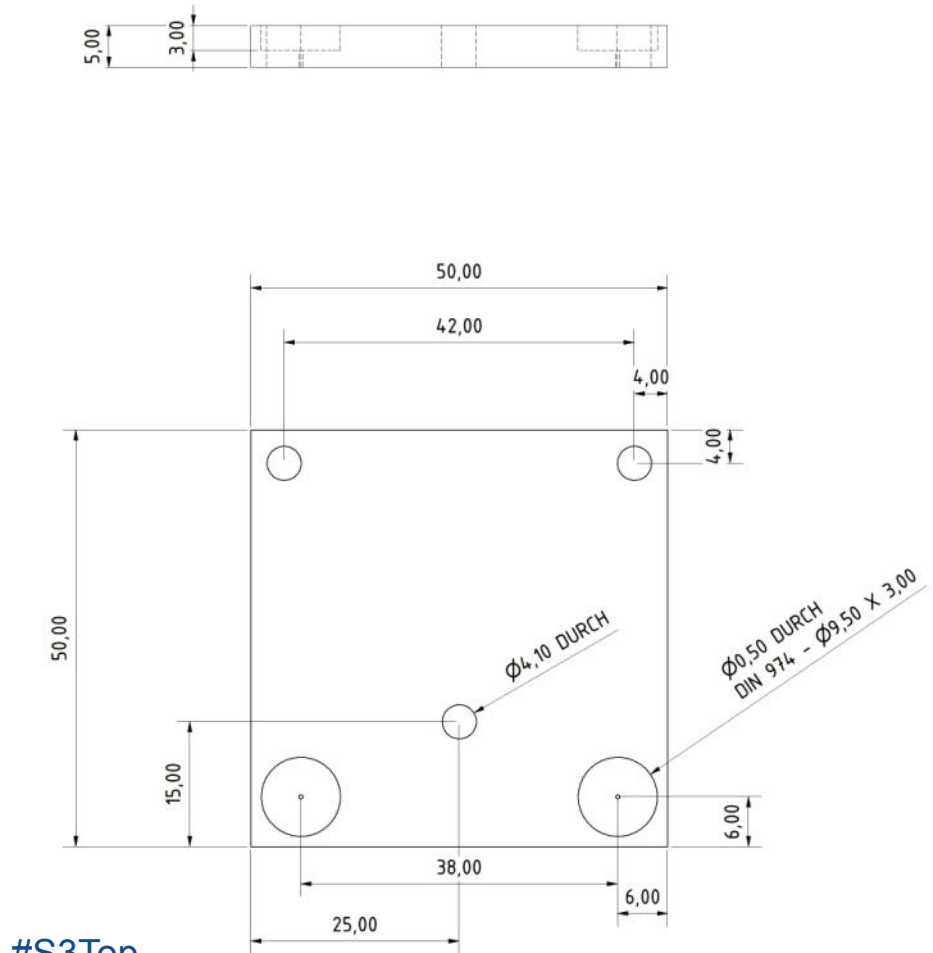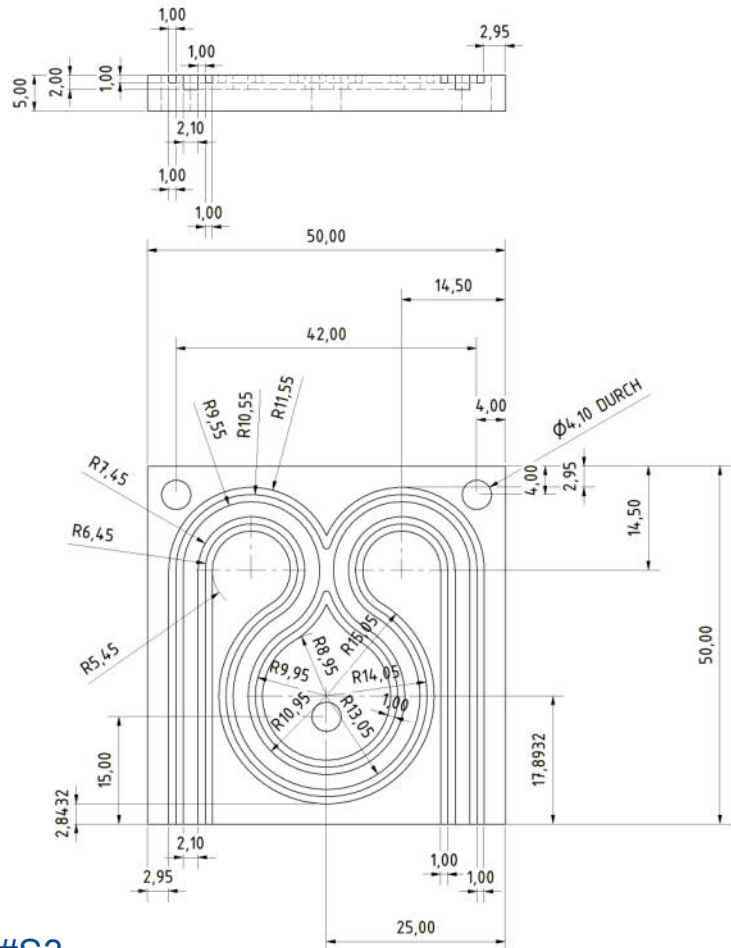
# Waveguide design
*Engineering drawings contd. III*

#D1
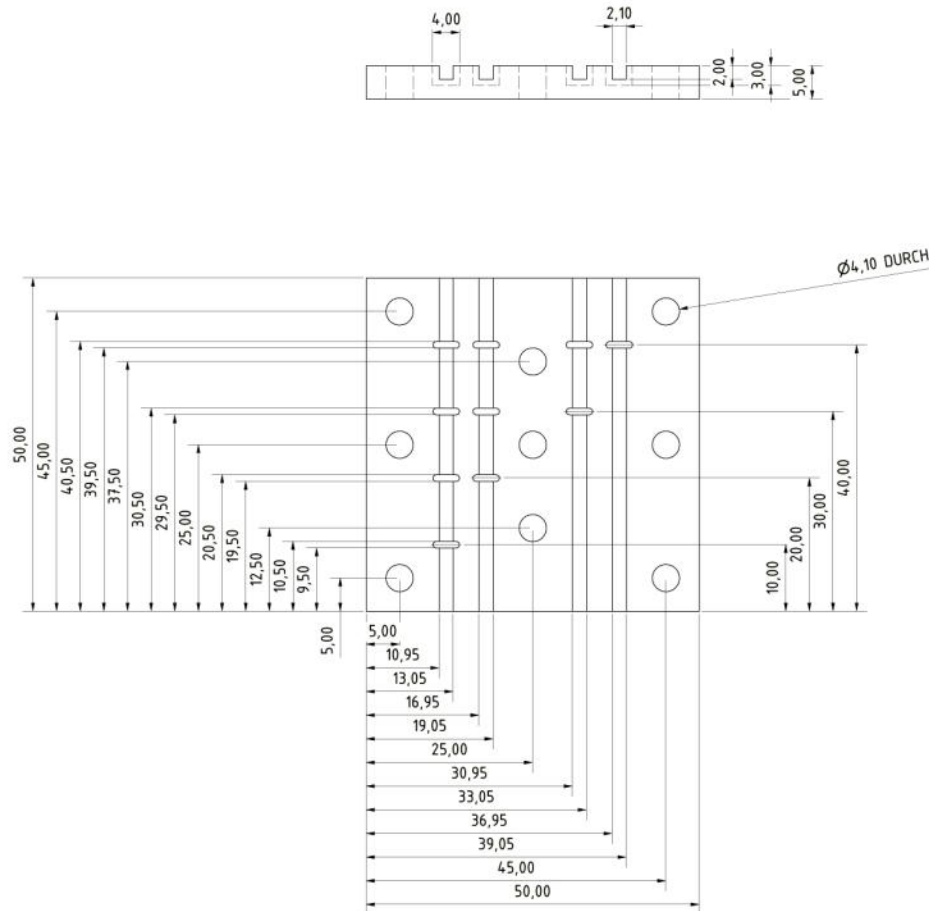
- **All engineering drawings are now finalized and forwarded to the Univ. Ulm workshop for fabrication.**

- **Shown here: orthographic projections from the top & front.**

- **D1 will be used to practice the pasting of small Au-coated silicon plates (max. size 3x3 mm) into the channels of devices D2-D4, thereby generating the retroreflecting end of the iHWG.**

Waveguide design
*Engineering drawings contd. IV*
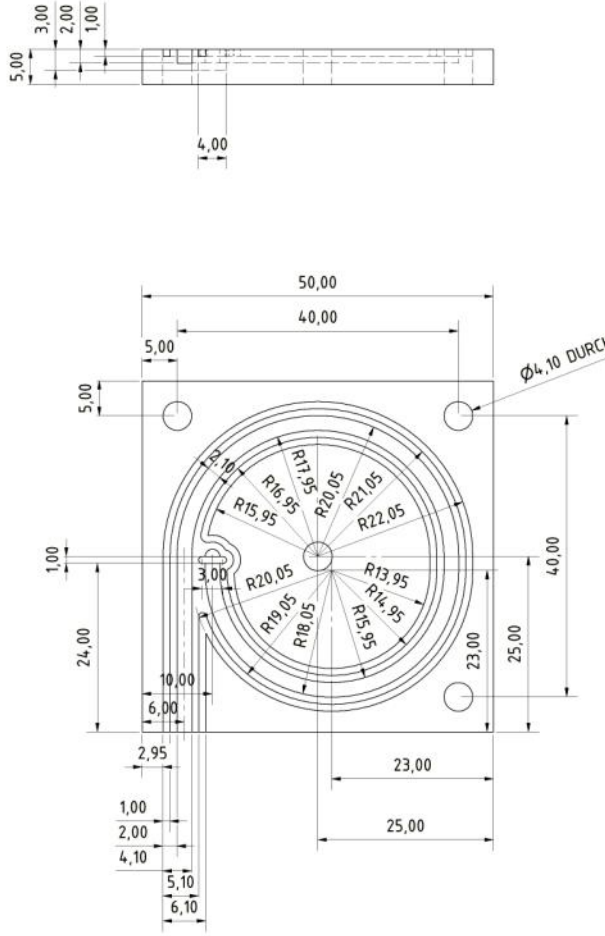
#D2
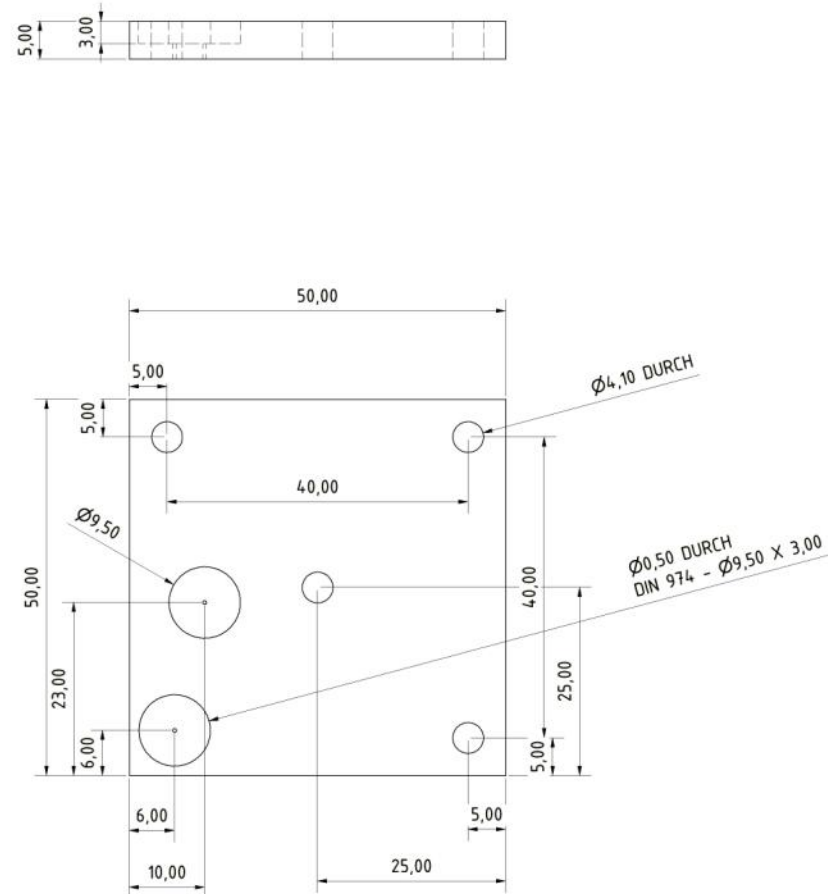
#D2Top

Waveguide design
Engineering drawings contd. V
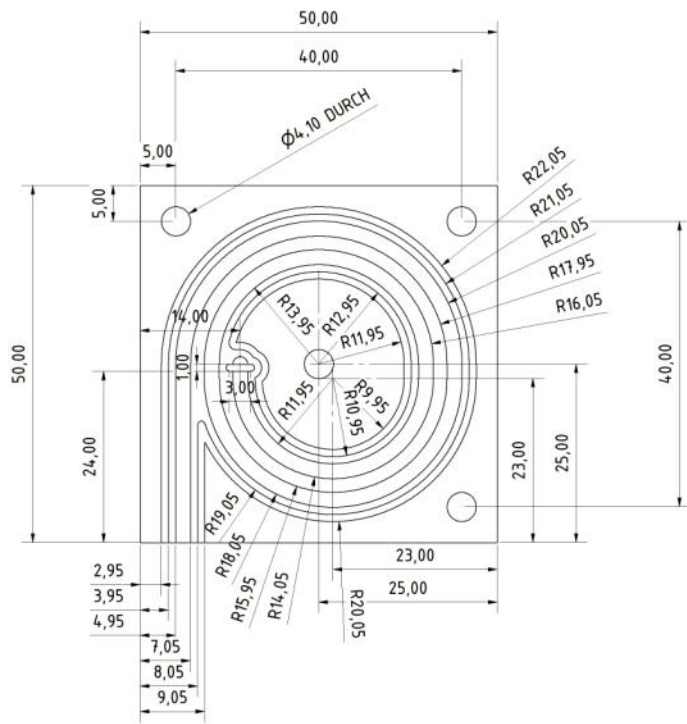
#D3
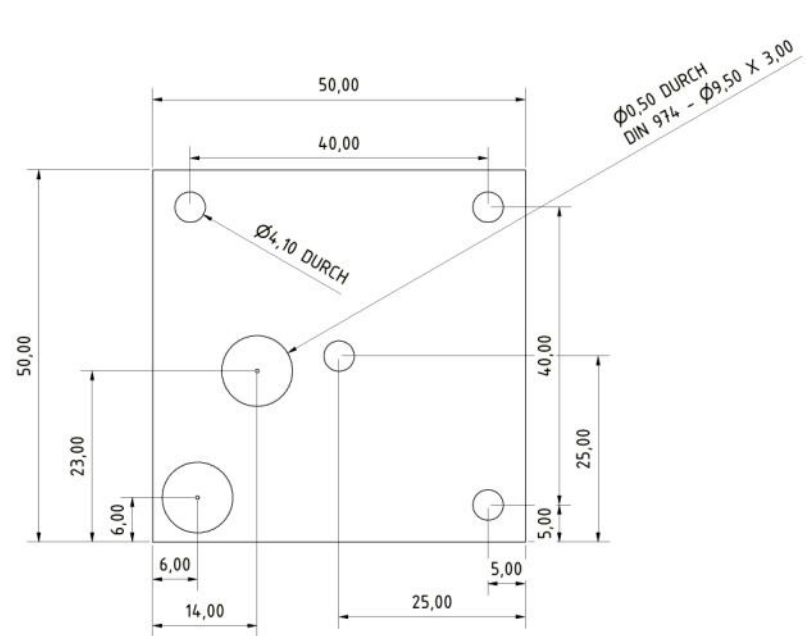
#D3Top

Waveguide design
Engineering drawings contd. VI
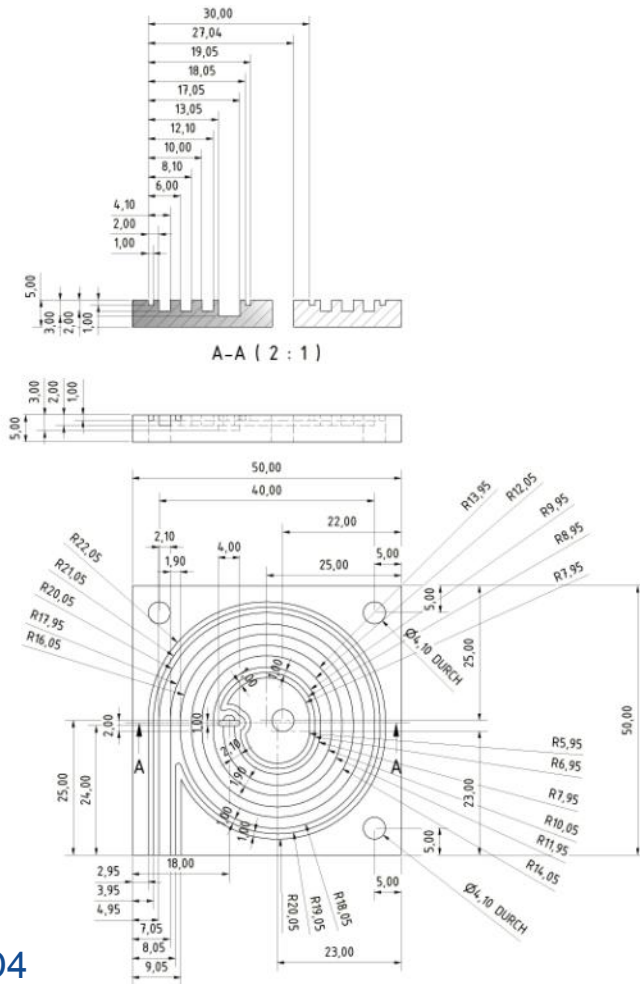
#D4
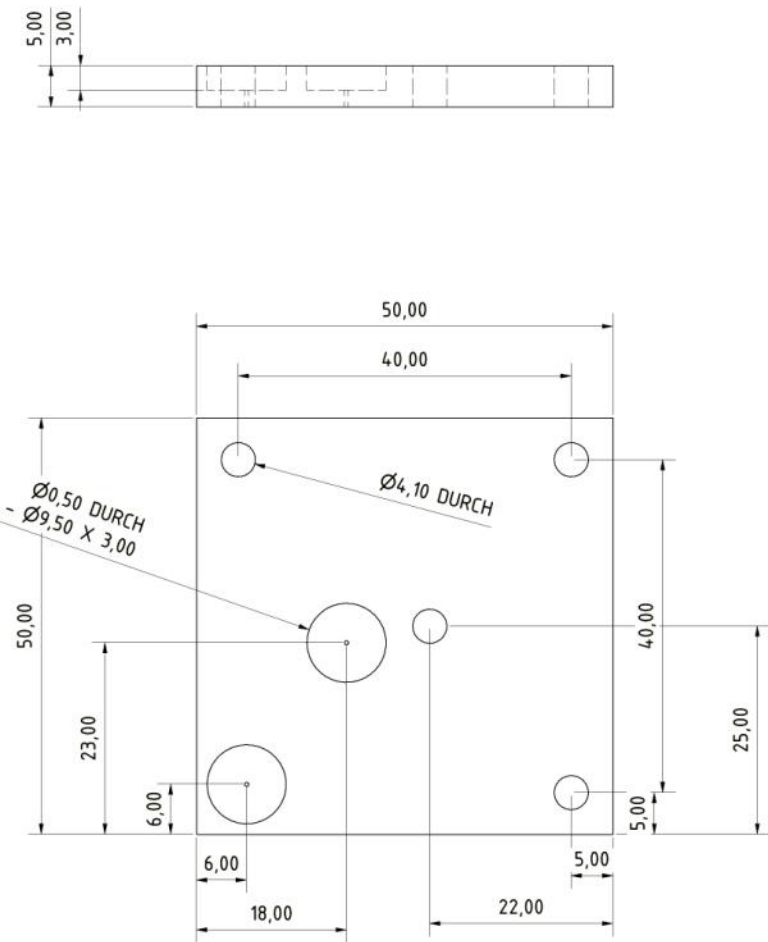
#D4Top

Waveguide simulation
3D objects
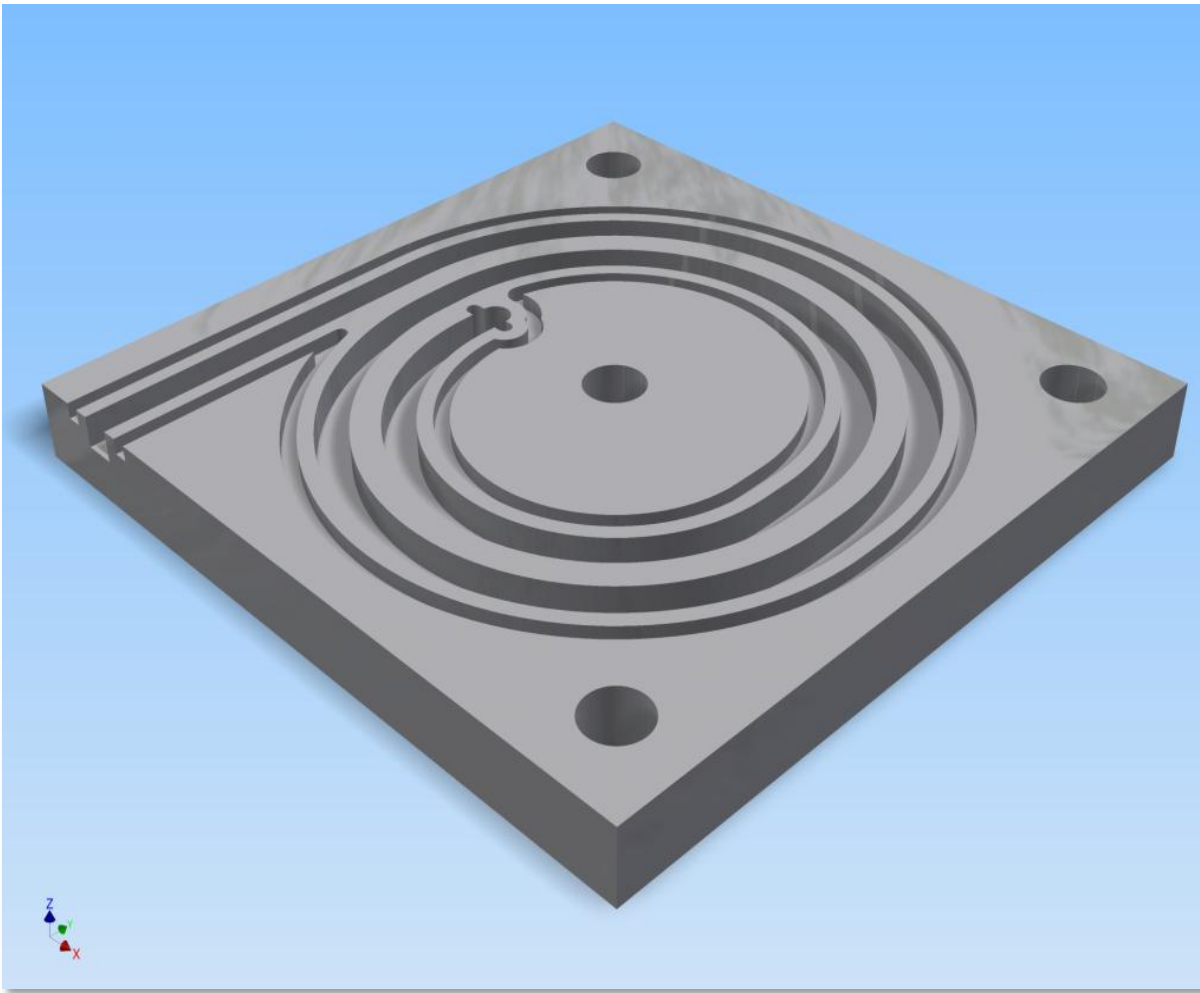
- **All possible waveguides have been drawn in 3D (Autodesk Inventor).**

- **These object designs could be used for possible future 3D ray tracing simulations.**

- **Exemplarily shown here: 3D rendering of device D3.**

Lawrence Livermore National Laboratory

Adhesive suitability experiments
Polished test samples

- **Fabrication of 10 mirror-like polished test samples (30x25mm) was completed.**

- **The samples will be used for absolute and angular reflectance measurements as well as adhesive characterization experiments.**

Waveguide design
Single- vs. double path

- **7 waveguide devices fabricated by the Fraunhofer IOF using macrofabrication technology. These represent our best devices to date in that the surface roughness is within our specifications of 100-200nm (rms) for IR gas sensing applications.**

Waveguide design
Single- vs. double path

- **Waveguide devices were also fabricated by the Uni Ulm workshop using macrofabrication technologies. The surface roughness of these devices in on the order of micron-sized features.**

Waveguide design
Single- vs. double path
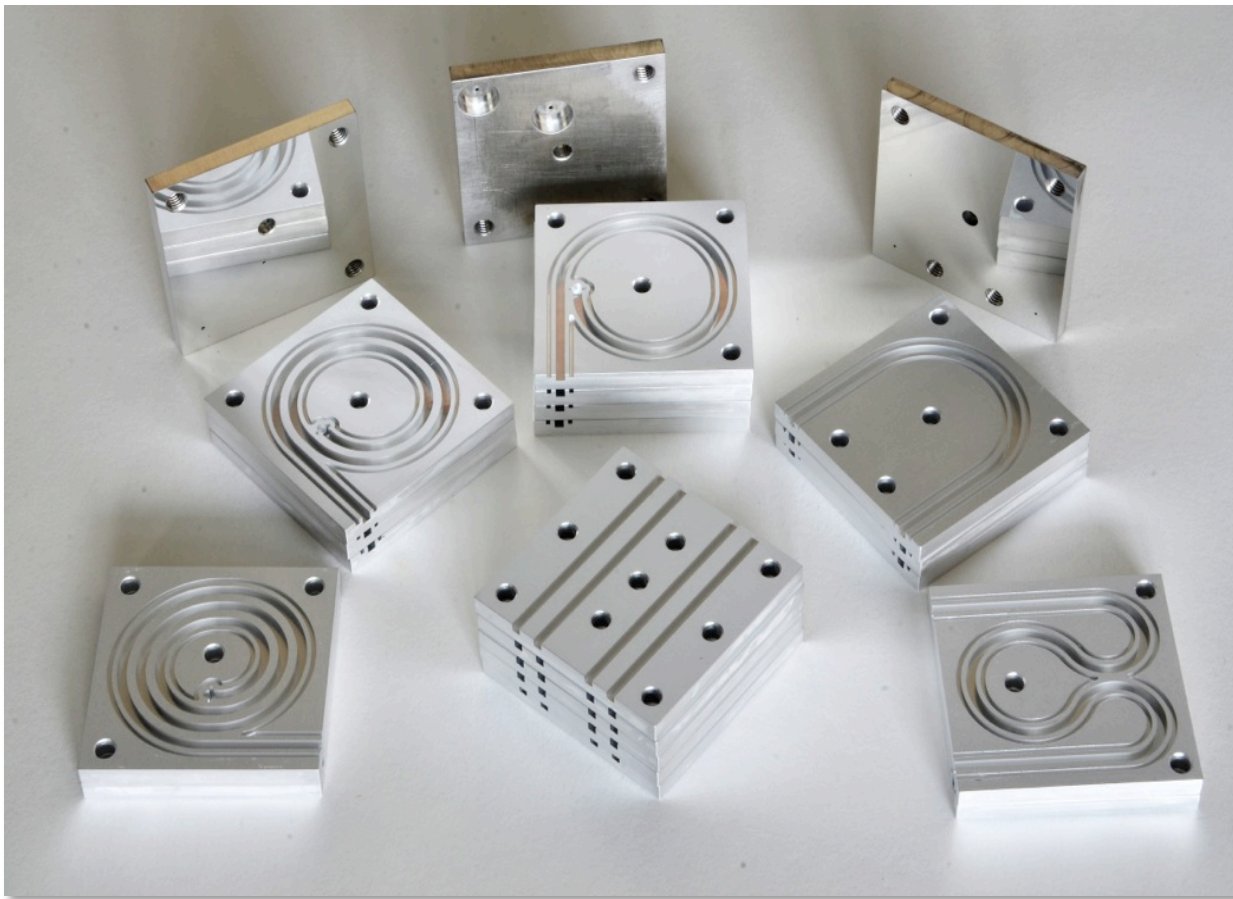
- **Waveguide devices with 3 top plates (the center plate features the unpolished backside showing two counterbored regions for gas line connections) are shown.**

Waveguide design
Single- vs. double path
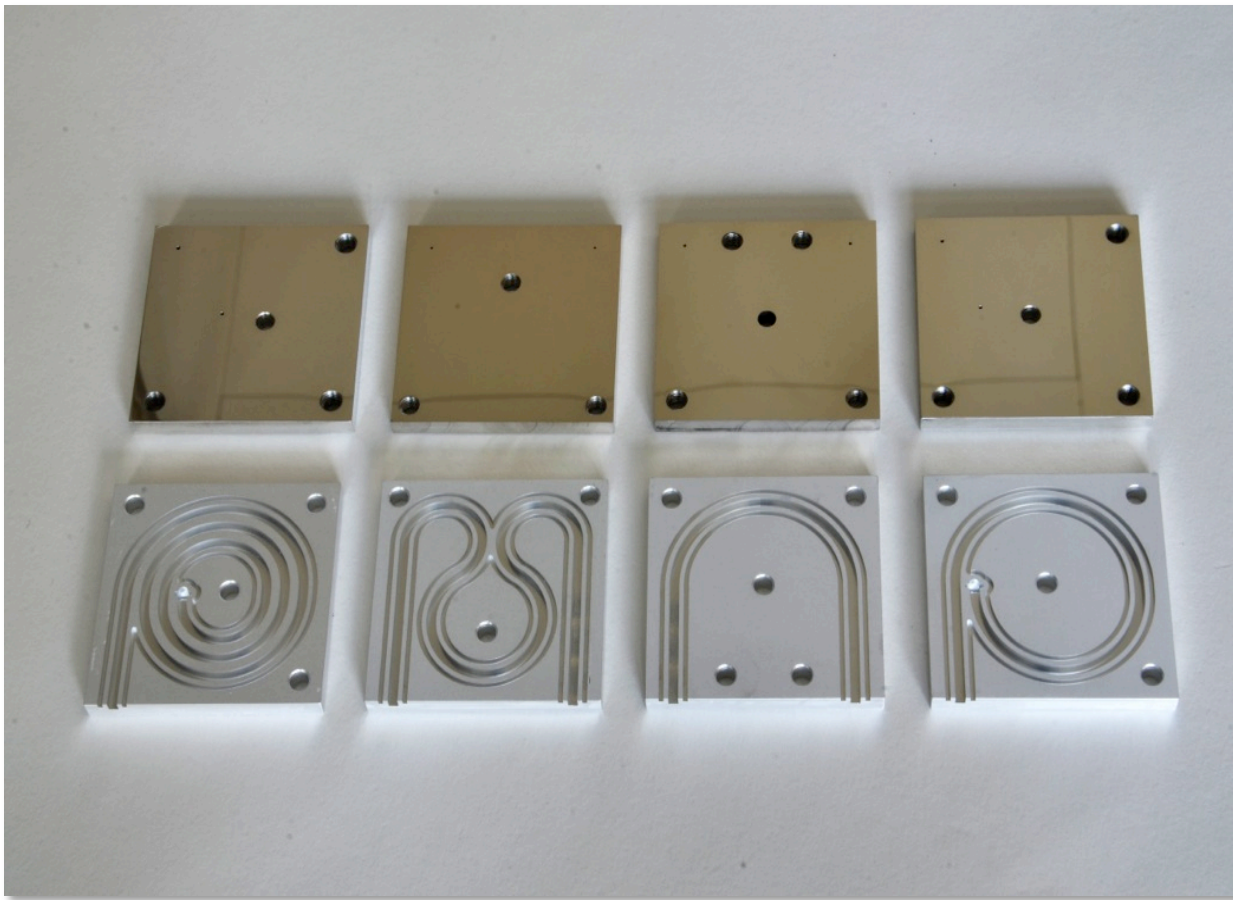
- **This image shows 4 different waveguide geometries alongside the matching top plate.**

- **Note the port locations for gas-in and gas-out connections are different for each waveguide design.**

**Lawrence Livermore National Laboratory**

Waveguide design
Single- vs. double path
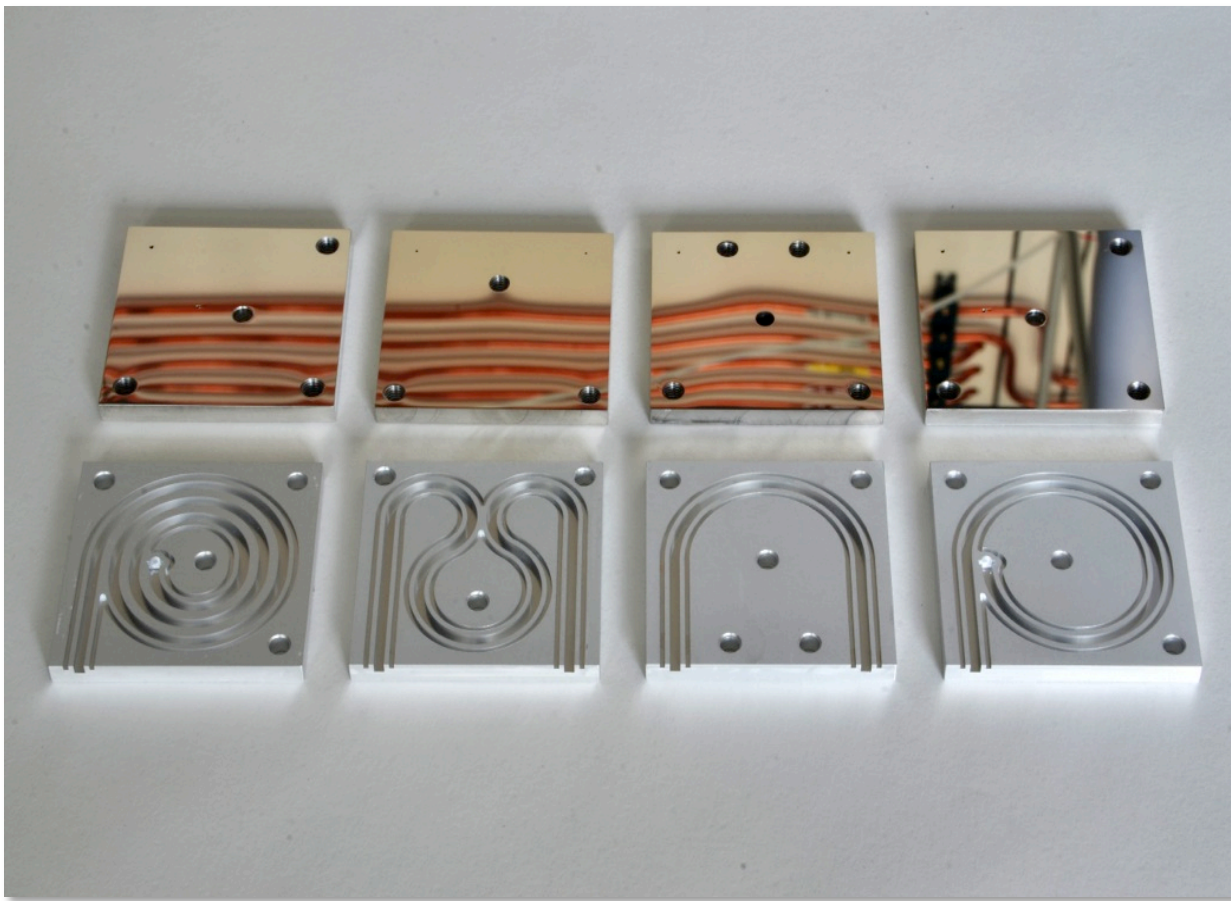
- **Same picture, except that here one can see the reflections of the copper gas supply lines to emphasize the mirror-like surface finish.**

Appendix B

Channel length calculation for the 8(° geometry
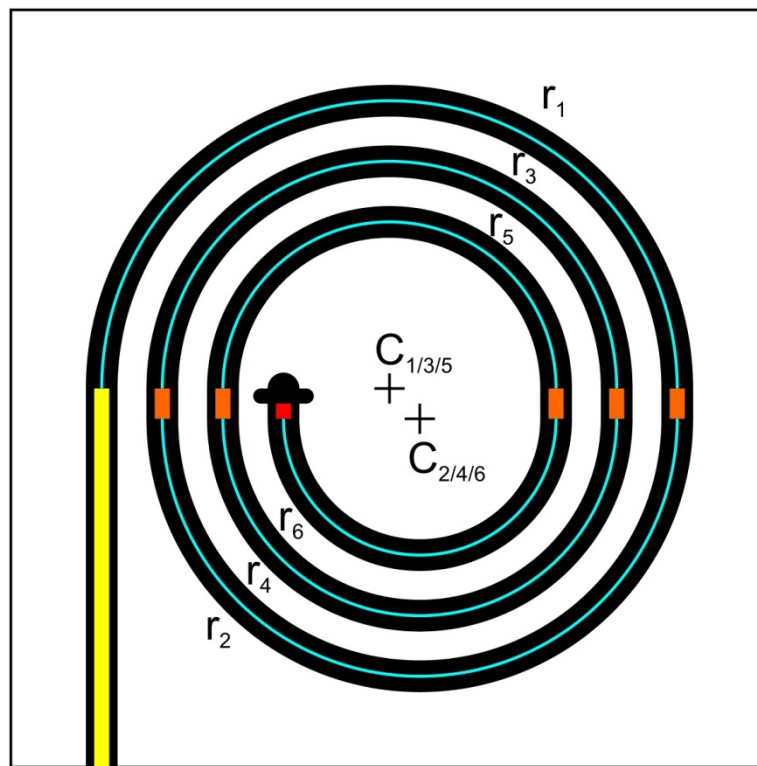
Explanation: ":=" means "per definition", i.e., the parameter used for the geometry D4

Substrate size =: 50 x 50 mm

Basic geometry := combination of half circles and straight sections

Individual length of straight sections:
Yellow:=   25.00 mm
Orange:=   2.00 mm
Red:=   1.00 mm

Radii of (half) circles:
r_1:=   19.00 mm
r_2:=   17.00 mm
r_3:=   15.00 mm
r_4:=   13.00 mm
r_5:=   11.00 mm
r_6:=   9.00 mm

➔ Arc lengths:

L_1:	$r_1\pi$ = 59.69 mm
L_2:	$r_2\pi$ = 53.41 mm
L_3:	$r_3\pi$ = 47.12 mm
L_4:	$r_4\pi$ = 40.84 mm
L_5:	$r_5\pi$ = 34.56 mm
L_6:	$r_6\pi$ = 28.27 mm

➔ The total geometrical path length (GPL) of the channel is

GPL(D4) = Yellow + 5Orange + Red + $L_1 + L_2 + L_3 + L_4 + L_5 + L_6$ = 299.89 mm.

➔ Accordingly, the GPLs of D3 and D2 are

GPL(D3) = Yellow + 3Orange + Red + $L_1 + L_2 + L_3 + L_4$ = 233.06 mm.

GPL(D2) = Yellow + Orange + Red + $L_1 + L_2$ = 141.10 mm.

➔ **As any ray will travel this distance both forwards & backwards, the optical path length approximately doubles:**

OPL(D4) $\cong$ 2*GPL(D4) = 599.79 mm.

OPL(D3) $\cong$ 2*GPL(D3) = 466.12 mm.

OPL(D2) $\cong$ 2*GPL(D2) = 282.19 mm.

Note that this value is NOT the OPL for the center ray, because the center ray will not smoothly follow the geometry, but will travel in a straight line, experiencing reflections at the side walls with $\theta_{in} = \theta_{out}$. It would be quite complicated to calculate the individual lengths of all those (straight) sections… I'd like to argue that in this case it should be sufficient to mention only the geometrical length of the channel.

Kern Evo Ultra Precision CNC Machine

Appendix C

High productivity with
ultra precision machining
±0.5 µm

KERN

Micro- und Feinwerktechnik

KERN Evo

Ultra Precision
## CNC Machining Centre
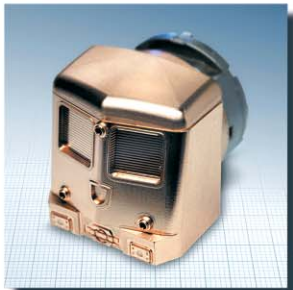
KERN Evo
Evolution
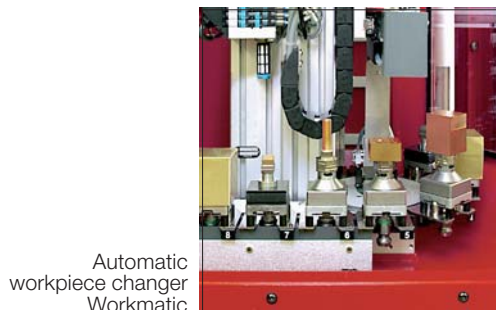
Specific machine characteristics:

The digital direct feed drives fitted to the KERN Evo ultra precision machining centre provide fast acceleration and feed rates. These forces are absorbed by the polymer concrete monobloc machine frame.

The KERN Evo is specially designed for applications requiring the following features:

- **Highest precision on the workpiece (deviation of position P_a ±0.5 µm according to VDI/DGQ 3441)**
- **Excellent surface quality Ra ≤ 0.1 µm**
- **Milling of critically machinable materials and hardened steel**
- **High productivity**
- **High acceleration rates**
- **High feed rates**
- **Automatic workpiece loading for batch production (available for 3 and 5 axes machining)**

Automatic workpiece changer Workmatic

Vector-controlled spindle HSK 25

Automatic tool changer HSK 25

Infrared touch probe for measuring of workpiece

Laser measuring system for tools

Interface for 4th/5th axis with digital drives

1957 mm

2189 mm
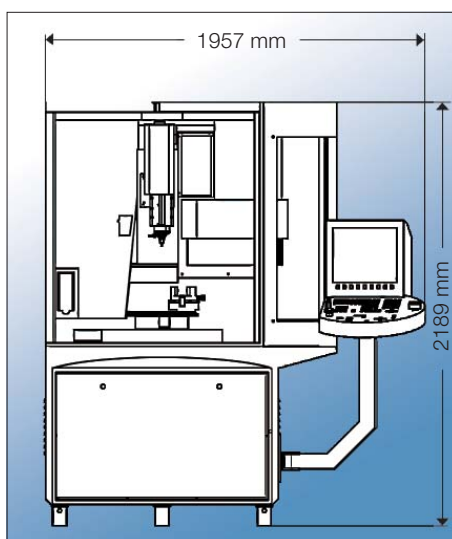
The KERN Evo ultra precision machining centre can be fitted with a wide range of accessories and options, e.g.:

- Powerful vector-controlled spindle (other spindle types available)
- Digital CNC precision dividing head (4th/5th axis)
- Automatic tool changer (ATC) with 32, 63 or 95 positions
- Automatic workpiece changer, integrated with 24 positions (picture), alternatively with 36, 60 and more positions (preparation for retrofitting at a later stage possible)
- Automatic measuring of the workpiece by a touch probe with data transfer by infrared beam (only for vector-controlled or oriented spindles)
- Automatic tool length and tool radius measurement with a laser measuring system

2

KERN Evo
Technical machine description

The engineering philosophy of KERN Micro- und Feinwerktechnik GmbH und Co. KG consists in obtaining the maximum machining accuracy. Hence all major machine components vital to reaching the highest precision are manufactured in house with the same precision principles linking the development, design and manufacture of our products.

Axis system (X, Y, Z)

The complex design principle of the axis system is fundamental to the high overall accuracy of KERN machines. High precision roller seated and backlash-free pre-stressed prismatic linear guides ensure constant positioning accuracies on a permanent basis. New digital direct drives optimise contour tracing on dynamic machining and permit high acceleration and high feed rates. Only specially selected precision machined ball screw spindles are used for integration into the axis centre next to the incremental Heidenhain glass scales (resolution 0.1 μm). Thanks to the central alignment of the major drive and command elements, jamming of the axes is avoided. All the slideways and ball screw spindles are permanently lubricated and are therefore maintenance-free.
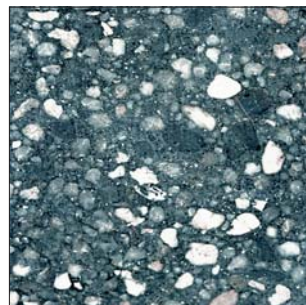
Machine design

The machine body of the KERN Evo is specially designed to take full advantage of the characteristics offered by the high tech material KERN polymer concrete:

- Maximum rigidity – static and dynamic
- Vibration absorption up to 10 times better than GG20
- Low sensitivity to temperature fluctuations

KERN Polymer Concrete

Spindles

KERN co-operates exclusively with proven spindle manufacturers sharing the same precision philosophy. High speed spindles are necessary to cater for the wide spectrum of application needs of our customers. Moreover, KERN machines can be fitted with several different spindles, these can be easily and quickly exchanged by the user.

Please do not hesitate to contact us for further information.

Ultra precision machining in hardened steel 47 HRC

Handwheel

Contouring Control

KERN machining centres are equipped with the latest Heidenhain contouring control systems. Even in their standard version, our Heidenhain controls are fitted with all the major functions required by a workshop. All Heidenhain contouring controls offer up to 5-axes interpolation, functions like rigid tapping, various milling and drilling cycles, parametric and subprogramming, teach-in programming, graphic display and simulation, tool management, tool radius correction for 5-axes simultaneous operation and DNC operation... but often with other manufacturers these features have to be ordered separately at additional cost.

Maintenance

The KERN machines are in general maintenance-free. They simply require regular thorough cleaning as well as high-level professionalism in their operation. Machine operators will be instructed in the technical details of their KERN machine during commissioning.

Environmental conditions

To obtain the best machining results, it is necessary to pay due care and attention to the working environment and avoid fluctuations in temperature.

5

KERN Evo
Options and accessories

Achieving the optimal results in machining operations depends on a variety of factors. One of these factors is the use of original KERN accessories.

Spindles

500 – 50,000 rpm	permanently grease lubricated, vector-controlled		0.8 Nm	3.4	kW
500 – 50,000 rpm	permanently grease lubricated, vector-controlled		1.5 Nm	6.4	kW
20,000 – 80,000 rpm	permanently grease lubricated			1.0	kW
30,000 – 90,000 rpm	permanently grease lubricated			0.17	kW
60,000 –160,000 rpm	oil-air lubricated			0.5	kW

Further spindle alternatives on request.

Tool changer
Standard 32 tools, optionally 63 or 95 tools
Tool changing time about 3 s
Average chip-to-chip time about 5 s
(depending on spindle configuration)
Tool length max. 105 mm
Tool diameter max. 50 mm
Tool shank diameter max. 10 mm

Digital CNC precision dividing head (4th/5th axis)
Rotational and swivelling axis, 2 axes or 1 axis system
Brushless servo motors, digital drive system
Diverse interfaces: collet chuck (max. chucking capacity Ø 26 mm, max. passage Ø 14 mm), System 3R or Erowa
Feed rate C/B 7000 / 3000 °/min
Max. swivelling range from -10° to +100°
Height of centres 100 mm
Positioning scatter $P_S \le 1"$, precision on the workpiece $\le 5"$
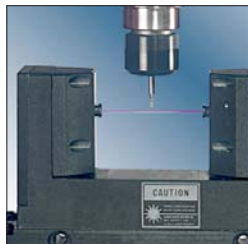
Tool length measuring: Laser
A laser beam with a diameter of 30 µm permits non-contact measuring of the smallest tool according to length, radius and concentric accuracy even at high spindle speeds. The measured data are transferred automatically into the Heidenhain contouring control and are taken into consideration in the active programme. In case of deviations from individually defined tolerances, for example automatic change of a sister-tool will take place (programmable).

Touch probe system with wireless infrared transmission

for measuring of the workpiece to be machined. An infrared touch probe which can be transferred automatically from the tool magazine to the spindle and measures the height and position of the workpiece. Can only be used in combination with vector-controlled or oriented spindle.

Vice with gripping jaws
for clamping of tools/collets in a collet chuck

Optical measuring device
Centring and controlling microscope with HSK interface
Magnification 30-times, alternatively 50- or 100-times

not illustrated:
Coolant device with temperature control
Oil mist lubrication / cooling unit
Special coolant system for temperature control of workpiece
Special coolant system for temperature control of spindle
Inductive shrink unit for
Shrink tool holder HSK 25 (KERN Special)
Tool holder HSK 25 (KERN Special)
EX 16 high precision collet chuck
ESX 16 precision collet chuck
D 14 high precision collet chuck
**Precision vice for workpieces**
etc.

3

Fully automatic
Machining Centres

KERN Micro- und Feinwerktechnik GmbH & Co. KG is a pioneer in the development of fully automatic workpiece loading systems for batch machining of high precision workpieces. The micro milling machine shop of KERN's subcontracting division has for some years used unmanned production systems for high precision parts.

Automatic workpiece pallet changing systems are available from different suppliers with a variety of pallets sizes, each being able to be integrated.

KERN HSPC with System 3R WorkPal

Automatic individual palletising for up to 32 different pallets for 3 to 5 axes machining. Workpieces are mounted onto System 3R Macro or Magnum holders.

KERN HSPC with Erowa

Automatic pallet changing for up to 90 different pallets for 3 to 5 axes machining. Workpieces are mounted onto Erowa ITS holders.

KERN Evo with integrated System 3R Workmatic

Automatic pallet changing for up to 36 different pallets for 3 to 5 axes machining. Workpieces are mounted onto System 3R Macro holders.

Maximum workpiece size: 70x70x100 mm

IMPORTANT space saving solution!

Additional integration of workpiece identification chips permits optimal control of the loading and machining process with maximum logistical flexibility using a cell computer.

Technical Data
KERN Evo

Axes:

Travel X/Y/Z	300/280/250 mm (11.81/11.02/9.84")
Clamping area max.	350 x 230 mm (13.78 x 9.06")
Drives	digital (AC Servo)
Workpiece weight max.	
(3-axis)	50 kg
Feed rate	0.01-16,000 mm/min (0.00039-629.92 "/min)
Acceleration	8 m/s² (314.96 "/s²)

Precision according to VDI/DGQ 3441:

Resolution	0.1 µm (0.0000039")
Positioning scatter P_S	±0.5 µm (0.0000196")
Positioning tolerance P	±1.0 µm (0.0000393")
Precision on the workpiece (3-axis)	±2.0 µm (0.0000787")

Choice of spindles:

	up to 50,000; 80,000; 90,000;160,000 rpm etc.
Taper	HSK 25 (using spindles up to 50,000 rpm max.)
Tool changer capacity	32 tools, optionally 63 or 95 tools
Tool diameter max.	50 mm
Tool changing time	approx. 3 s
Chip to chip	approx. 5 s

4th / 5th axis:

Rotational	360° continuous
Swivelling	-10° up to +100°
Precision	≤5"
Feed rate	C/B 7000 / 3000 °/min

Automation:

Automatic workpiece changing system	24, 36, 60 and more positions

Kern Evo:

Space requirements min.	2.80 x 2.50 x 2.20 m (110.24 x 98.43 x 86.61")
Weight	approx. 3,000 kg
Controller	Heidenhain

Subject to technical changes

Machine design with polymer concrete
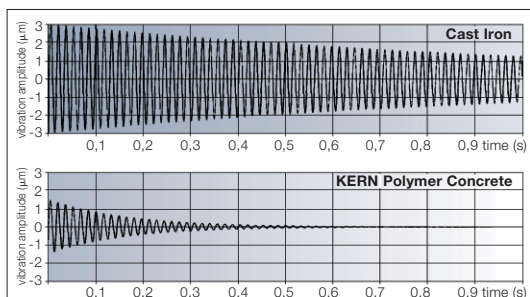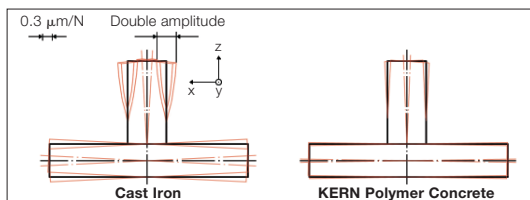
Maximum rigidity – static and dynamic
Cross-sections with exceptionally big dimensions are used on the KERN machines, thanks to the 1.8 tonnes polymer concrete construction on a 2.5 m² footprint. The static and dynamic rigidity inherent in our polymer concrete machine frame is much higher than the limits of a cast iron structure.

Vibration absorption 10 times better
The vibration dampening characteristics of the monobloc frame are of paramount importance to balance the high dynamic forces exerted by our digital direct feed drives. Polymer concrete monobloc absorbs up to 10 times more vibrations than cast iron, resulting in longer tool life of up to 30 % and superior surface quality with Ra ≤ 0.1 µm.

Low sensitivity to temperature fluctuations
The polymer concrete monobloc frame of KERN machines is known to have a 50 % lower heat conductibility than that of a steel or cast iron design. Polymer concrete does not react to short temperature fluctuations. The very low thermal conductivity minimises any deformation due to temperature variations. This in turn increases the workpiece accuracy.

01/2008e

Atomic Force Microscopy
Images of Test Samples

Appendix D

# Atomic Force Microscopy of test samples
Surface roughness
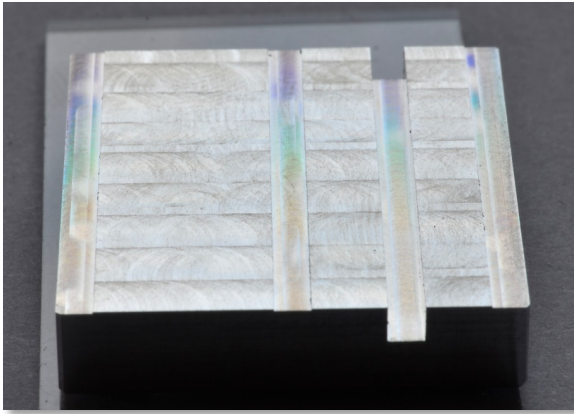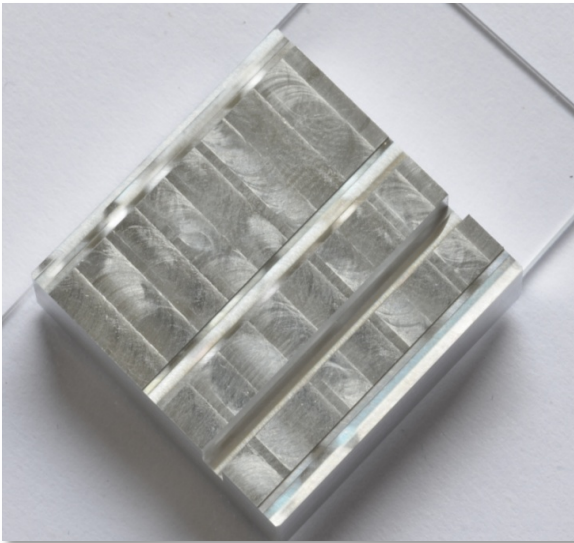
- **We received a 2x2 cm test sample of a straight iHWG fabricated by an external company (bottom left picture). The channels were are also made using conventional machining (hence the iHWGs from our own workshops are alike), but on a state-of-the-art milling machine** (KERN Evo Ultra Precision CNC Machining Center, KERN Micro- und Feinwerktechnik GmbH & Co. KG, Eschenlohe, Germany; PDF attached to this report) and a solid carbide end mill (HAM 430, Hartmetall-Werkzeugfabrik Andreas Maier GmbH, Schwendi-Hörenhausen, Germany; PDF attached, page #7)**.**

- **If the channels are viewed in the correct angle, diffraction creates rainbow colors (iridescence) due to the periodically structured surface (i.e., the grooves act as a diffraction grating; top right picture). This phenomenon already indicates that the size of the surface structures are in the same dimension as the wavelength of visible light.**

Lawrence Livermore National Laboratory

Fabrication progress
## *High precision milling*
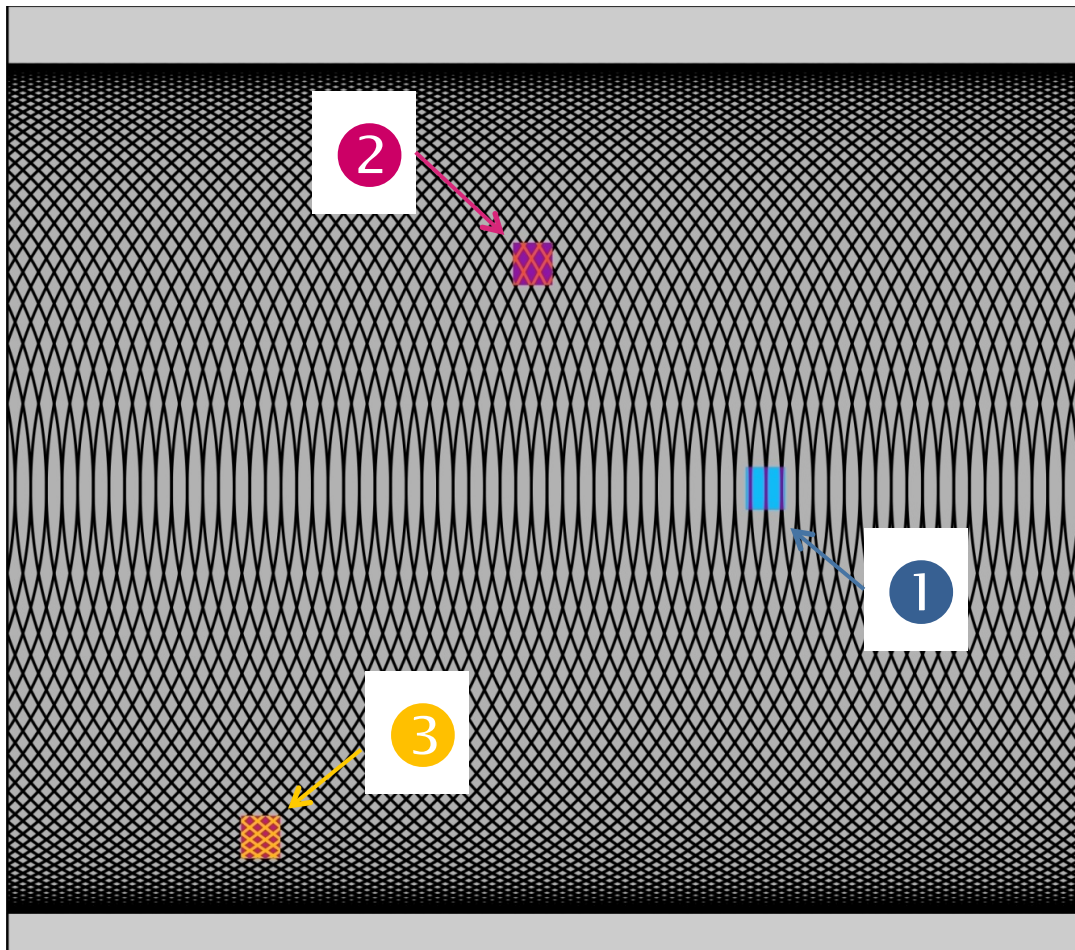
- The edges of the forward moving milling tool always create a pattern on the bottom surface like the one shown to the left.

- In order to estimate the RMS roughness of the channel we performed atomic force microscopic (AFM) measure-ments at three different sites, differing mainly in their distance from the channel's central axis (named (1) to (3) in the following).

Lawrence Livermore National Laboratory

Fabrication progress
High precision milling

1
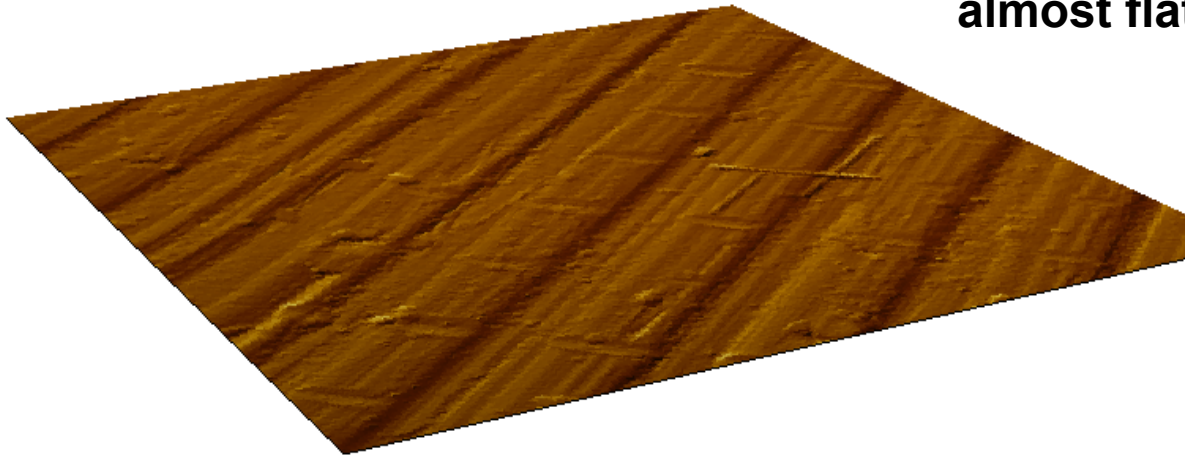
- **The areas of all measured sites were 50x50 μm.**

- **Without any height amplification applied, the surface looks almost flat.**

Fabrication progress
High precision milling
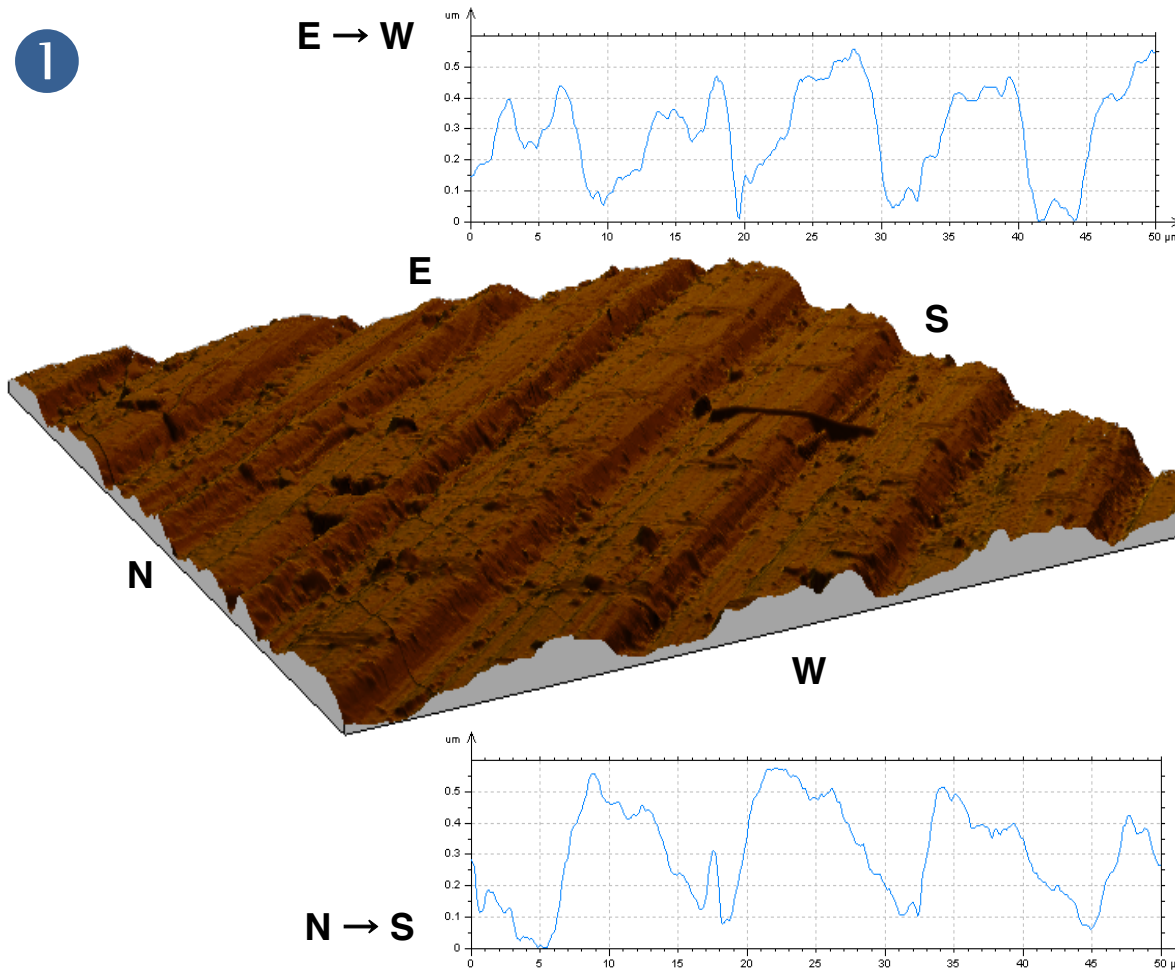
- **For better visibility however we chose a different scale of the z-axis.**

- **Also shown here: height profiles both in east-west and north-south direction.**

Fabrication progress
High precision milling

② (pink marker)

③ (yellow marker)
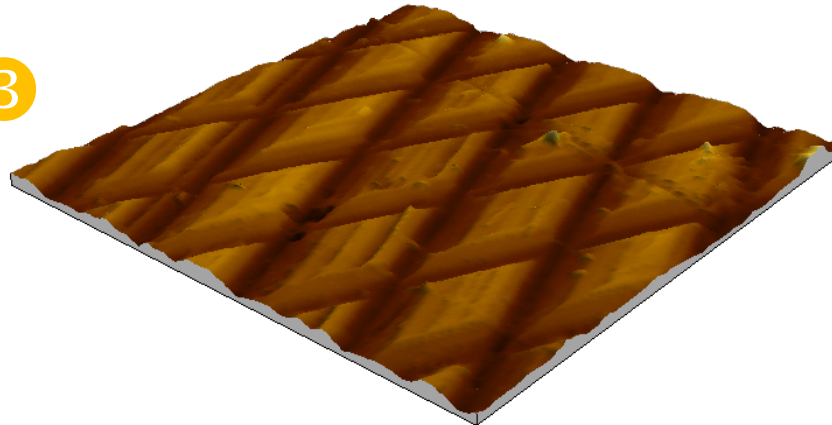
- To the left: 3D AFM pictures at sites (2) and (3).

- The individual readings for the surface roughness (expressed as RMS height) were

  - ❶ 157 nm

  - ❷ 153 nm

  - ❸ 141 nm

- As the MIR spectral regime (i.e., the guided radiation is between 2 and 20 µm), the surface quality of the channels is now sufficient enough to **fulfill the l/10th criterion**.

- Compared to the previously reported [5] RMS values of the channels (270 & 387 nm) produced at the Uni Ulm workshops, the **surface quality enhanced significantly**.

[5] LLNL Project outline - Planar HWG chip, 11-02-07 v1.pptx

Lawrence Livermore National Laboratory

HAM Precision Milling Tools

Appendix E

Ab 01.07.2012
+ 3%
Teuerungszuschlag

HAM
PRÄZISION

Über
40
Jahre

Präzisionswerkzeuge in Vollhartmetall zum Fräsen
Auswahlprogramm für Ihre Fertigung
Precision milling tools in solid carbide
program choices for your production

Sonderaktion
special campaign

NEU

HAM Vollhartmetall-Hochleistungsfräser für höchste Ansprüche
HAM solid carbide high performance end mills for highest demands

Gültig ab 01.09.2011
valid from September 01, 2011

HAM PRÄZISION

HAM 430 — Vollhartmetall-Schaftfräser
solid carbide end mill

VHM	Z 3	45° rechts	Werk Norm
Typ N		SHRINK FIT
HA	HB

Konstruktions-Daten
- bis Ø 3,0 mm und Ø d2 = 3,0 mm,
  3 Schneiden bis Mitte schneidend
- ab Ø 3,0 mm und Ø d2 = 6,0 mm,
  eine Schneide über Mitte schneidend
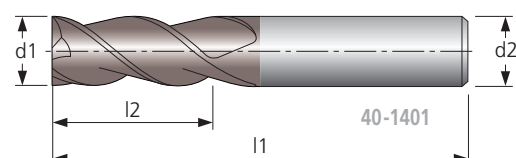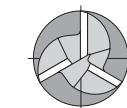
Engineering data
- *up to Ø 3,0 mm and Ø d2 = 3,0 mm,*
  3 cutting edge centre cutting
- *from Ø 3,0 mm and Ø d2 = 6,0 mm,*
  1 cutting edge over centre

40-1400

d1 | d2 | l2 | l1
40-1401
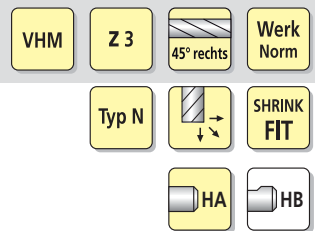
Material	Alu	Alu > 9% Si	Stahl < 800 N/mm²	Stahl < 1200 N/mm²	Stahl < 1600 N/mm²	Stahl < 55 HRC	Stahl < 60 HRC	Stahl < 66 HRC	INOX < 800 N/mm²	INOX > 800 N/mm²	GG	GGG	hochw. Legierungen	Titan	NE Metalle Cu-Leg.	Graphit Faser-verbund	MMS	max.	ohne	AIR
40-1400	O	O	●	●	O				●	●	●	●	O	●	O		●	●	O	O
40-1401	O	O	●	●	O				●	●	●	●	O	●	O		●	●	O	O

● sehr gut geeignet / *very suitable*   O geeignet / *suitable*

Ø d1 (e8) mm	40-1400	40-1401 TA	l2 mm	l1 mm	Ø d2 (h6) mm
0,4	7,20	9,10	2	38	3
0,6	7,20	9,10	2	38	3
0,8	7,20	9,10	3	38	3
1	7,20	9,10	3	38	3
1,2	7,20	9,10	4	38	3
1,5	7,20	9,10	5	38	3
1,6	7,20	9,10	5	38	3
1,8	7,20	9,10	6	38	3
2	7,20	9,10	6	38	3
2,4	7,20	9,10	7	38	3
2,5	7,20	9,10	7	38	3
2,8	7,20	9,10	7	38	3
3	7,00	8,90	7	38	3
3,5	12,40	14,90	7	57	6
4	9,70	11,60	12	40	4

Ø d1 (e8) mm	40-1400	40-1401 TA	l2 mm	l1 mm	Ø d2 (h6) mm
4,5	13,70	16,10	8	57	6
5	12,40	14,90	14	50	5
5,75	13,70	16,10	10	57	6
6	12,40	14,90	10	57	6
7	17,10	20,80	13	63	8
8	14,30	18,00	16	63	8
9	25,40	29,80	16	72	10
10	23,00	27,70	19	72	10
12	32,50	37,50	22	83	12
14	42,40	50,50	22	83	14
16	57,50	66,90	26	92	16
18	82,60	94,40	26	92	18
20	89,90	102,70	32	104	20
25	149,90	167,40	40	110	25

Alle Preise in € pro Stück / *all price in €/pcs*

Bestellbeispiel / *Order example*:   HA-Schaft / *shank*   40-1400-4,5-57
HB-Schaft / *shank*   40-1400-4,5-57-HB

| Eckenfase / *chamfer at corner*	d1	b
45° b	≥ Ø 4,0	0,05
	≥ Ø 8,0	0,10
	≥ Ø 14,0	0,15
	≥ Ø 18,0	0,20

Optical Fiber Probe for
Double-Pass Waveguide Coupling

Appendix F

Considerations on single- vs. double-pass
Coupling using fiber probes

Rectangular iHWG:
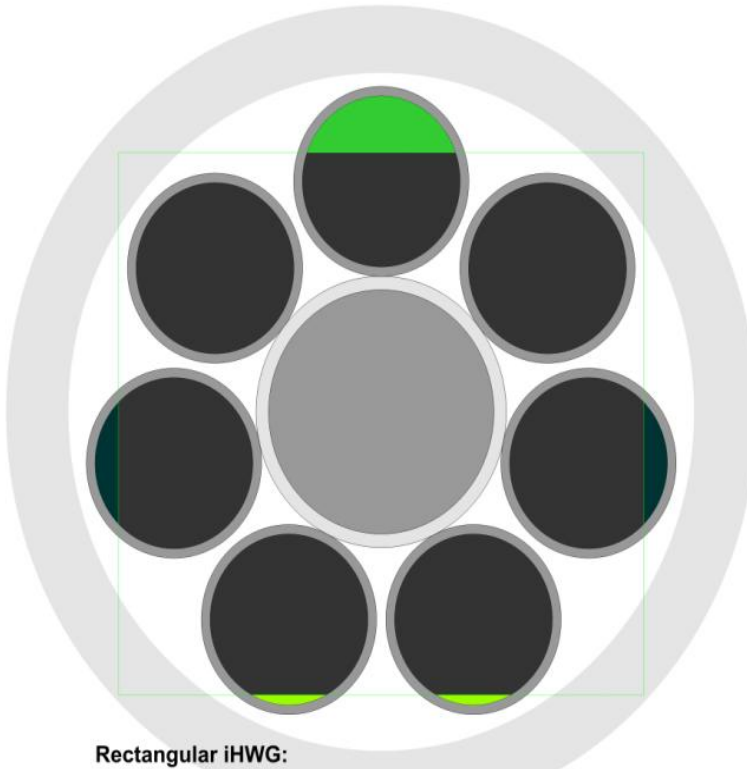
Area of iHWG = 2.1000 mm x 2.0000 mm = 4.200 mm^2
Covered area of outcoupling fibers = 2.019 mm^2

Outcoupling ratio = 48.07 %

- Double-pass configurations require both in- and outcoupling fibers to be linked to the same iHWG end facet.

- As a consequence either the end facet of the iHWG would require widening in order to accomodate both single fiber terminators, or – alternatively – fibers could be bundled in one common terminator.

- The first option (i.e., the side-by-side coupling) can only be achieved at the cost of significantly increased outcoupling losses (i.e., the outcoupling ratio can only be as high as the ratio A/B with A=the overlapping area of fiber and iHWG end facet (cross section), and B=the iHWG cross section).

- For the bundled fiber option compare the picture to the left, demonstrating the situation exemplary for a 7-around-1 configuration, leading to an outcoupling ratio of ~8% (which is indeed the theoretical maximum for the current 2.1x2mm waveguide channel dimensions).

Lawrence Livermore National Laboratory

Interface
Complete overlap: optimum for quadratic iHWG
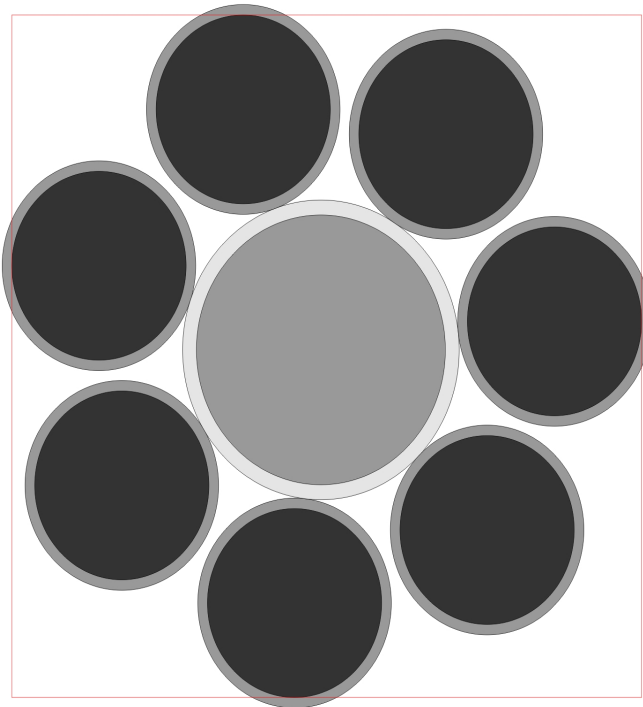
Quadratic iHWG (enlarged):

Area of iHWG = 2.2770 mm x 2.2770 mm = 5.185 mm^2
Area of outcoupling fibers = 7·(63 mm/2)$^2\pi$ = 2.182 mm^2

Outcoupling ratio = 42.09 %

- **To the left we depict the same fiber bundle (7 – 630/700 micron diameter collection fibers & 1 – 900/1000 micron diameter IR delivery fiber) from slide 2. If all collecting fibers should cover the iHWG completely, and the iHWG cross section shall be quadratic, its width and height must be 2.277mm, resulting in an coupling ratio of 42.09% (i.e., the area covered).**

Lawrence Livermore National Laboratory

Interface
Complete overlap: optimum for rectangular iHWG
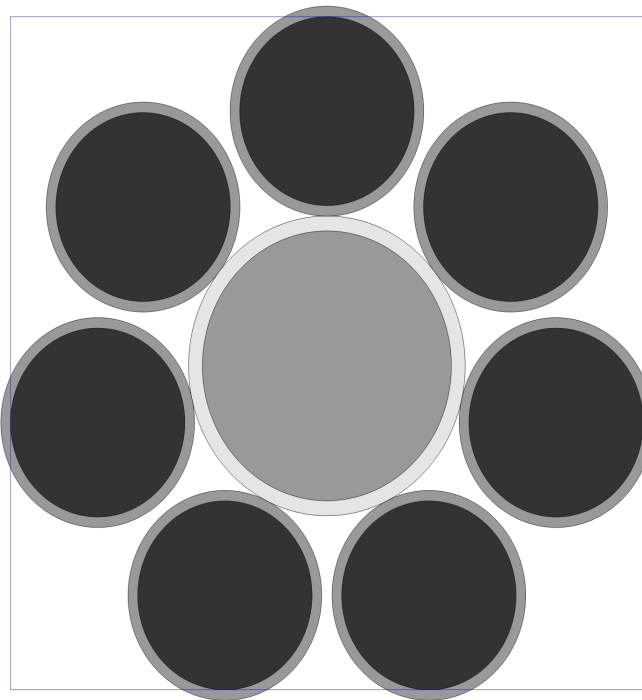
Rectangular iHWG (enlarged):

Area of iHWG = 2.28738 mm x 2.24582 mm = 5.137 mm^2
Area of outcoupling fibers = 7·(63 mm/2)$^2\pi$ = 2.182 mm^2

Outcoupling ratio = 42.48 %

- **If the iHWG's cross-section is allowed to be rectangular (indeed our current iHWG is rectangular as well), the coupling ratio could be increased from the previous slide, but only very slightly - roughly 0.4%).**

Interface
Partial overlap: optimum for current (rectangular) iHWG
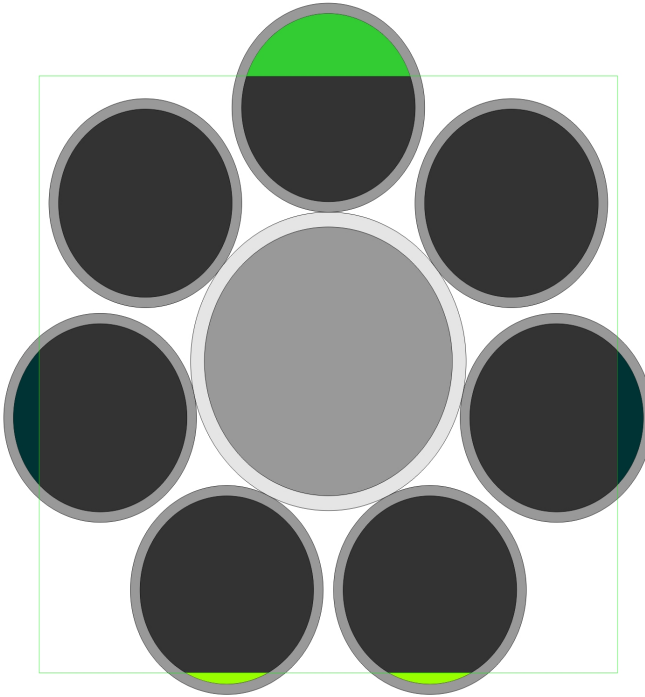
Rectangular iHWG (current configuration):

Area of iHWG = 2.1000 mm x 2.0000 mm = 4.200 mm^2
Covered area of outcoupling fibers = 7·(63 mm/2)^{2}π -
- 2·0.007421 mm^2 - 0.090213 mm^2 - 2·0.028957 mm^2 =
=2.019 mm^2

Outcoupling ratio = 48.07 %

- **However, if we stay with the current iHWG cross section (2.1mm wide, 2mm high) the geometric coupling ratio can increase to > 48% (assumed a perfect alignment; shown at the left), although not all fibers do overlap completely with the iHWG end facet.**

Lawrence Livermore National Laboratory

Interface considerations
Conclusion

- **Widening the whole channel or expanding the coupling end is counterproductive for coupling purposes (although widening the whole channel is always advantageous for throughput).**

- **Best for coupling is leaving the channel dimensions unaltered and do a butt-coupling (or alternatively drill a hole so that the device can accomodate the fiber:**

Lawrence Livermore National Laboratory

The iHWG Configured as a Gas Cell for Tier 0 Gas Testing

Appendix G

Detector mount
Construction

Front-, side- and top view
Dark grey: Angle bracket (base)
Light grey: Top plate

Top view
Light grey: Angle bracket (base)
Dark grey: Top plate
Arrows: fixation screws
Material: aluminum
Surface: black anodized
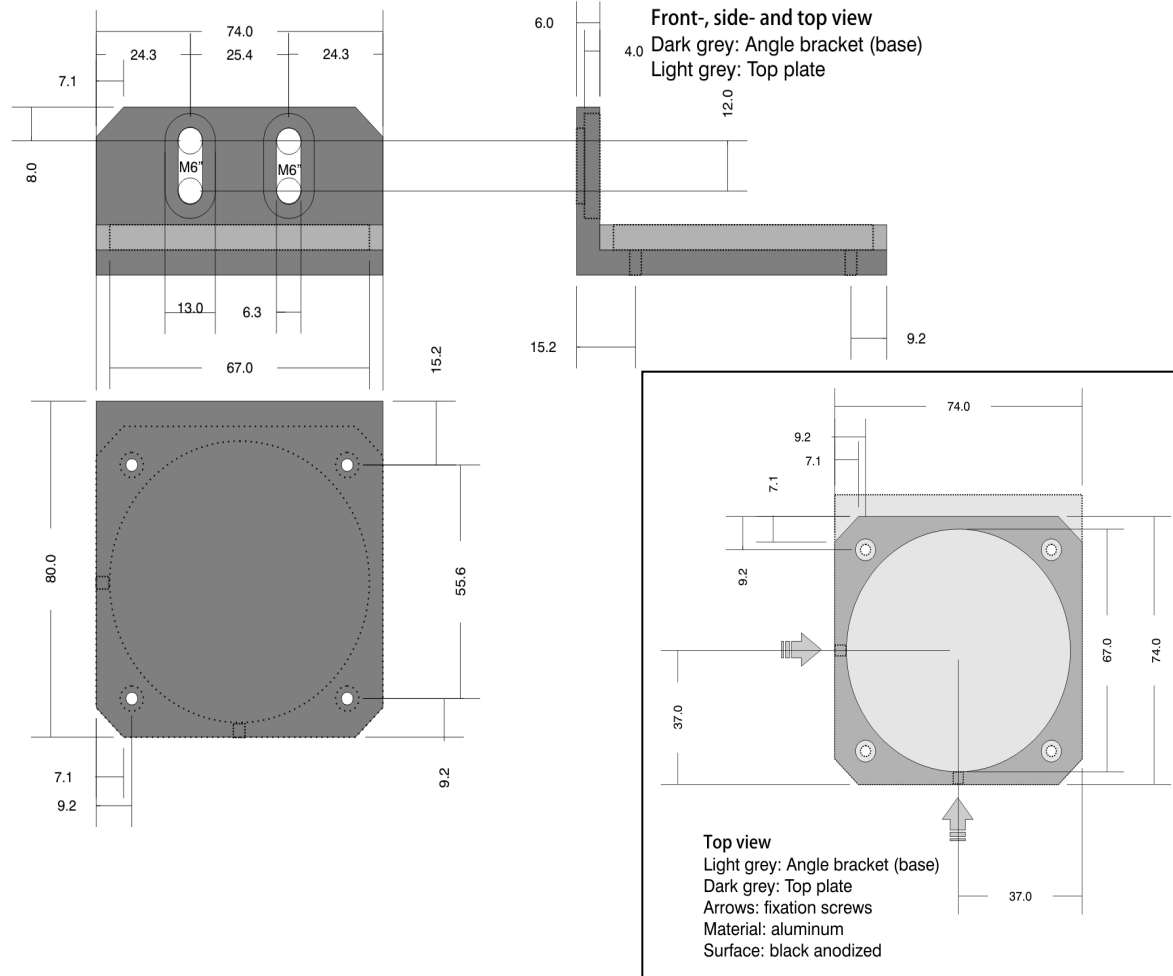
- **A detector mount was custom-made in order to ensure secure and precise positioning of the MCT detector on the xyz-positioning stage.**

Detector mount
Finished device
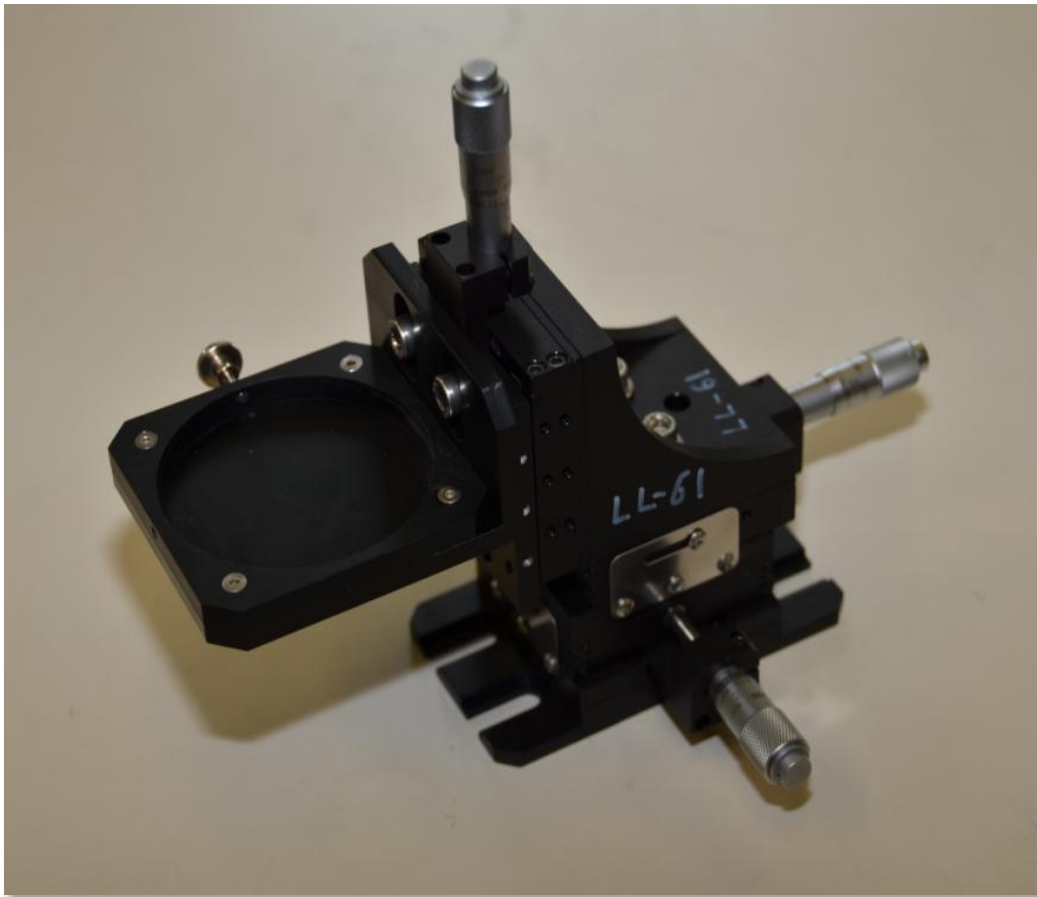
- **The device is shown to the left, assembled to a xyz-positioning stage.**

Detector
FTIR-16-2.0

MCT element
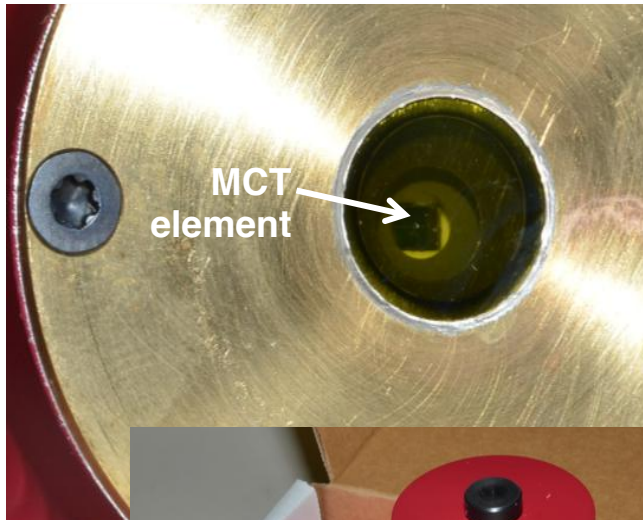
Detector response (sensitivity)[1]
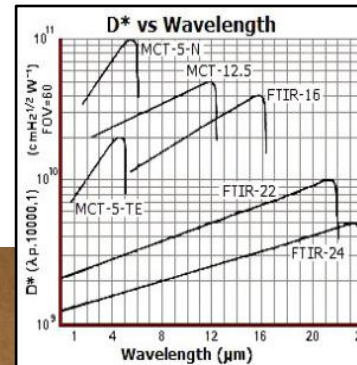
- **iHWG cross section (end facet) (or alternatively fiber cross section) determines the minimum spot size of the focal point at the detector element (assuming perfect refocusing optics).**

- **Accordingly, a highly sensitive detector with a 2x2 mm MCT element (InfraRed Associates FTIR-16-2.0) was selected to match the iHWG channel cross section.**

- **Using two 90° Au-coated OAPMs, almost 100% capture of the emitted light is anticipated.**

- **Even when using fibers for outcoupling the large area detector is perfectly suited.**

Lawrence Livermore National Laboratory

Serial interface

Connection of preamplifier and spectrometer

to the detector

to the spectrometer
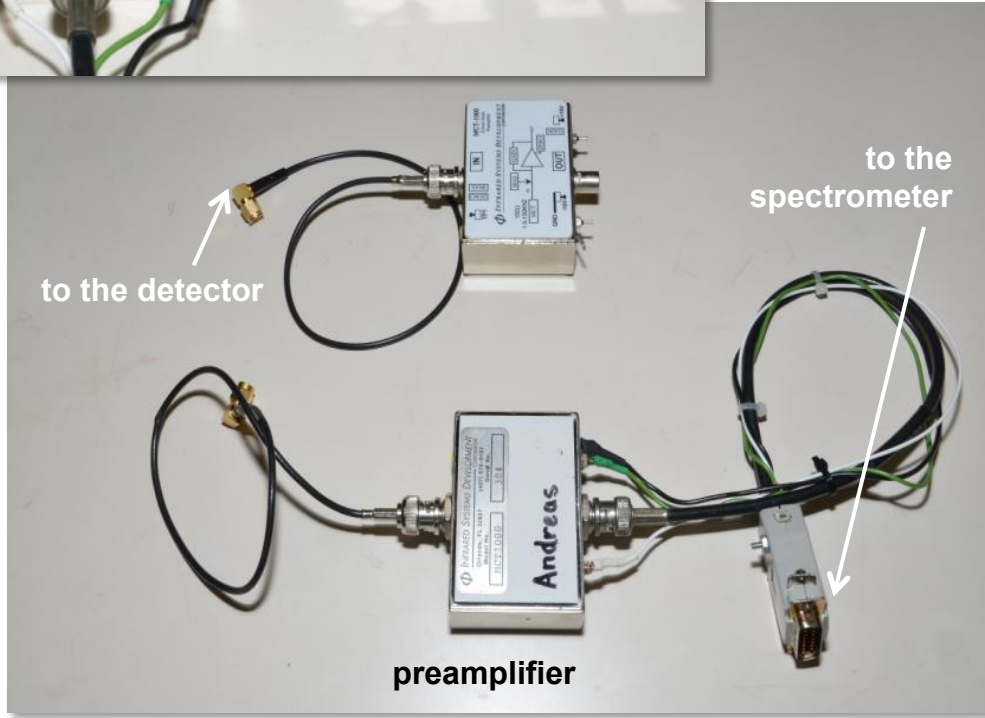
preamplifier

- **Interface cable is necessary for communication (data transfer) between the preamplifier and the Bruker Ircube spectrometer.**

- **This cable is not included in the shipping and had to be custom made.**

Clamp
Construction finished

Gap
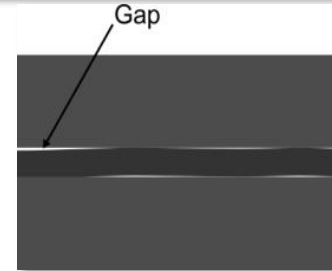
- **Referring to our previous FY11 year-end report, 'gaps' were evident due to the non-planarity of the parts of the sandwiched iHWGs.**

- **Pressing the parts tightly together by applying enough force using a custom-made highly robust clamp was evaluated.**

- **The image to the left shows the clamp prototype (disassembled).**

Clamp
Construction complete
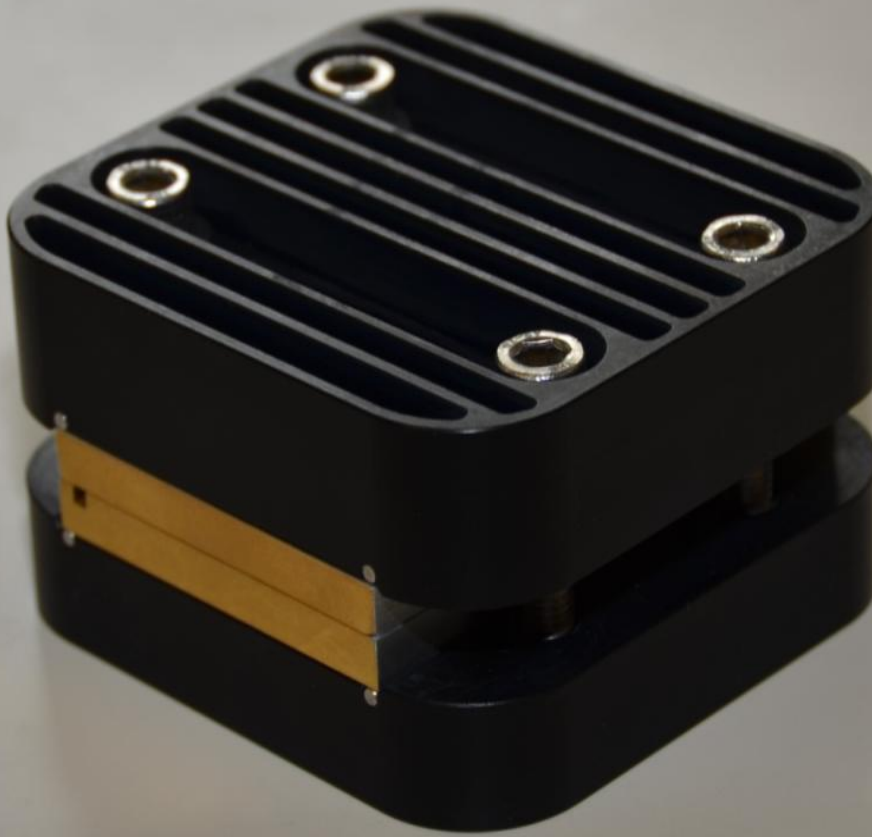
- **Image shows the clamp in action (a 2-piece-iHWG is shown assembled).**

- **Although the new clamp improved the planarity somewhat, gaps were still evident.**

- **Glueing the iHWG components together appears to be the most viable option (also for weight reduction). For laboratory purposes requiring flexible assemblies, the developed clamp is sufficient.**

Clamp modification
Transformation of the iHWG into a gas cell
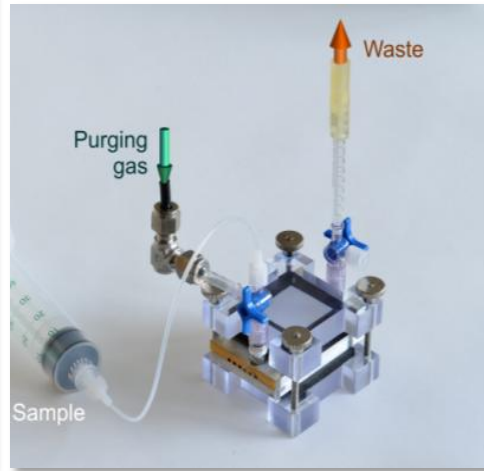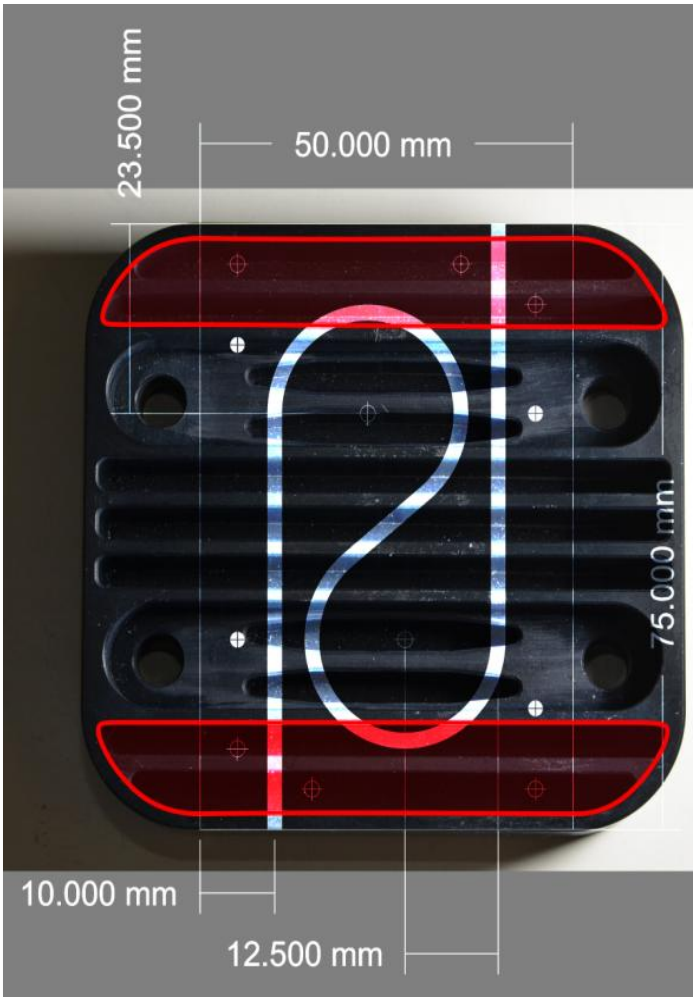
- We intend to remove the areas highlighted in red (left picture) in order to configure the iHWG as a gas cell similar to the one shown in the FY11 year-end report (small picture bottom right).

Lawrence Livermore National Laboratory

Gas cell assembly
4-piece Yin-Yang iHWG gas cell finalized
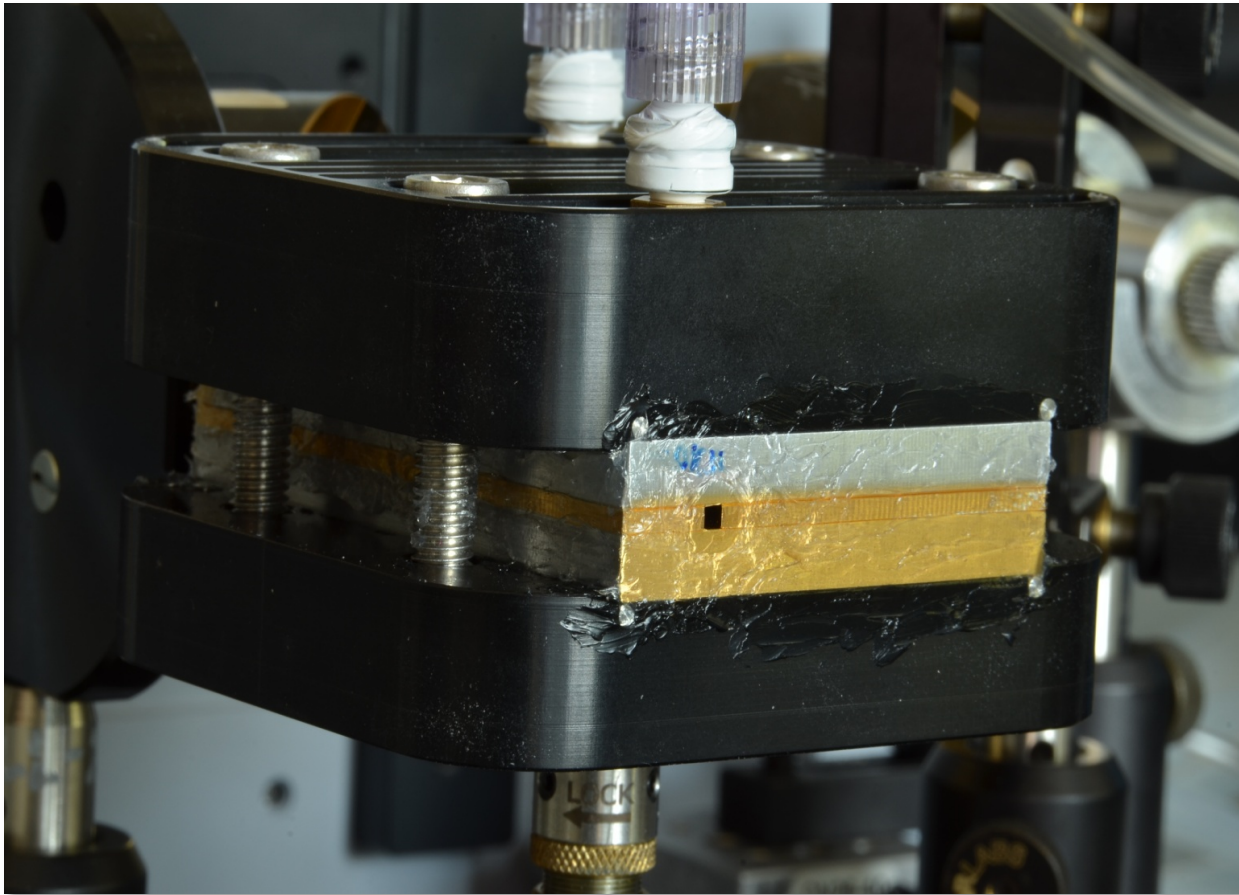
- We finalized the assembly of the single-pass, 4-piece waveguide (yin-yang) gas cell (compare picture).

- Most noticeable is the BaF_2 window. Two were glued to seal the in- and outcoupling facets of the iHWG, respectively.

- Silicone rubber is used as sealant and as glue. The sealant was generously applied, surrounding the entire iHWG in order to make the cell as a whole absolutely air tight.

- On the very bottom of the picture (in the center) the mount (translating optical post, Thorlabs) is visible. On the very top you can see the Luer Lock connections for gas supply.

[1] LLNL Monthly progress report - Substrate-integrated HWGs, 2012-06.pptx

Lawrence Livermore National Laboratory

Gas cell assembly
4-piece Yin-Yang iHWG gas cell finalized
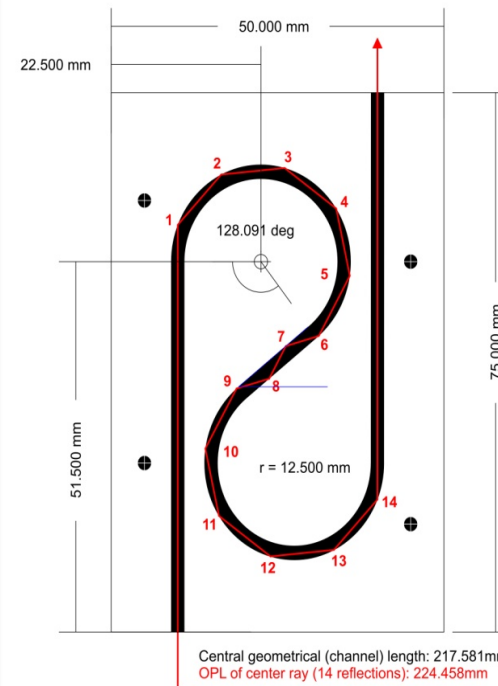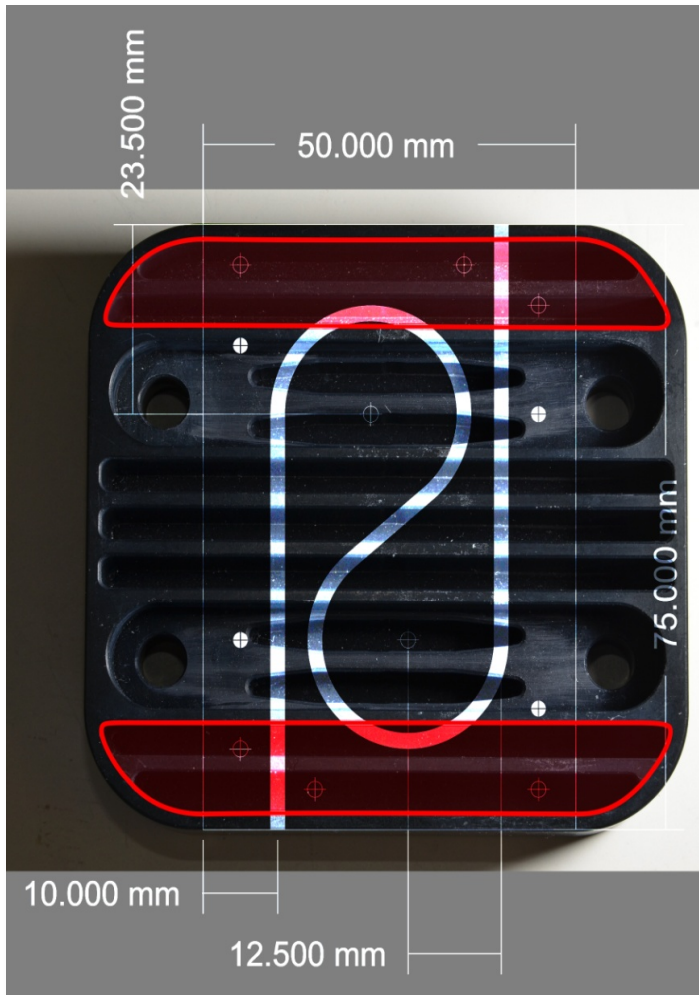
- **The image to the far left shows an overlay of the clamp and the channel geometry. The red fields indicate the areas where the original clamp had been modified**

- **The image on the near left shows the propagation of the center ray, this time alongside with the exact iHWG dimensions.**

- **The central channel length can be calculated as 217.6mm, whereas the average OPL exceeds this value (for the center ray it is already 224.5mm).**

[1] LLNL Monthly progress report - Substrate-integrated HWGs, 2012-06.pptx   [2] LLNL Project outline - Planar HWG chip, 11-06-21 v5.pptx

Lawrence Livermore National Laboratory

Sensor assembly, iHWG
Experimental setup, overview
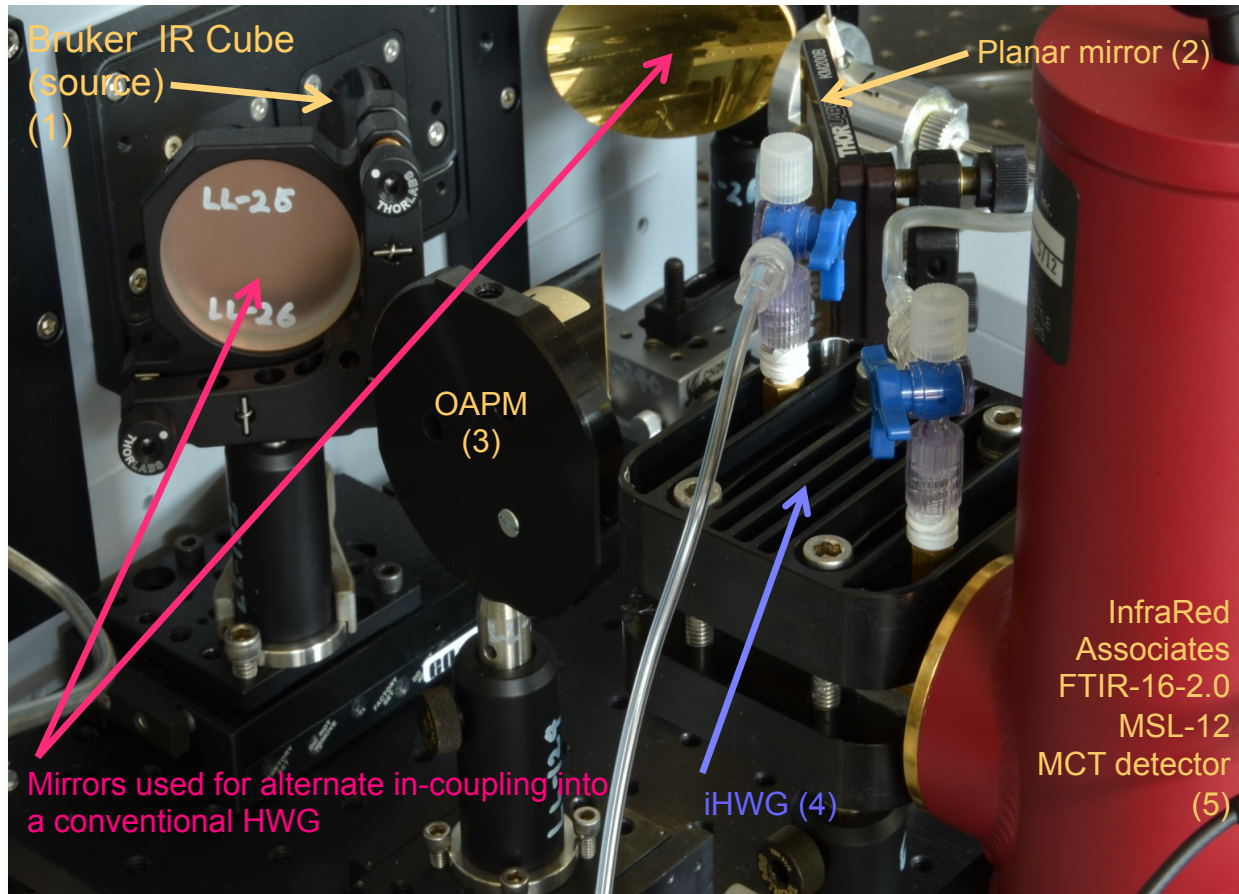
- **The complete sensor looks like this.**
- **The beam propagates from (1) to (5).**

Sensor assembly, iHWG
Experimental setup, detail

gap
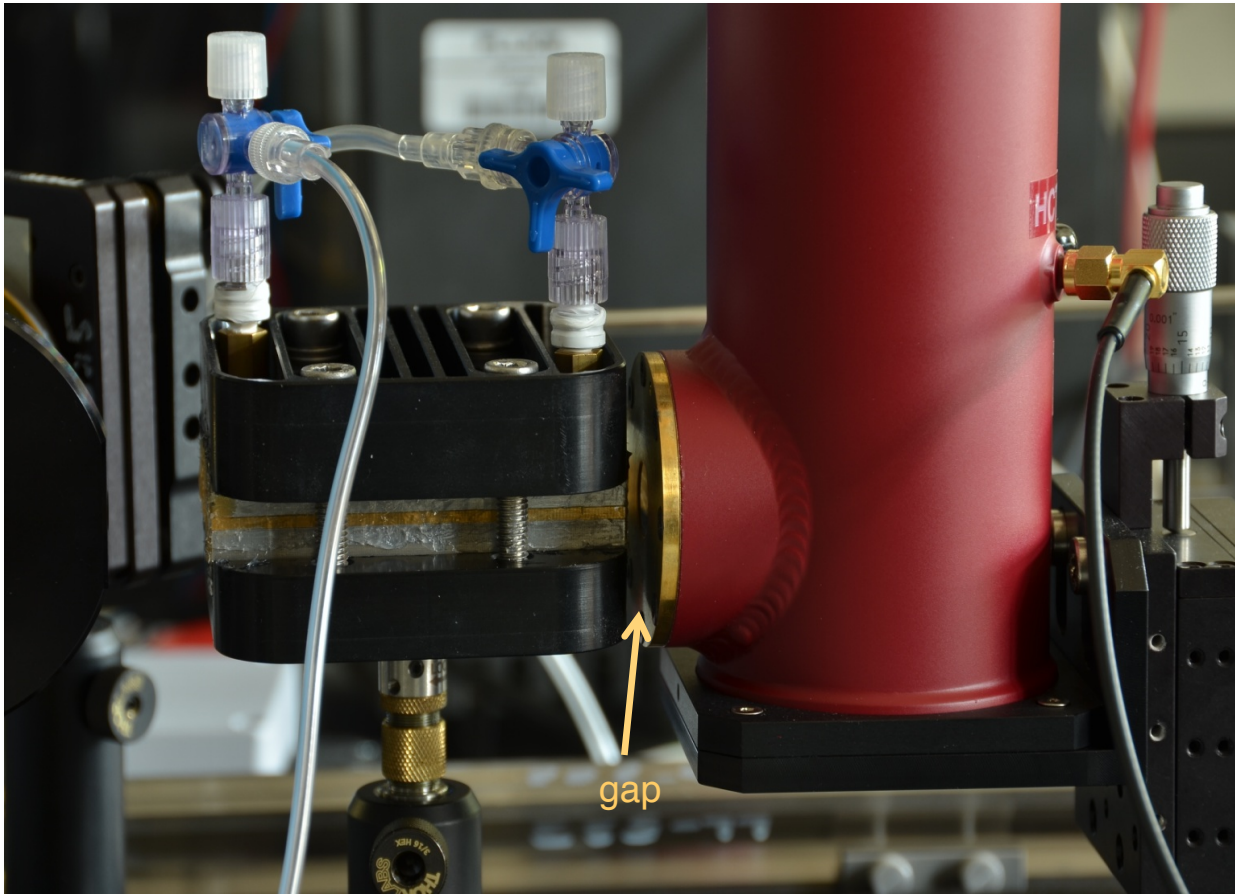
- **As you might have noticed already on the previous slide, this optical setup goes without any refocusing optics.**

- **Most remarkably there is a ~5 mm gap between the outcoupling facet of the iHWG (i.e., the focal point) and the incoupling ZnSe window of the detector sitting in the optical axis (i.e., within the center of the outcoupled radiation cone).**

- **Nonetheless *this coarse alignment is sufficient to obtain more than 29'000 ADC counts***

Lawrence Livermore National Laboratory

Sensor assembly, iHWG
Experimental setup, including GMS
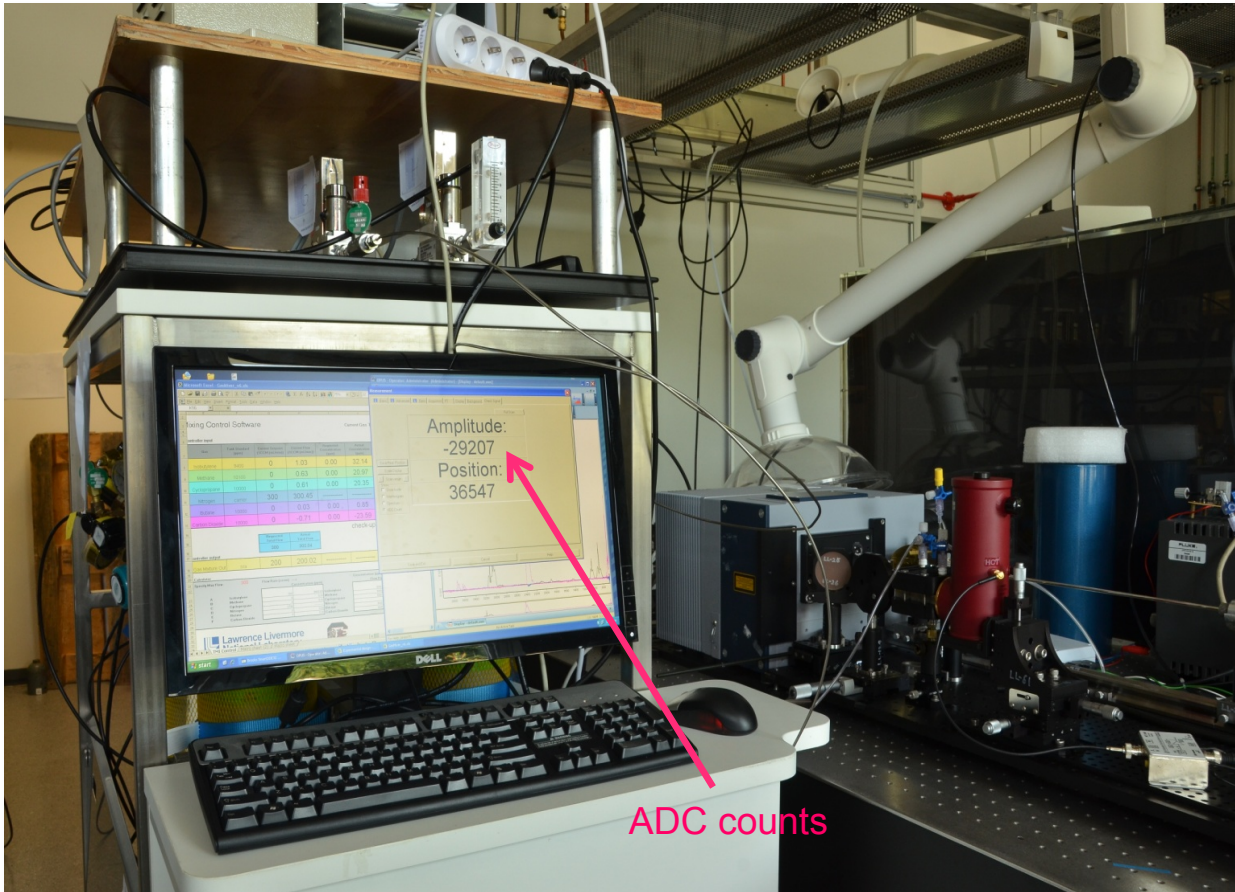
ADC counts

- In fact the current sensor is limited by the ADC count value. Hence the optical components had to be misaligned on purpose; perfect alignment (or even a slightly less misaligned optical setup) would cause detector saturation (occurring at 32'768 counts (= 2^{15}) due to the analog-digital conversion process).

- We assume that the observed ADC counts have their foundation mainly in the usage of a highly sensitive & large cross-sectioned MCT element, rendering the results not directly comparable to the ones previously reported on different MCT detectors.

- That said, the new detector should give us plenty scope to either further decrease the achievable LOD (using even longer OPLs, and leaving the counts unchanged at the same time), or to compensate the losses that have to be expected when using fiber coupling.

Lawrence Livermore National Laboratory

Gas Mixing & Calibration System

Appendix H

Gas mixing system
Contents

- **Portable cart construction**
- **Adapting between US standard and German standard regulators**

- **Purchase and installation of gas standards based on LLNL's tier 0 test matrix**
- **Development of a robust MFC back pressure calibration procedure**
- **Testing of the control software**

Gas mixing system
System and transportability

- **A gas mixing system (GMS) was constructed and tested at LLNL and then transferred to the University Ulm for gas mixing and calibration.**

- **Design and construction of a transport trolley for the gas mixing system (GMS) was completed by the University Ulm workshop according to specifications.**

- **The final design features a mobile yet robust platform that can be used in different laboratories in combination with variable spectrometers.**

- **The trolley has a small footprint (i.e., it occupies same area as the GMS itself, as everything is stacked vertically).**

- **It is made from stainless steel, and includes storage for computer and control units.**

- **The trolley can comfortably accommodate six 10L-gas bottles; a maximum of 8 bottles.**

- **Each bottle is locked into place with 2 lashing straps to meet safety requirements.**

- **Images of the fully assembled GMS are included in the following slides.**

Lawrence Livermore National Laboratory

Gas mixing system
Pressure regulators

US parts

Replacements (new)

flammable

non-flammable

pressure regulator side
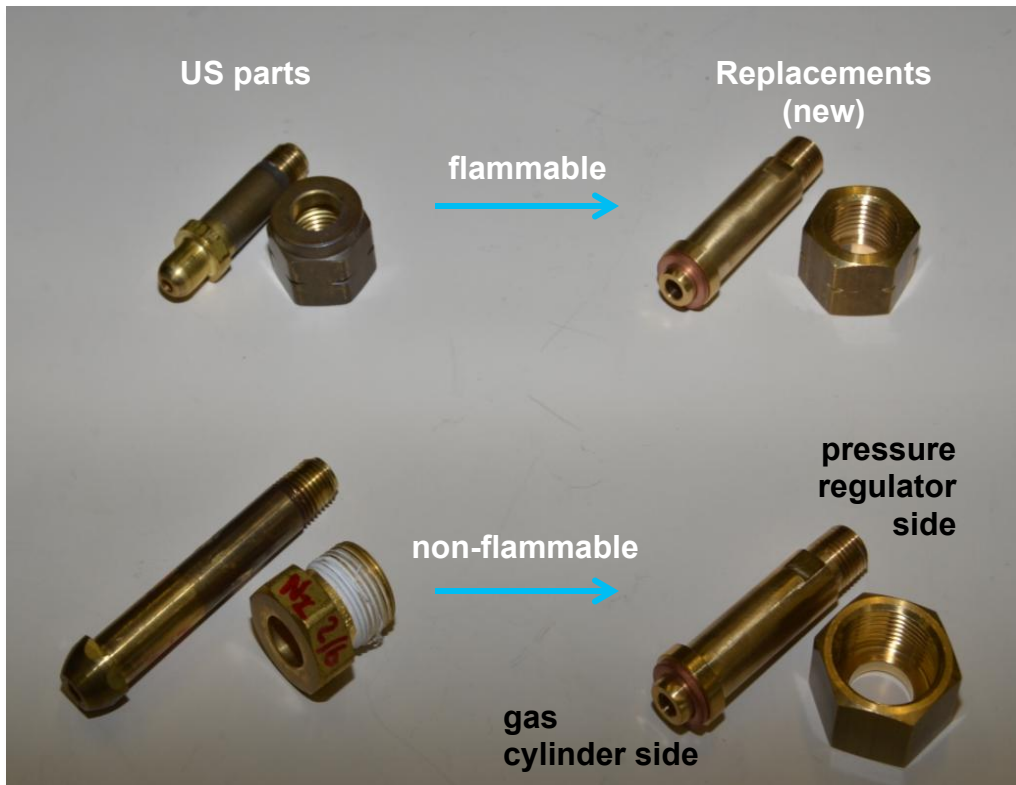
gas cylinder side

- **The connecting bolts (input connections) of all pressure regulators had to be exchanged in order to match the valve threads of German gas cylinders.**

- **Modification of the thread of commercially available input connections was done in the University workshop by cutting new threads at the pressure regulator side to match the US standard regulators.**

Gas mixing system
Pressure regulators

- **Exemplarily: one of the new input connections is shown to the left (completely assembled).**

Gas mixing system
Overview—gas mixing system and transportable cart

- **All the units are integrated:**

  - **Portable cart**

  - **Gas standards**

  - **Gas mixing unit**

  - **Power supply**

  - **Communication box**

 - **Control and Data acquisition computer**

Gas mixing system

Detailed view – Power supply, interface box, final MFC, waste line MFC
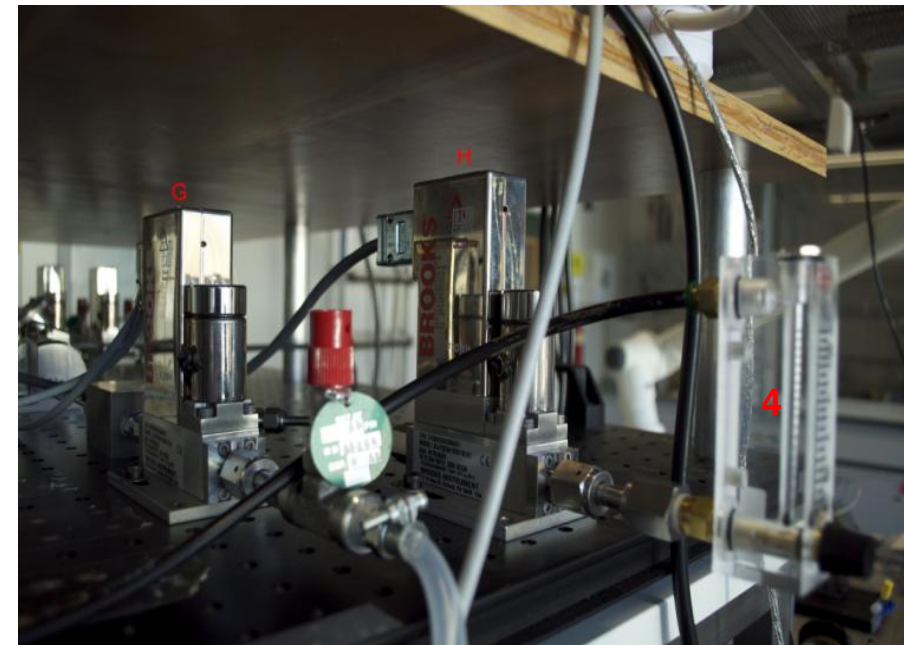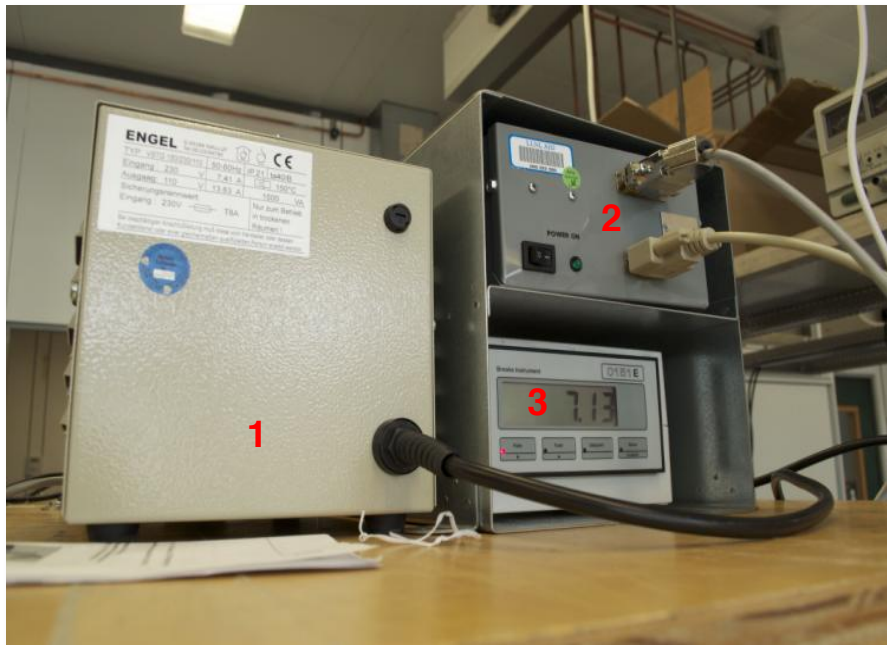
- 1 – power supply
- 2 – computer interface box with MFCs
- 3 –control unit for MFC #H
- G – delivery (output) MFC
- H – excessive gas dumping (overflow) MFC
- 4 – flow meter for waste gas line

Lawrence Livermore National Laboratory

Gas mixing system
Detailed view – individual gas MFCs
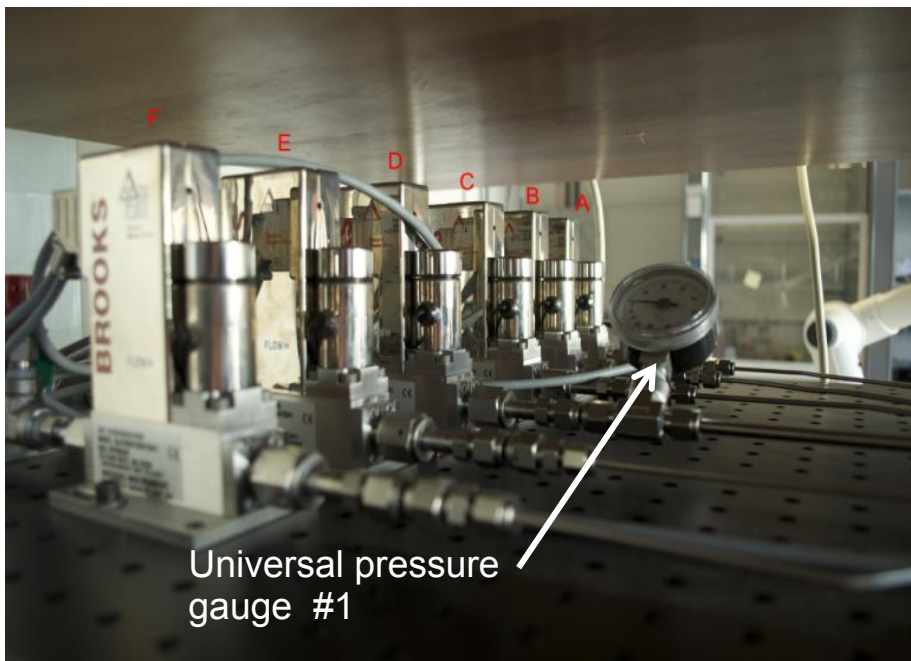
Universal pressure gauge #1

- **A ~ F – individual gas MFCs (5 gas standards and one carrier gas)**

GMS initialization procedure
Calibration of MFC pressure input/output using the universal pressure gauge
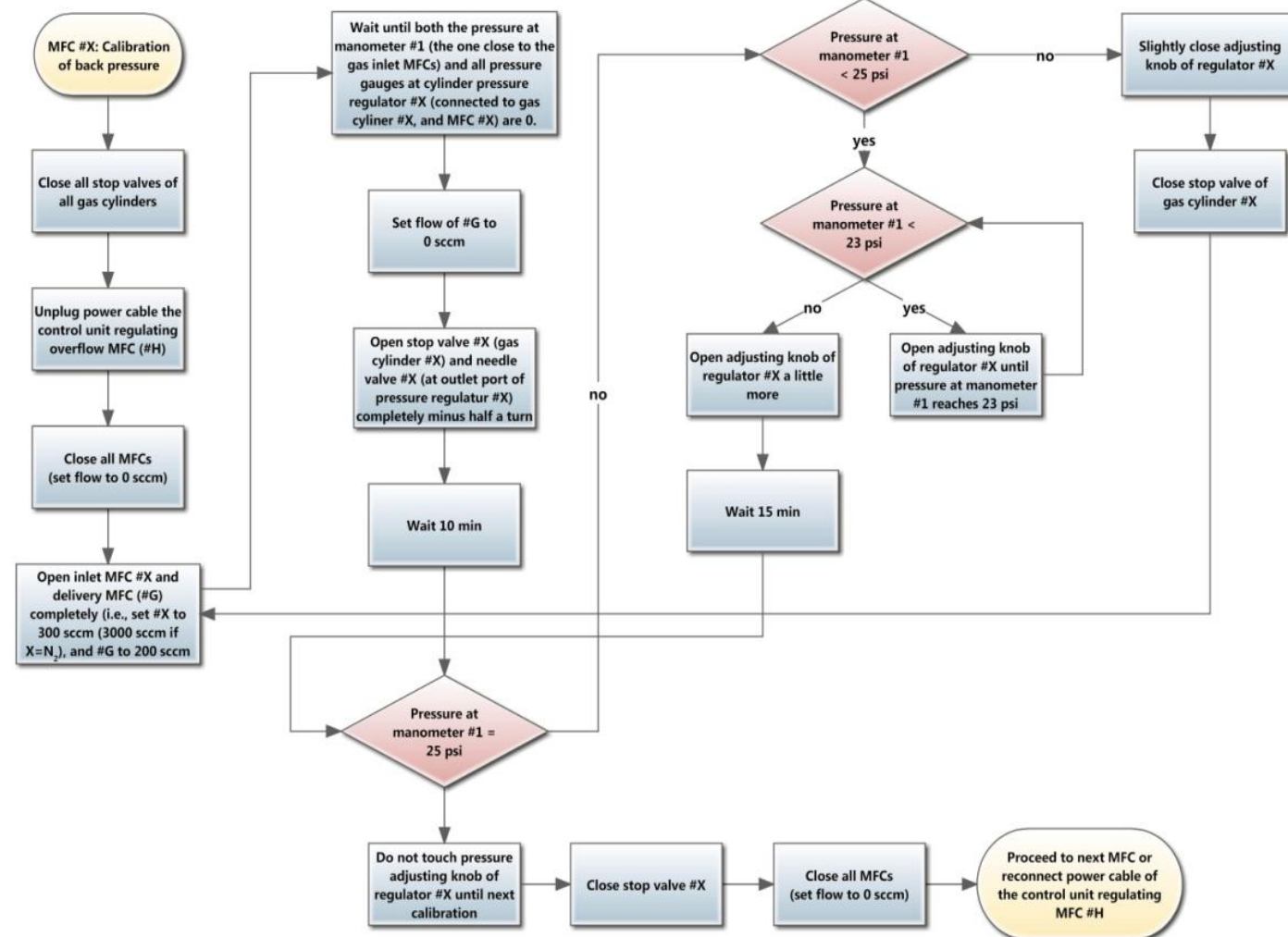
Gas Mixing System (GMS) software issues resolved
New control software versions were successfully installed at Ulm

- **Working computer software to control the GMS:**

  - **Operating System: Window XP Professional Version 2002 Service Pack 3.**

  - **Computer Interface Software: Brooks Instrument Inc. Brooks Smart DDE32 Build 2.0.0.27**

    — **Setting; Baudrate = 19200, RS-232, refresh rate = 2500 msec. minimal response time = 50 msec.**

- **Control Front Panel Software:**

  - **A. GasMixer_v6 version 6, July 24 2008 – MS Excel based interface**

  - **B. Gas-O-Matic – Labview based interface**

- **Both Excel control program and Labview control program have been successfully configured. The GMS is operational as of June 2012.**

Future Plan: Since Windows XP operating system becomes outdated and MS does not provide technical support for XP anymore, we need to move to newer OS such as Windows 7 or 8. However, the current Excel program (GasMixer v6) is not compatible with Windows 7 OS. Accordingly, it is necessary to develop a control front panel software compatible with Windows 7.

Lawrence Livermore National Laboratory

Gas Mixing System (GMS), Software
Control front panel software – Excel vs. Labview
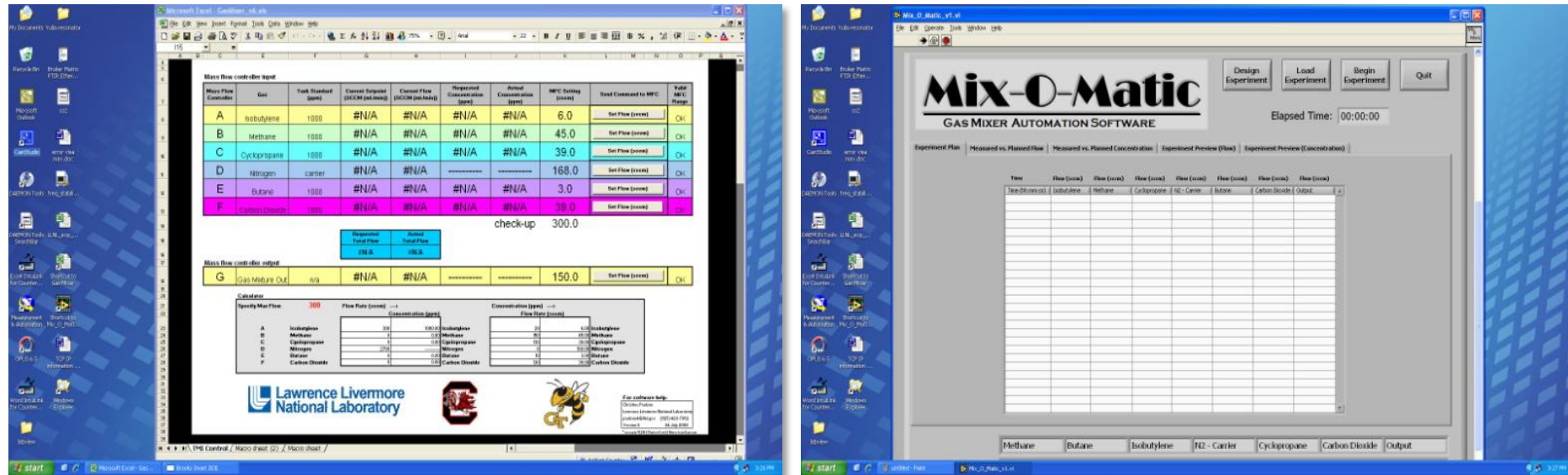
- **Pros and Cons:**
  - **Labview based Mix-O-Matic is more advanced version of GMS control program.**
  - **Excel based GasMixer v6 is simple and easy to use. It also allows instantaneous change of set-value during experiments, while Mix-O-Matic is able to perform more complicated tasks. It allows automated mixing routines.**

Lawrence Livermore National Laboratory

Gas Mixing System (GMS) Gas Standards
Gas standards installed based on LLNL's tier 0 test matrix

Index	Name	Chemical Formula	Concentration (%)		Cylinder Size (L)
			Nominal	Actual	
1	i-Butene	$i\text{-}C_4H_8$	1.00	0.94	10.00
2	Methane	CH_4	1.00	1.01	10.00
3	Cyclopropane	C_3H_6	1.00	1.00	10.00
4	Carbondioxide	CO_2	1.00	1.00	10.00
5	Butane	$n\text{-}C_4H_{10}$	1.00	1.00	10.00

Vendor: Westfalen AG http://www.westfalen-ag.de

Lawrence Livermore National Laboratory

Mid-IR Gas Sensing Results
for Tier 0 Gas Matrix Testing

Appendix I

0 ppm
Blank measurements, overview spectrum
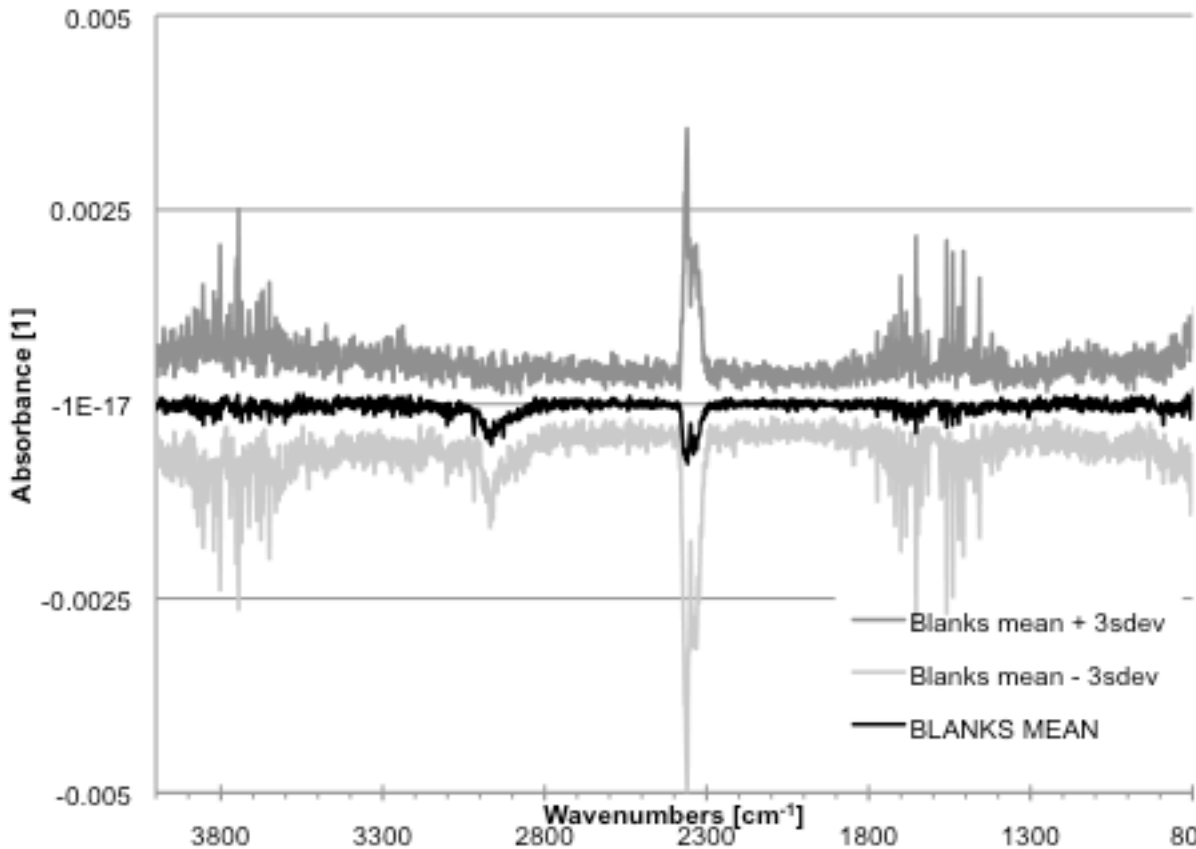
- **Spectrum was measured with the 4-piece yin-yang iHWG sensor described in Appendix G.**

- **Grey curves: mean spectrum plus/minus three times the standard deviation of those 15 spectra, meaning statistically that 99.7% of the blank spectra population lie within this interval.**

0 ppm
Blank measurements, interpretation

15 blank measurements
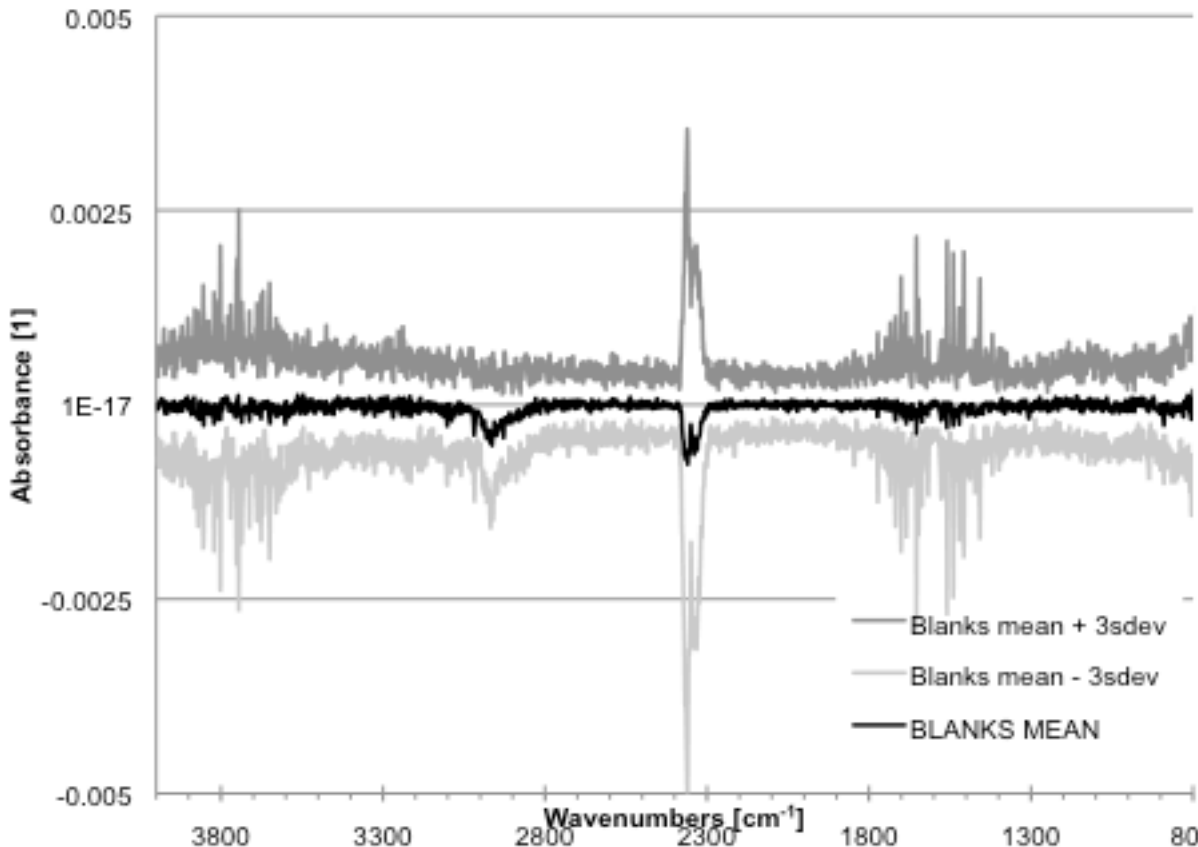
- Note the small "dip" of the baseline at around 2800 to 3000 WN. This is an artifact of the flushing time of 90s, which itself is a compromise between measurement time and accuracy. In this case the blanks were measured subsequently to other samples containing – amongst others – the strong absorber butane. The dip indicates that butane was not flushed/ eliminated completely prior to the start of the acquisition of the blank background spectrum.

- The peaks @ 3600-4000 & @ 1400-1900 wavenumbers (WN) are from water, and the ones @ 2300-2400 WN from CO_2. Remember that the sensor was not shielded from the ambient atmosphere, hence shows increased fluctuations in those regions.

Lawrence Livermore National Laboratory

1000 ppm
CO_2, overview spectrum

- **Spectrum was measured with the 4-piece yin-yang iHWG sensor as described in Appendix G.**

- **The „BLANKS MEAN" is the black curve shown on slides #2 & 3.**

Lawrence Livermore National Laboratory

1000 ppm
CO_2, spectrum section

only carbon dioxide band
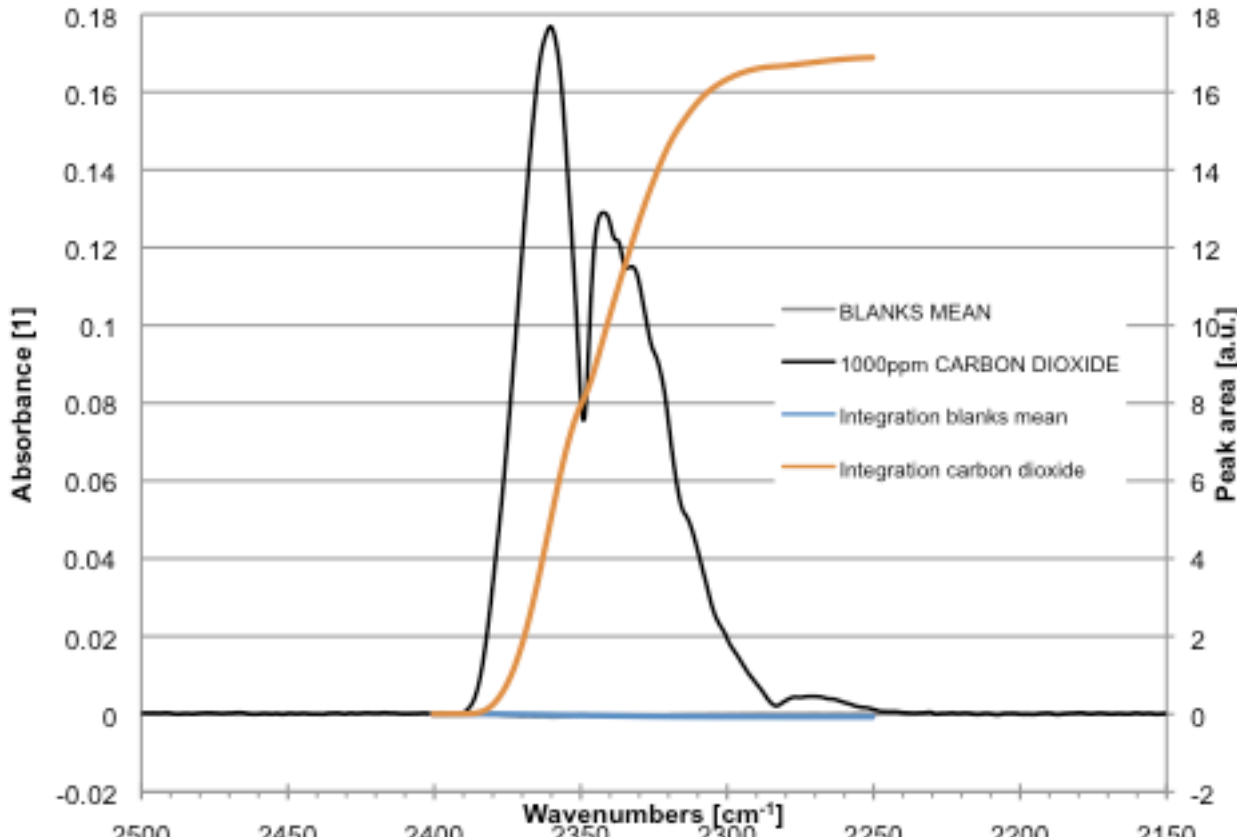
- **This diagram illustrates the univariate SNR by showing the integration of both background and signal.**

- **Note: the displayed integration was performed in Excel, not using the (more sophisticated) OPUS method. The results are still similar, but not identical.**

1000 ppm
Butane, overview spectrum

- **Spectrum was measured with the 4-piece yin-yang iHWG sensor as described in Appendix G.**

- **The „BLANKS MEAN" is the black curve shown on slides #2 & 3.**

1000 ppm
Butane, spectrum section
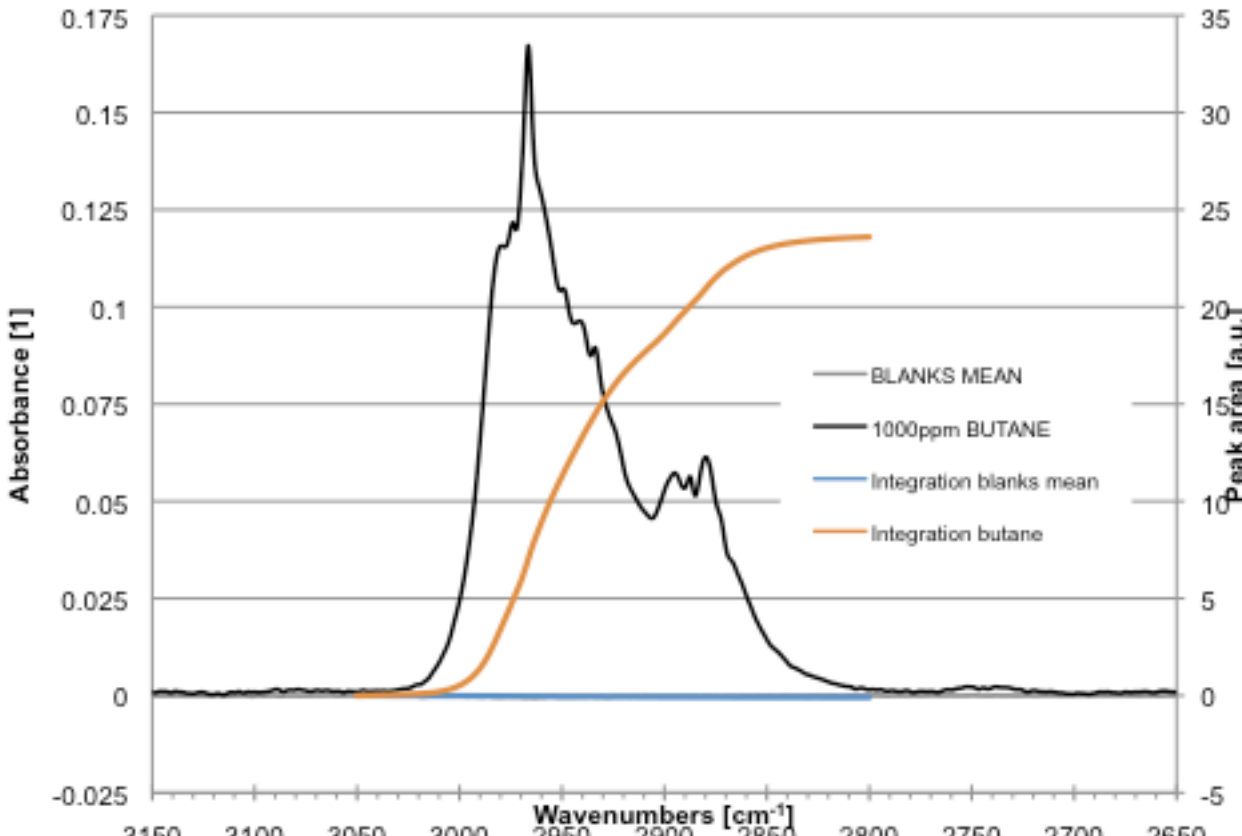
- **This diagram illustrates the univariate SNR by showing the integration of both background and signal.**

- **Note: the displayed integration was performed in Excel, not using the (more sophisticated) OPUS method. The results are still similar, but not identical.**

1000 ppm
Methane, overview spectrum

- **Spectrum was measured with the 4-piece yin-yang iHWG sensor described in Appendix G.**

- **The „BLANKS MEAN" is the black curve shown on slides #2 & 3.**

1000 ppm
Methane, spectrum section
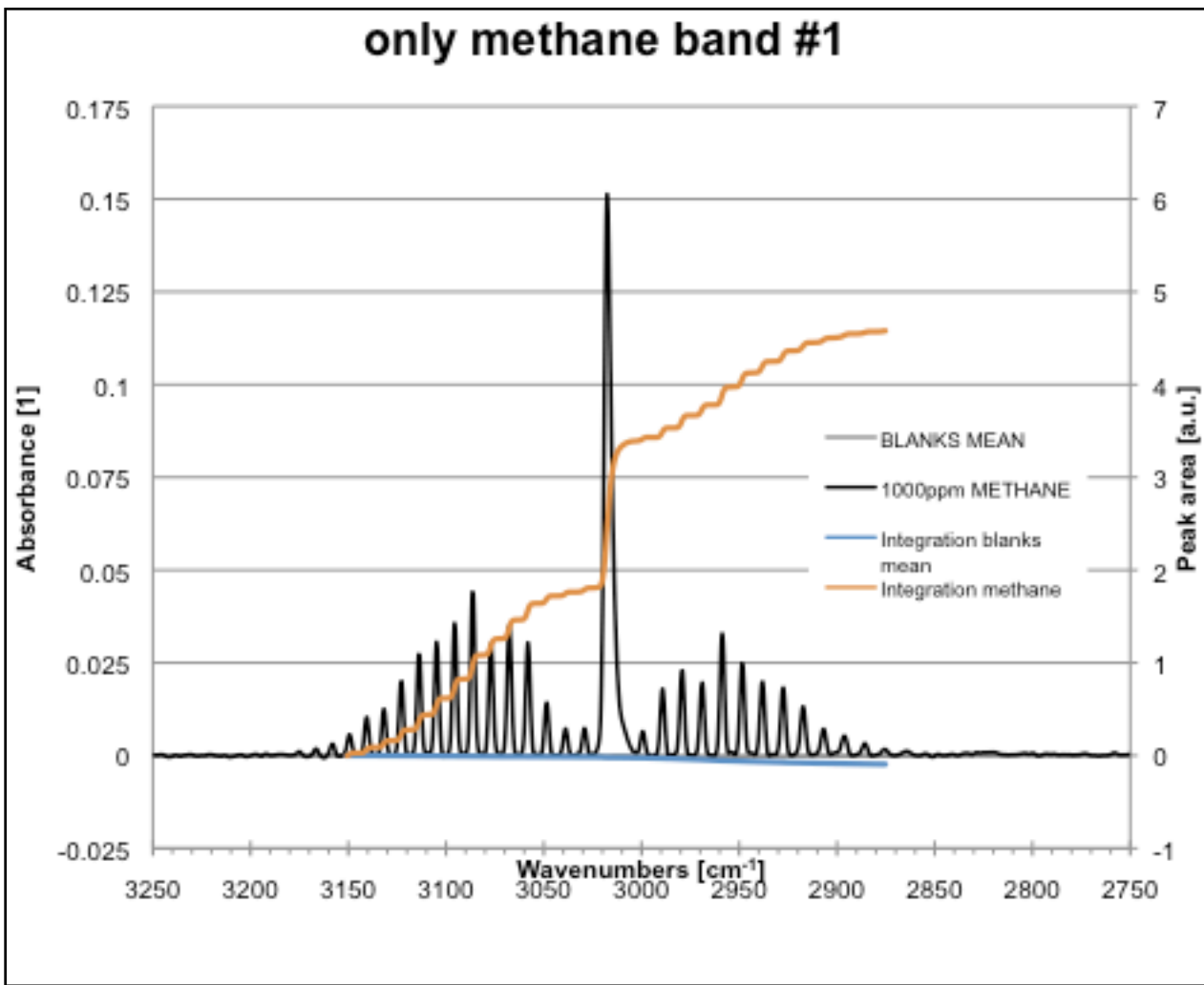

- **This diagram illustrates the univariate SNR by showing the integration of both background and signal.**

- **Note: the displayed integration was performed in Excel, not using the (more sophisticated) OPUS method. The results are still similar, but not identical.**

1000 ppm
Cyclopropane, overview spectrum

1000ppm cyclopropane + mean of blanks
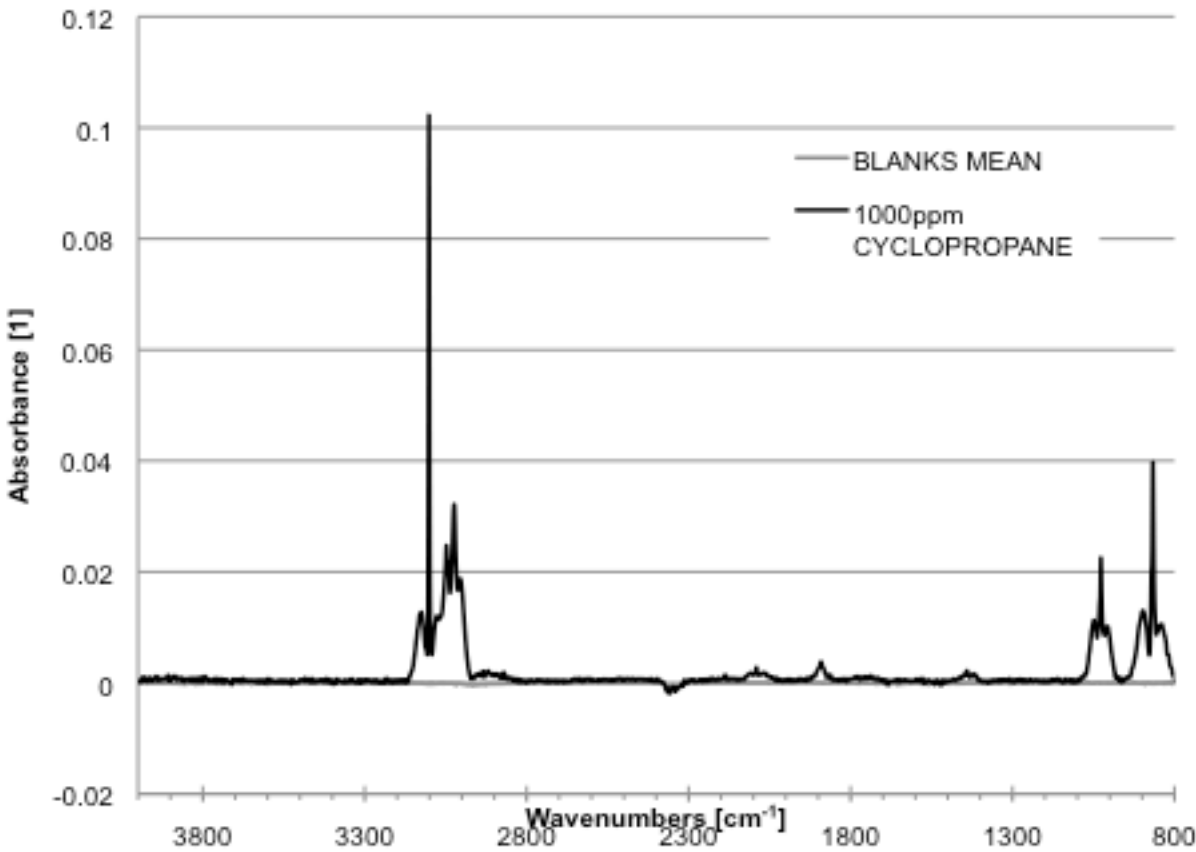
- **Spectrum was measured with the 4-piece yin-yang iHWG sensor as described in Appendix G.**

- **The „BLANKS MEAN" is the black curve shown on slides #2 & 3.**

Lawrence Livermore National Laboratory

I-10

1000 ppm
Cyclopropane, spectrum section
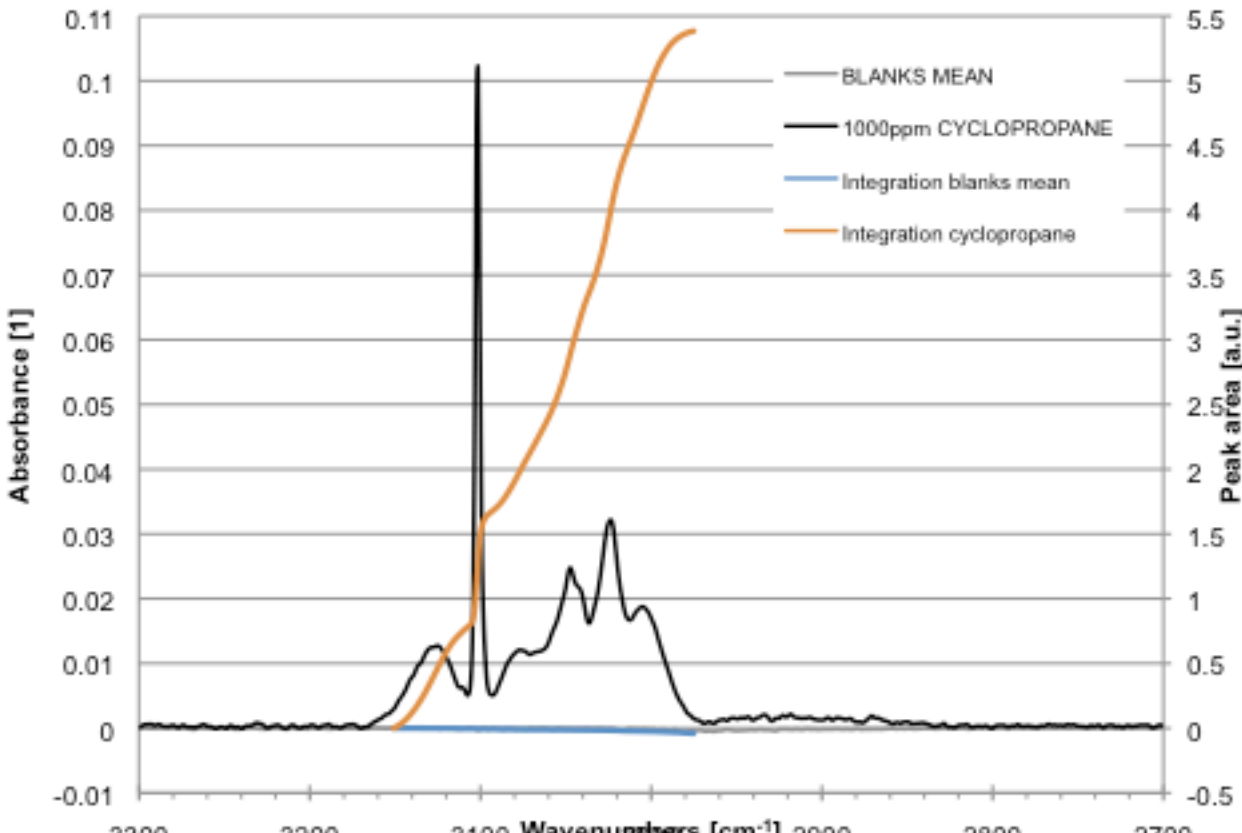
- **This diagram illustrates the univariate SNR by showing the integration of both background and signal.**

- **Note: the displayed integration was performed in Excel, not using the (more sophisticated) OPUS method. The results are still similar, but not identical.**

# 1000 ppm
Isobutylene, overview spectrum

- **Spectrum was measured with the 4-piece yin-yang iHWG sensor as described in Appendix G.**

- **The „BLANKS MEAN" is the black curve shown on slides #2 & 3.**

1000 ppm
Isobutylene, spectrum section

only isobutylene band #1
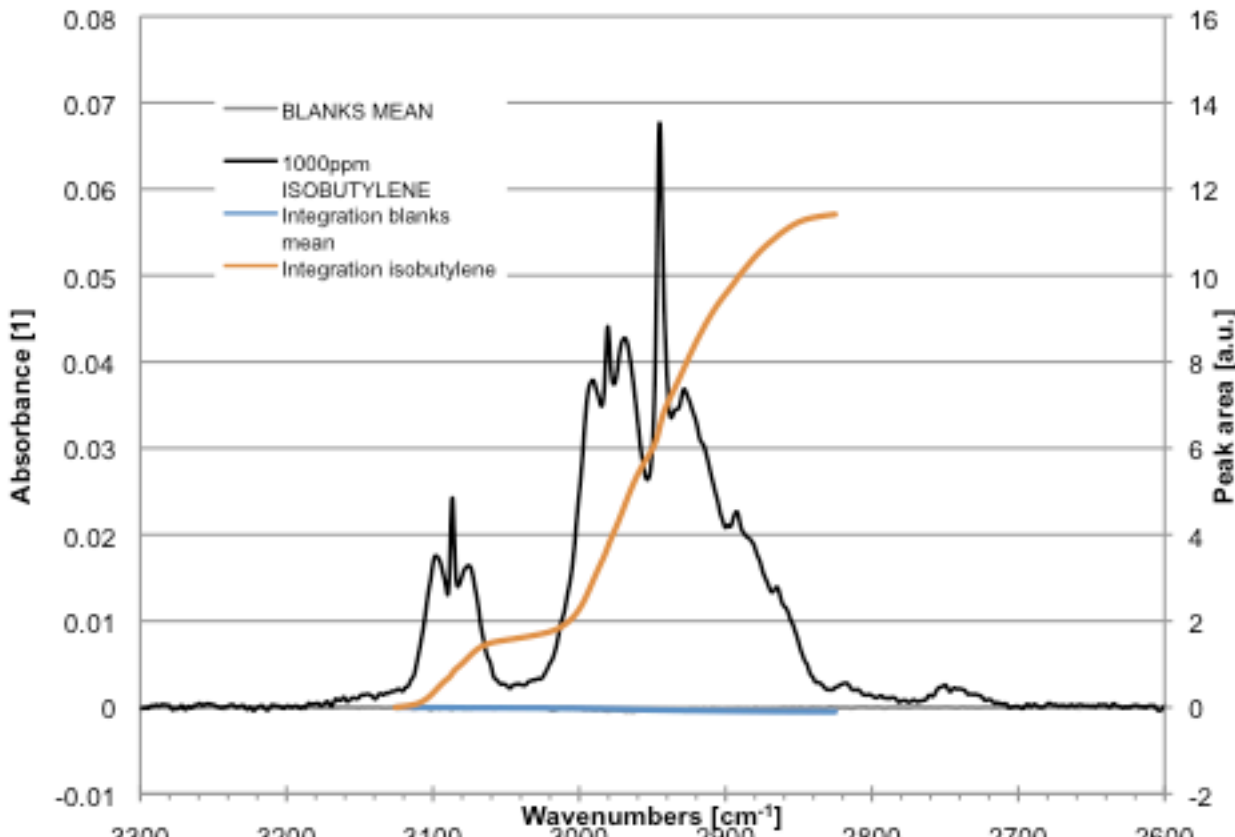
- **This diagram illustrates the univariate SNR by showing the integration of both background and signal.**

- **Note: the displayed integration was performed in Excel, not using the (more sophisticated) OPUS method. The results are still similar, but not identical.**

Summary
Univariate SNR & Detectable concentration limit (LOD) estimation

4-piece yin-yang iHWG		
Analyte	UNIVARIATE SNR	UNIVARIATE LOD (ppm)
Isobutylene	324	10.2 (2)
Methane	314	10.5 (2)
Cyclopropane	337	9.77 (C)
Butane	507	6.50 (1)
Carbon dioxide	156	21.1 (1)

Lawrence Livermore National Laboratory

Mixture spectrum
Tier 0 Gas Mixture
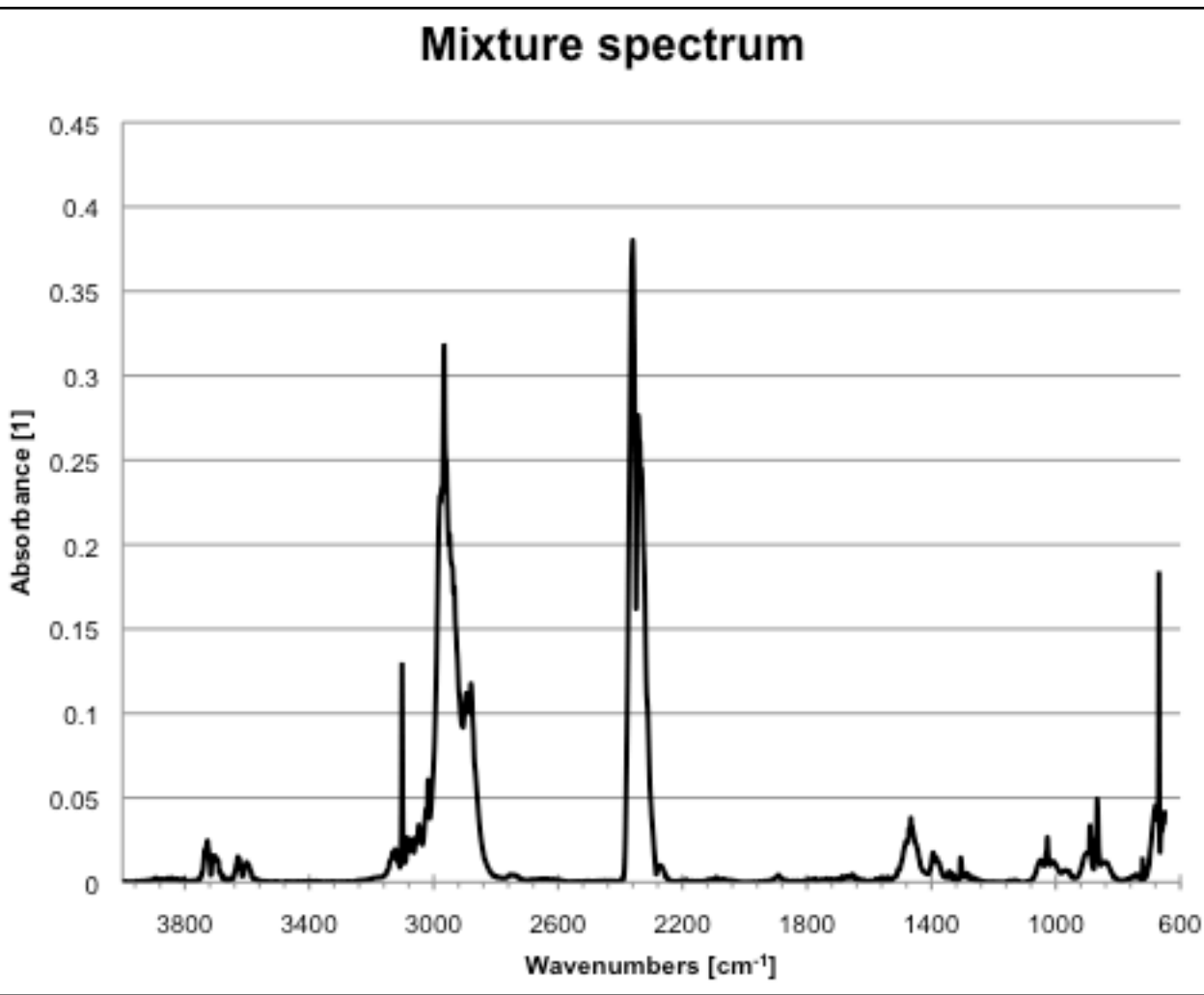
- **All previously shown spectra were pure analyte spectra.**
- **This is a single example of a mixture spectrum; containing**
- **200 ppm methane,**
- **2200 ppm carbon dioxide,**
- **200 ppm isobutylene,**
- **1800 ppm butane, and 1200 ppm cyclopropane.**

Lawrence Livermore National Laboratory

Mixture spectrum
Decomposition

- **As labeling of the peaks is quite difficult due to the highly unequal absorption strengths and analyte concentrations (i.e., in this case the spectrum is dominated by CO_2 and butane), each individual spectrum has been decomposed to visualize the individual analyte contributions to the mixture.**

- **For decomposition I used the (pure) 1000ppm spectra of the target analytes, and executed a linear scaling of their absorption values to resemble the corresponding concentrations in the mixture. E.g., every single absorption value of the 1000ppm CO2 spectrum was multiplied with a factor of 2.2, which estimates CO2 at 2200ppm (i.e., its concentration in the mixture). Accordingly, e.g., the absorbance values of the 1000ppm methane spectrum were multiplied with 0.2, estimating the spectral response of 200ppm methane.**

Mixture spectrum
Carbon dioxide

Mixture decomposed
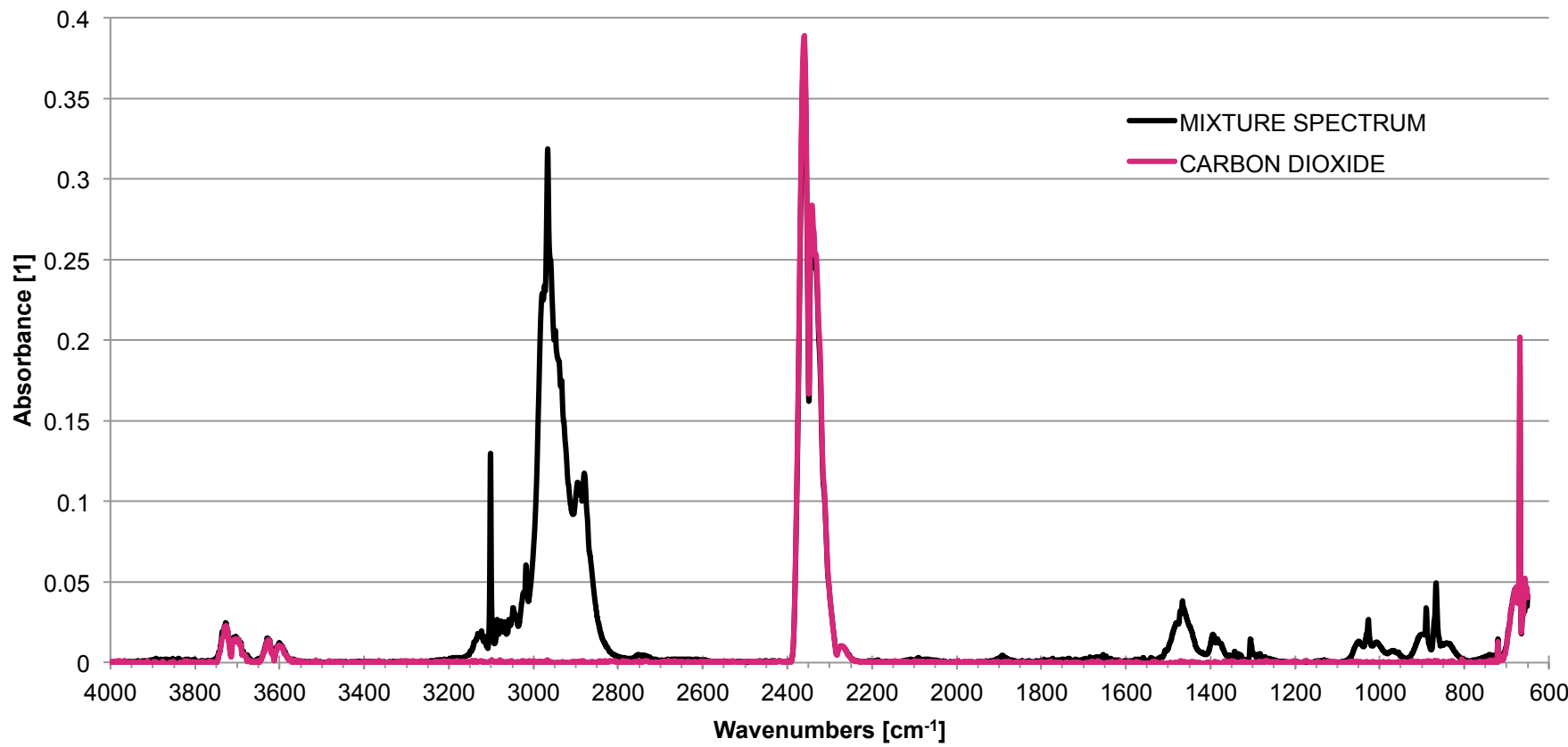
Mixture spectrum
Isobutylene

Mixture decomposed
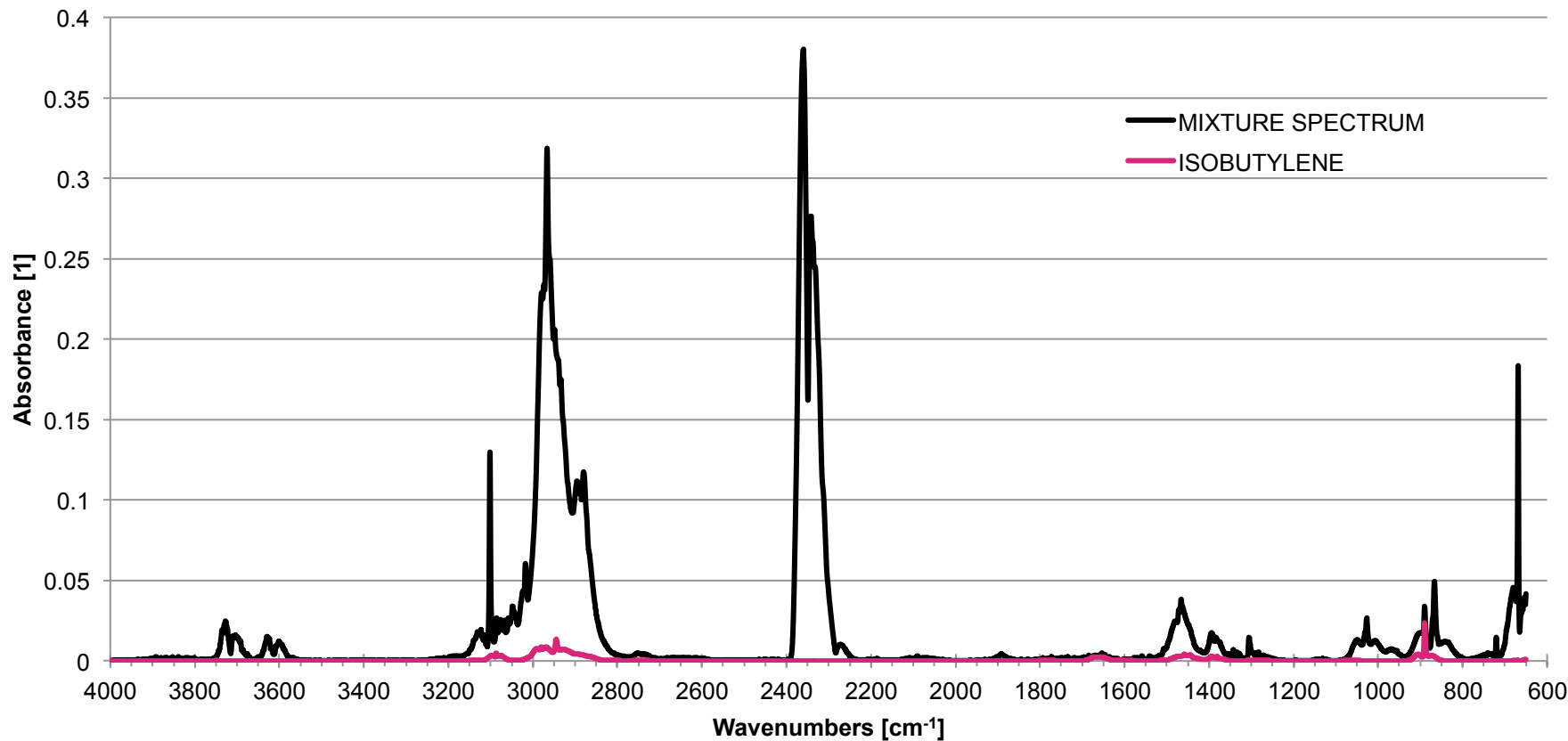
Mixture spectrum
## *Cyclopropane*

Mixture decomposed
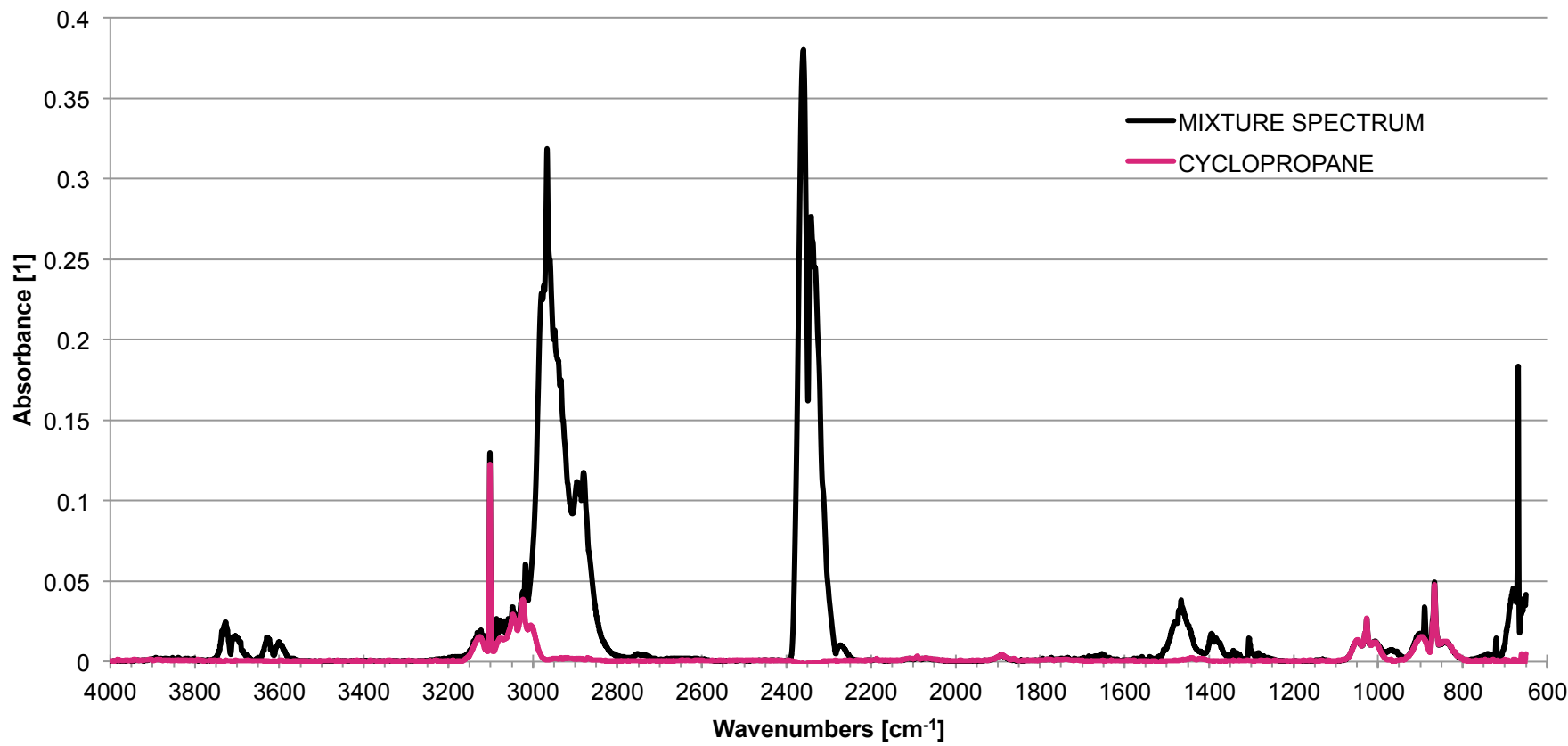
Mixture spectrum
Methane
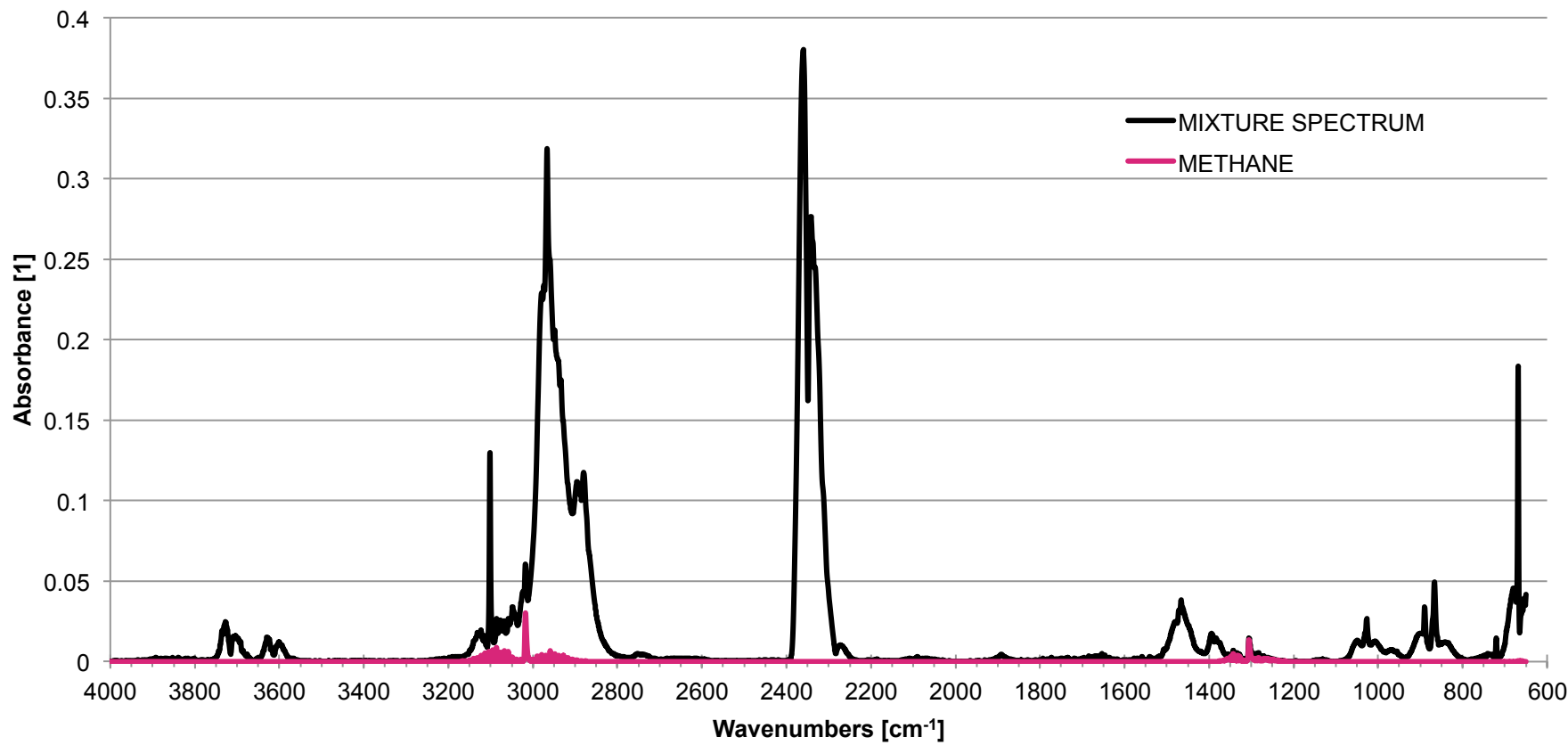
Mixture spectrum
Butane
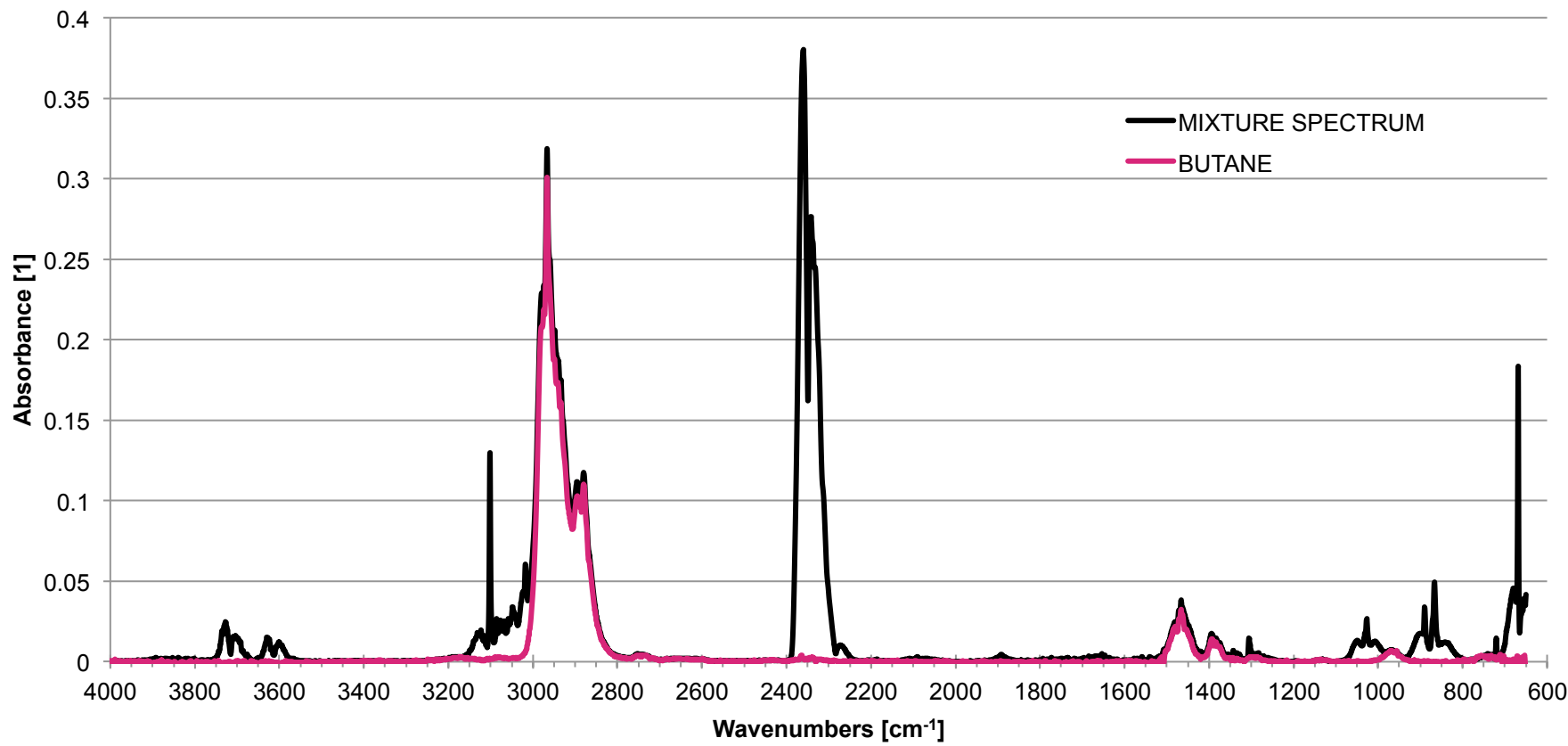
Verification of the decomposition

Synthetic mixture: this is the sum spectral response of all 5 (pink) decomposed spectra

Lawrence Livermore National Laboratory